MEDNARODNA
PODIPLOMSKA ŠOLA
JOŽEFA STEFANA

5. ŠTUDENTSKA KONFERENCA MEDNARODNE PODIPLOMSKE ŠOLE JOŽEFA STEFANA

Zbornik - 2. del

5th JOŽEF STEFAN INTERNATIONAL POSTGRADUATE SCHOOL STUDENTS' CONFERENCE

Proceedings - Part 2



23. 05. 2013, LJUBLJANA

Zbornik 5. Študentske konference Mednarodne podiplomske šole Jožefa Stefana
(Proceedings of the 5th Jožef Stefan International Postgraduate School Students Conference)

Uredniki:
Nejc Trdin
Andraž Rešetič
Majda Pavlin
Božidara Cvetković

Založnik:
Mednarodna podiplomska šola Jožefa Stefana, Ljubljana

Tisk:
TISKARNA PLEŠKO d.o.o.

Naklada:
150 izvodov

Ljubljana, maj 2013

IPSSC organizira študentski svet Mednarodne podiplomske šole Jožefa Štefana
(IPSSC is organized by Jožef Stefan International Postgraduate School - IPS student council)

CIP - Kataložni zapis o publikaciji
Narodna in univerzitetna knjižnica, Ljubljana

5/6(082)
378.046-021.68:001.891(497.4)(082)

MEDNARODNA podiplomska šola Jožefa Stefana. Študentska konferenca (5 ; 2013 ; Ljubljana)
Zbornik = Proceedings / 5. študentska konferenca Mednarodne podiplomske šole Jožefa Stefana = 5th Jožef Stefan International Postgraduate School Students Conference, 23. maj 2013, Ljubljana, Slovenija ; [organizira študentski svet Mednarodne podiplomske šole Jožefa Štefana = organized by Jožef Stefan International Postgraduate School - IPS Student Council] ; uredili, edited by Nejc Trdin ... [et al.]. - Ljubljana : Mednarodna podiplomska šola Jožefa Stefana, 2013

ISBN 978-961-92871-5-6
1. Trdin, Nejc 2. Mednarodna podiplomska šola Jožefa Stefana (Ljubljana)
266944512

5. ŠTUDENTSKA KONFERENCA MEDNARODNE PODIPLOMSKE ŠOLE JOŽEFA STEFANA

Zbornik - 2. del

5th JOŽEF STEFAN INTERNATIONAL POSTGRADUATE SCHOOL STUDENTS' CONFERENCE

Proceedings - Part 2

Uredili / Edited by

Nejc Trdin, Andraž Rešetič, Majda Pavlin in Božidara Cvetković

23. 05. 2013, Ljubljana

Kazalo (Table of Contents)

Ekotehnologija (Ecotechnology)

Optimization of derivatization process for human metabolites of common cytostatics cyclophosphamide and ifosfamide

Marjeta Česen[1,2], **Tina Kosjek**[1,2], **Ester Heath**[1,2]

[1] Department of Environmental Sciences, Jožef Stefan Institute, Ljubljana, Slovenia

[2] Jožef Stefan International Postgraduate School, Jamova 39, 1000 Ljubljana, Slovenia

marjeta.cesen@ijs.si

Cyclophosphamide and ifosfamide are drugs, mainly used in chemotherapy to treat cancer and some autoimmune diseases. After chemotherapy, these compounds undergo metabolism in human body and are finally excreted *via* urine in initial form and as metabolites. There is still little known about the occurrence and transformations of cytostatic drugs in aqueous environment and even less about the fate of their human metabolites. In our study, we will develop an analytical method for determination of human metabolites of cyclophosphamide and ifosfamide in low environmental concentrations in aqueous matrices. We have already optimized the first step – derivatization process, which is necessary for chemical analysis with gas chromatography coupled to mass spectrometry. Following step will be optimization of solid phase extraction of aqueous samples, which will enable us to quantitatively determine their presence in Slovene wastewaters and surface waters. In addition, we will perform laboratory-scale experiments for degradation studies of selected metabolites of cyclophosphamide and ifosfamide (N-dechloroethyl-CP, 3-dechloroethyl-IF, 2-dechloroethyl-IF and keto-CP).

MEDNARODNA PODIPLOMSKA ŠOLA JOŽEFA STEFANA
JOŽEF STEFAN INTERNATIONAL POSTGRADUATE SCHOOL

OPTIMIZATION OF DERIVATIZATION PROCESS FOR HUMAN METABOLITES OF COMMON CYTOSTATICS CYCLOPHOSPHAMIDE AND IFOSFAMIDE

Marjeta Česen, Tina Kosjek, Ester Heath
Jožef Stefan International Postgraduate School
(programme Ecotechnology)
Supervisor: Assoc. Prof. Dr. Ester Heath
Jožef Stefan Institute, Department of Environmental Sciences, Ljubljana, Slovenia

INTRODUCTION

The increasing consumption of cytostatics raises concerns about their presence and effects in the environment. Among them, cyclophosphamide (CP) and ifosfamide (IF) are one of the most commonly prescribed drugs in chemotherapy. CP and IF undergo partial metabolism in human body, which is followed by their elimination *via* urine as parent compounds and metabolites. Pharmacokinetic data together with unknown effects of CP's and IF's metabolites in aqueous environment reveal the need to develop analytical method for their quantification. The aim of this study is to optimize derivatization process, which improves sensitivity of GC-MS analysis by transformation of such highly polar substances to more volatile derivatives.

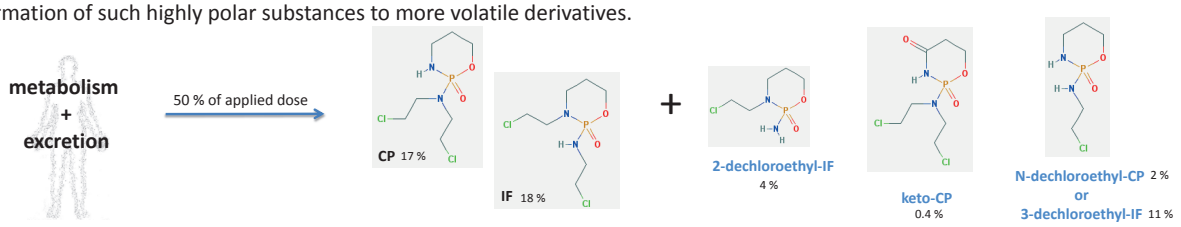

Optimization of DERIVATIZATION PROCESS

I. derivatizing agents

Type	agent
Silyating agents	MSTFA
	MTBSTFA
	MTBSTFA with 1 % TBDMCS
Acylating agents	HFBA
	TFAA
	HFBI
	MBTFA
	PFBCl
	AC_2O
Alkylating agent	PFBBr
Other	PFBHA

II. solvents:
- ethyl acetate
- toluene
- dichloromethane
- acetone
- acetonitrile

IV. volumes of appropriate solvent (0.25 mL – 1 mL) and agent (5 µL – 30 µL)

GC-MS analysis
- HP 6890 series (Agilent) GC-MS
- column DB-5 MS 30 m × 0.25 mm × 0.25 µm (Agilent J&W)
- carrier gas: He
- Injected V = 1 µL (splitless)
- GC oven: an initial T 65 °C held for 3 min, then ramped at 20 °C min^{-1} to 280 °C and held for 2 min

III. diverse reaction conditions (60 – 90 °C; 16h – 32 h)

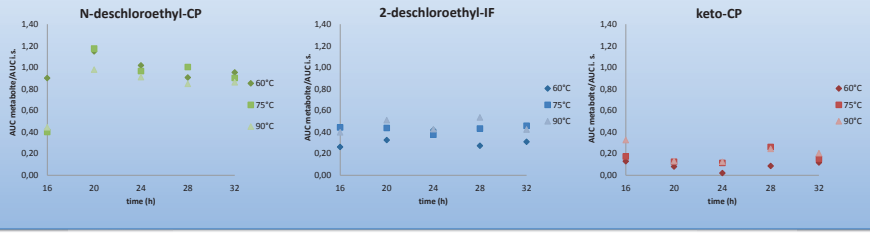

RESULTS AND FURTHER WORK

Derivatization process was optimized and will be followed by next step in analytical method, solid phase extraction. Once analytical method is developed and validated, it will be applied in further investigations:

- quantitative **analysis of Slovene wastewaters and surface waters ecotoxicological tests** for parent compounds + metabolites
- **degradation studies** under biotic and abiotic treatments

compound	retention time (min)	characteristic ion fragments	conditions	solvent	$V_{solvent}$	V_{agent}
N-dechloroethyl-CP	12.84	308, 280, 195	20 h at 75 °C	acetonitrile	0.25 mL	15 µL
2-dechloroethyl-IF	13.15	257, 255, 136	20 h at 75 °C	toluene	0.25 mL	30 µL
keto-CP	13.65	297, 295, 242	16 h at 90 °C	acetonitrile	0.25 mL	15 µL

Acknowledgements
This work was financially supported by the EU through the EU FP7 project CytoThreat (Fate and effects of cytostatic pharmaceuticals in the environment and the identification of biomarkers for and improved risk assessment on environmental exposure (grant agreement No.: 265264) and by the Slovenian Research Agency (Program Group P1-0143 and Young Researcher grant to M. Č.).

Determination of the isotopic composition of polycyclic aromatic hydrocarbons in environmental samples

Marinka Gams Petrišič[1,2], **Nives Ogrinc**[1,2]

[1] Department of Environmental Sciences, Jožef Stefan Institute, Ljubljana, Slovenia

[2] Jožef Stefan International Postgraduate School, Ljubljana, Slovenia

marinka.petrisic@ijs.si

The identification and quantification of organic compounds present in the environment are major areas of application in modern analytical chemistry. However, it is still scarcely recognized that, in addition to the chemical identity and concentration of organic compounds, there is more information to be found about their source and fate in the environment from their isotope composition. Isotope ratio mass spectrometry (IRMS) following on-line combustion (C) of compounds separated by gas chromatography (GC-C-IRMS) has been commercially available only since 1990. Our understanding of the isotope composition of organic compounds in different studies is therefore still somewhat limited.

In this work, the stable isotope approach was further used to identify the sources of polycyclic aromatic hydrocarbons (PAHs) in sediments, which was not possible based only on the concentration distribution of individual PAH.

MEDNARODNA PODIPLOMSKA ŠOLA JOŽEFA STEFANA

JOŽEF STEFAN INTERNATIONAL POSTGRADUATE SCHOOL

DETERMINATION OF THE ISOTOPIC COMPOSITION OF POLYCYCLIC AROMATIC HYDROCARBONS IN ENVIRONMENTAL SAMPLES

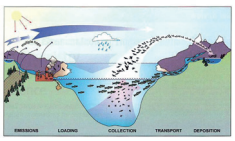

MARINKA PETRIŠIČ, univ. dipl. kem., prof. kem.
Študijski program: **Ekotehnologija (4. letnik),**
Mednarodna podiplomska šola Jožefa Stefana
MENTORICA: **izr. prof. dr. NIVES OGRINC**
Institut "Jožef Stefan", Jamova cesta 39, 1000 Ljubljana

INTRODUCTION

- PAH constitute a large group of Persistent Organic Pollutants (POP) containing from two to six fused benzene rings.
- Certain PAH are among the most carcinogenic substances known and can be acutely toxic or genotoxic, depending on the number and configuration of the benzene rings and the presence and position of their substituents.
- PAH exhibit different molecular distribution according to their origin formed during incomplete OM combustion (**pyrolytic origin**) or natural and anthropogenic fossil fuel combustibles (**petrogenic origin**).
- Source identification using stable isotopes is only possible if organic compounds are resistant to chemical and biological alteration processes.
- The primary objectives of the proposed study were:
  - to determine the precision and accuracy of the isotopic composition of PAH in standards using GC-C-IRMS.

Figure 1: Lake Bled.

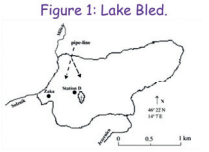

Figure 2: Sampling site location.

Figure 3: Corer.

Figure 4: Soxhlet extraction.

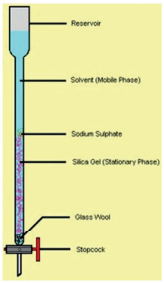

Figure 5: Fractionation.

Figure 6: GC-MS.

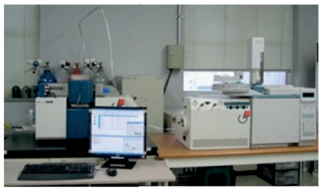

Figure 7: GC-C-IRMS.

SAMPLING → **EXTRACTION** → **FRACTIONATION** → **DETECTION**

RESULTS

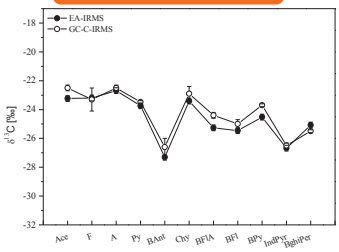

Figure 8: Comparison between $\delta^{13}C$ values obtained for the PAH pure standards using conventional EA-IRMS and GC-C-IRMS.
Ace = Acenaphthene; F = fluorine; Ph = phenanthrene; A = anthrancene; Fl = fluoranthene; Py = pyrene; BaA = benz(a)anthracene; ChY = chrysene; BbFl = benzo(b)fluoranthene; BaPy = benzo(a)pyrene; BghiPer = benzo(ghi)perylene; IndPy = indeno(123-cd)pyrene.

Table 1: $\delta^{13}C$ values of individual PAH in Lake Bled sediments in the W basin.

PAH	$\delta^{13}C$ (‰)	
	12-14 cm	14-16 cm
Fluorene (F)	-28.2	-25.9
Phenantrene (Ph)	-26.3	-23.4
Anthracene (A)	-23.9	-28.4
Fluoranthene (Fl)	-22.4	-25.4
Pyrene (Py)	-21.7	-22.7
Chrysene (Chy)	-29.4	-29.5
Benzofluoranthene (BF)	-26.4	-26.1
Benzopyrene (BP)	-25.1	-25.7

- CSIA was performed on individual PAH pure standards and in the standard mixture of PAHs with a precision of 0.2 to 0.4‰ and an accuracy ranging between 0.3 and 1.0‰.
- GC-C-IRMS measurements in sediment samples were performed with a precision of 0.3‰ for well separated PAH compounds and up to 1.0‰ for some coeluting isomers.
- The overall trend in PAH $\delta^{13}C$ values ranging between –29.5‰ and –21.7‰ were quite distinct and were useful to identify possible source of contamination.
- The dominant signatures identified at the depth of 12-14 and 14-16 cm in sediments of Lake Bled were mainly attributed to a coal/wood burning source, but PAH from carsoots could also contributed to the overall isotope signatures at the depth of 12-14 cm.
- The 12-14 cm and 14-16 cm depths in sediments correspond to the period 1953-1961 and 1944-1953, respectively.
- This study indicates that isotopic composition of PAH is a useful parameter to obtain more detailed source identification of organic pollutants in environmental samples including sediments.

Implementation and results of Research Fund for Coal and Steel funded project CoGasOUT at Coal-Mine Velenje

Sergej Jamnikar[1], **Jerneja Lazar**[1], **Simon Zavšek**[1], **Ludvik Golob**[1]

[1] Premogovnik Velenje (Coal-Mine Velenje), Velenje, Slovenia

sergej.jamnikar@rlv.si

CoGasOUT is a research and development project with interdisciplinary international partner project group funded by European Comission Research Fund For Coal and Steel. Project group includes scientific and industrial partners as listed: Imperial College, Mine Rescue Service Limited, Coal-Mine Velenje, DMT, K-UTEC, Glowny Instytut Gornictwa, Hullera Vasco Leonesa, AITEMIN and Hornonitrianske bane Prievidza. CoGasOUT project started with a Kick-off meeting in July 2010, and will conclude in July 2013 project with final activities, dissemination and reports.

Key aspect of project is design and development of novel techniques for safer underground mining concerning coal gas hazards. Project work is divided into theoretical background set-up and revision of existing data, followed by experiment design and digital model creation and final implementation of designed experiment. Experimental results will be used in digital model creation and its calibration.

Over project's 3-years duration time, several research campaigns, experiments, tests, analyses and revision have been performed. Coal-Mine Velenje is the major partner for field work and underground in-situ measurements. On the basis of the preliminary and preparation activities we focused on final deliverable of Coal-Mine Velenje's part of CoGasOUT project – underground gas drainage of excavation pillar.preparation activities we are focused on a final deliverable of Coal-Mine Velenje's part of CoGasOUT project – underground gas drainage of excavation pillar.

EXECUTION AND RESULTS OF RFCS* FUNDED PROJECT CoGasOUT AT COAL-MINE VELENJE

Sergej Jamnikar, Jerneja Lazar, Simon Zavšek, Ludvik Golob
Coal Mine Velenje, Partizanska 78, Velenje, Slovenija

INTRODUCTION AND PROJECT STRUCTURE (WORK PACKAGES)

CoGasOUT is research and development project with multiple international partner project group under the funding of European Comissions' Research Fund For Coal and Steel.
Project group combines multiple scientific and industrial partners as listed: Imperial College, MRSL, Coal-Mine Velenje, DMT, KUTEC, GIG, HVL, AITEMIN and HBP.
CoGasOUT project started with a Kick-off meeting in July 2010, followed by annual project group meetings and reports for EU Commission TGC 1 evaluators group.
By July 2013 project will conclude with final activities, dissemination and reports.

Key aspect of project is design and development of novel techniques for safer underground mining concerning coal gas hazards. Project work is divided into theoretical background set-up and revision of existing data, followed by experiment design and digital model creation and final implementation of designed experiment.
Experimental results will be used in digital model creation and its calibration together with seam gas drainage pilot test.

Over project's 3-years duration time, several research campaigns, experiments, tests, analyses and revision has been done.
Coal-Mine Velenje is the major partner for field work and underground in-situ measurements.
On basis of preliminary and preparatory activities we are focused on final deliverable of Coal-Mine Velenje's part of CoGasOUT project – underground gas drainage of excavation pillar.

Coal-Mine Velenje share include existing data review, field and laboratory investigations, in-situ monitoring, mine experiment preparations, modelling and pilot trials.

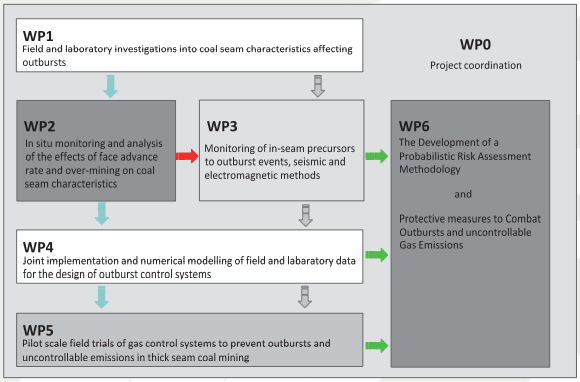

Figure 1: Project structure

MINE MONITORING AND MEASUREMENTS

Underground measurement and monitoring campaigns at excavation pillars and long-wall faces in Coal-Mine Velenje included:
- seam gas pressure measurements,
- seam gas composition measurements and gas isotopic composition analyses,
- seam gas content experiments,
- geo-technical parameters measurements,
- long-wall face ventilation data monitoring and
- execution of seismic measurements (micro-seismic tomography, seismic source and strength).
All of listed activities led to final deliverable of project - Pilot seam gas drainage trials.

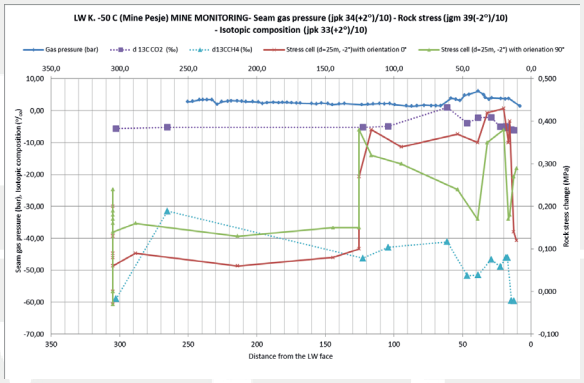

Figure 2: Seam gas pressure, gas composition and rock stress measurements in dependence of long-wall face advance (Long-wall face K. -50 C)

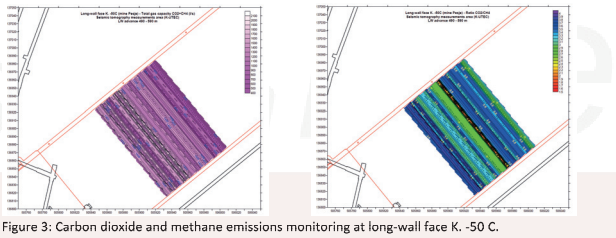

Figure 3: Carbon dioxide and methane emissions monitoring at long-wall face K. -50 C. Total gas content (left) and gas ratio (right).

RELATED ACTIVITIES

Over the procedure of CoGasOUT project Coal-Mine Velenje hosted several scientific groups from related institutions. As an example, GIG and KUTEC performed their seismic monitorings and measurements. Many samples were sent to partner's laboratories in order to test coal samples with alternative methodologies.

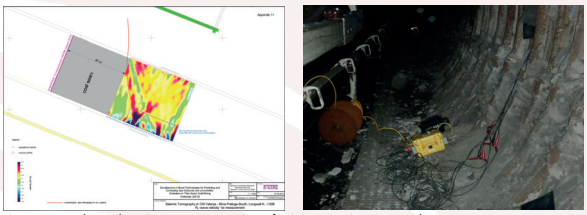

Figure 4: Results and equipment preparation of Micro-seismic tomography measurements at long-wall face K. -130 B (KUTEC, 2012)

PILOT GAS DRAINAGE TRIALS

On basis of multiple mine monitoring results and analysis we designed pilot underground gas drainage trials at long-wall face K. -65 F. Main objective of trials is optimisation of drainage setup (drainage wells, vacuum pump, monitoring, pipeline) for continuous gas drainage in future.

Figure 5: Pilot gas drainage trial set-up. Pipe line with water settler (left), vacuum pump and monitoring sensors (right).

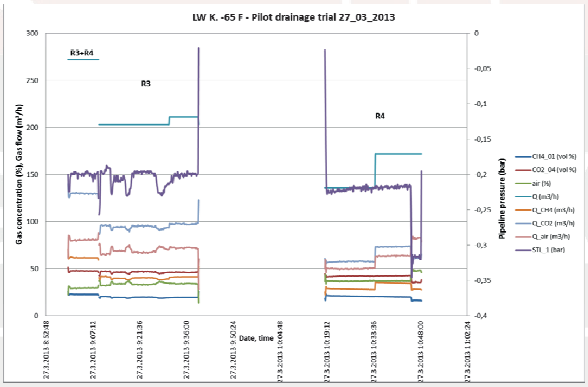

Figure 6: Results of daily pilot gas drainage trial. Gas concentrations, pipe-line pressure and total gas flow are measured. Single gas quantities are calculated.

REFERENCES

- CoGasOUT Annual Reports (2011 - 2013)
- Razplinjevanje odkopnega stebra na odkopni plošči k. -65 F v jami Pesje, Rudarski projekt

A novel method for speciation of Pt in human serum incubated with cisplatin, oxaliplatin and carboplatin by conjoint liquid chromatography on monolithic disks with UV and ICP-MS detection

Anže Martinčič[1,2], Radmila Milačič[1,2], Maja Čemažar[3], Gregor Serša[3], Janez Ščančar[1,2]

[1] Department of Environmental sciences, Jožef Stefan Institute, Ljubljana, Slovenia

[2] Jožef Stefan International Postgraduate School, Ljubljana, Slovenia

[3] Institute of Oncology, Department of Experimental Oncology, Ljubljana, Slovenia

anze.martincic@ijs.si

Our work is based on monolithic chromatography, which offers several advantages over standard (particle packed) chromatographic columns. Monolithic supports have high permeability and therefore allow thorough cleaning during regeneration after each separation run. This enables great robustness of such chromatographic columns which in turn enables higher throughput of samples. Monolithic supports are also cheaper and offer possibilities to be applied in numerous chromatographic separations of compounds in environmental and biological samples.

Combining affinity and anion exchange monolithic disks enables us to construct so called conjoined liquid chromatography columns (CLC) that can perform 2D chromatographic separations in a single run.

MEDNARODNA PODIPLOMSKA ŠOLA JOŽEFA STEFANA

JOŽEF STEFAN INTERNATIONAL POSTGRADUATE SCHOOL

A novel method for speciation of Pt in human serum by conjoint liquid chromatography on monolithic disks with UV and ICP-MS detection

Anže Martinčič*#, Radmila Milačič*#, Maja Čemažar**, Gregor Serša** and Janez Ščančar*#

*Jožef Stefan Institute, Jamova 39, 1000 Ljubljana, Slovenia
#Josef Stefan International Postgraduate School, Jamova 39, 1000, Ljubljana
**Institute of Oncology, Zaloška cesta 2, 1000 Ljubljana, Slovenia

INTRODUCTION

In speciation analysis of platinum in human serum, ion exchange (IE) chromatography is frequently used. As an alternative to classic – particle packed IE columns, monolithic supports have been successfully applied. They have several advantages over classical columns (e.g. greater robustness) but both are unable to separate unbound drug from immunoglobulins (IgG), which co-elute at the same retention time t_0 (Figure 1) [1]. To overcome this problem a conjoint liquid chromatography (CLC) column containing one CIM Protein G and one CIM DEAE monolithic disk in a single housing was constructed. Such set up allows two dimensional separation in one chromatographic run. CIM Protein G disk (affinity chromatography) binds Fc region of IgG thus separating free Pt-based drug from portion that is bound to IgG, while on a weak anion exchange CIM DEAE disk serum transferrin and albumin were separated.

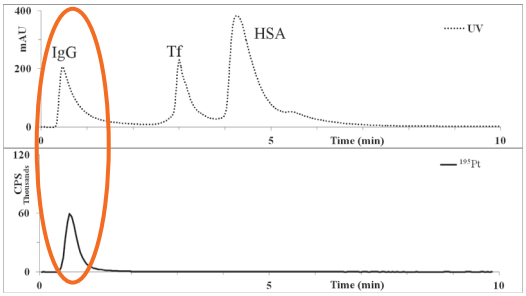

Figure 1: Co-elution of unbound drug and IgG. Chromatogram of the mixture of serum proteins (above). Chromatogram of cisplatin diluted in buffer A (below).

METHODS

Chromatographic separation on Agilent 1200 HPLC and elemental detection by Agilent 7700x ICP-MS

1. CIM DEAE and CIM protein G disks

- 0.05 M Tris HCl + 0.03 M $NaHCO_3$, pH 7.4 (buffer A)
- 0.05 M Tris HCl + 1 M NH_4Cl, pH 7.4 (buffer B)
- 0.5 M AcOH, (eluent C)
- Sample volume: 0.1 mL
- Flow 1 mL/min
- Analysis time: 14 min; 1st min isocratic at 100 % buffer A, next 9 min gradient elution from 100 % A to 100 % B, and the last 4 min eluent C.
- Column regeneration time: 9 min

Figure 2: CIM Protein G disk column

2. UV detection at 278 nm

3. ICP-MS

- RF power: 1550 W
- Carrier gas: 0.35 L/min, dilution gas: 0.82 L/min
- Integration time on m/z 195 and 194: 0.7 s
- Time resolved analysis: 14 min

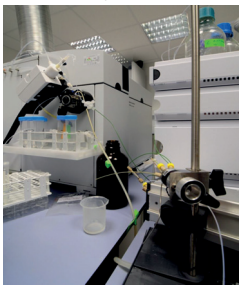

Figure 3: Instrument setup

RESULTS AND DISSCUSSION

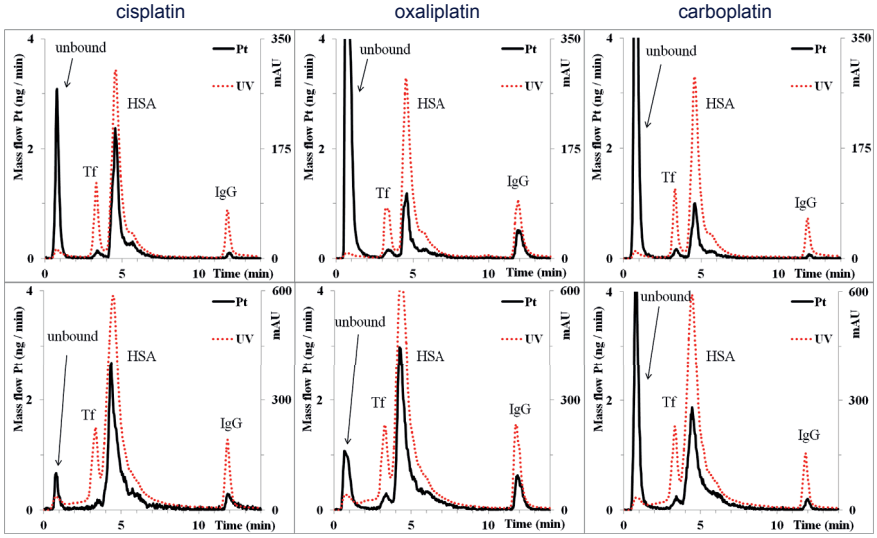

Figure 4: Chromatographic separation of a synthetic mixture of serum proteins (top) and human serum (bottom) spiked with a single Pt-based drug (100 to 200 ng Pt mL^{-1}, incubation time 24 h).

As can be seen from Figure 2, the developed method separates all the major Pt species found in human serum. The use of post-column ID adequately compensated the changes in eluent composition, while also providing the means for quantifying our results (table 1).

Table 1: Distribution of Pt in human serum

Pt drug	Incubation time (h)	Pt spike added	Unbound Pt	Pt bound to Tf	Pt bound to HSA	Pt bound to IgG	Column recovery
		(ng mL^{-1})	(ng mL^{-1})	(ng mL^{-1})	(ng mL^{-1})	(ng mL^{-1})	(%)
Cisplatin	24 h	137.4±1.1	19.5±0.1	2.50±0.02	103.5±0.8	5.00±0.04	95
Oxaliplatin	24 h	153.7±1.2	27.0±0.2	4.01±0.03	102.1±0.8	16.0±0.1	97
Carboplatin	48 h	165.6±1.3	77.5±0.6	3.02±0.02	75.5±0.6	3.01±0.03	96

CONCLUSIONS

The developed method is uniquely able to separate unbound drug from drug bound to IgG while preserving all the advantages of monolithic chromatography, mainly speed and robustness.

Chromate cannot exist in food samples

Breda Novotnik[1,2], **Tea Zuliani**[1], **Janez Ščančar**[1,2], **Radmila Milačič**[1,2]

[1] Department of Environmental Sciences, Jožef Stefan Institute, Ljubljana, Slovenia

[2] Jožef Stefan International Postgraduate School, Ljubljana, Slovenia

breda.novotnik@ijs.si

Recently several papers have been published on the presence of Cr(VI) in tea infusions, bread samples and plants in spite of the well known fact, that Cr(VI) cannot exist in these samples as it is readily reduced by organic matter. The assumptions were made on the basis of total Cr determination in alkaline and aqueous sample extracts by ETAAS, without applying any speciation analysis. If Cr(VI) really exists in bread samples and tea infusions, consuming bread and tea would represent a long-term chronic exposure to Cr(VI) and health threat for most of human population. To confirm our hypothesis that the data published in the literature is erroneous, the aim of our work was to repeat the extraction procedures described in the literature and with speciation analysis using HPLC-ICP-MS confirm or negate the data on the presence of Cr(VI) in bread and tea samples. To follow Cr species interconversions stable isotopes of ^{50}Cr(VI) and ^{53}Cr(III) were added to the samples. Our results have shown that Cr(VI) concentrations in the samples were below the limit of detection. Additionally, ^{50}Cr(VI) that was added to tea and bread samples was reduced by organic matter in spite of the high pH (12), providing additional proof that Cr(VI) cannot exist in food samples.

MEDNARODNA PODIPLOMSKA ŠOLA JOŽEFA STEFANA

JOŽEF STEFAN INTERNATIONAL POSTGRADUATE SCHOOL

Chromate cannot exist in food samples

Breda Novotnik[1,2], Tea Zuliani[1], Janez Ščančar[1,2] and Radmila Milačič[1,2] .[1] Department of Environmental Sciences, Jožef Stefan Institute, Ljubljana, Slovenia. [2] Jožef Stefan International Postgraduate School, Ljubljana, Slovenia. <bnovotnik@ijs.si>

Introduction

Chromium is a common environmental contaminant. In the environment Cr(VI) is readily reduced to Cr(III) by organic matter. Therefore, in biological samples Cr is exclusively present as Cr(III) except shortly after exposure. Despite this known fact, several papers have been published in recent years on the presence of total Cr(VI) in tea leaves[1], bread samples[2] and plants based on alkaline extraction and determination of Cr with ETAAS (electrothermal atomic absorption spectrometry) without performing any speciation analysis. Based on ETAAS determination of Cr content in tea infusions, its concentration was prescribed to be soluble Cr(VI)[1]. These presumptions were again made without applying speciation analysis.

Aim of work

The aim of our work was to repeat the experiments of Mandiwana *et al.*[1] and Soares *et al.*[2] and to apply speciation analysis of Cr by high performance liquid chromatography – inductively coupled plasma mass spectrometry (HPLC-ICP-MS) using Cr stable isotopes to follow species interconversions during the extraction procedures.

Materials and methods

Cr in tea infusion: 2.0 g of sample + 200 mL of boiling water, double spike 10 ng mL ^{50}Cr(VI) and 10 ng mL^{-1} ^{53}Cr(III)

Alkaline extraction of tea leaves: 0.25 g of tea leaves + boiling 0.1 mol L^{-1} Na_2CO_3 + 10 ng mL ^{50}Cr(VI) and 10 ng mL^{-1} ^{53}Cr(III)

Alkaline extraction of bread: 1.0 g of dried bread + 0.01 mol L^{-1} NaOH + 10 ng mL ^{50}Cr(VI) and 10 ng mL^{-1} ^{53}Cr(III), shaken for 17 h, then NH_4NO_3 was added and sample was centrifuged. Supernatant was filtered and analyzed.

Speciation analysis: High performance liquid chromatography with inductively coupled plasma mass spectrometry HPLC-ICP-MS.[3]

Results and discussion

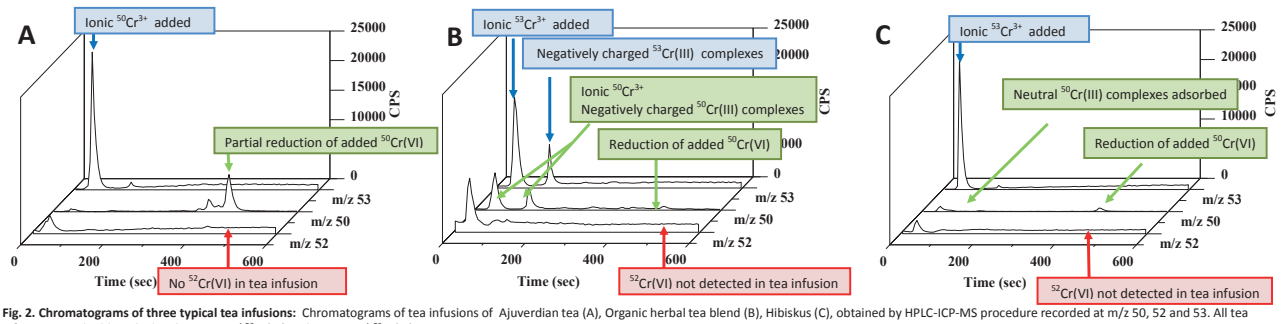

Fig. 2. Chromatograms of three typical tea infusions: Chromatograms of tea infusions of Ajuverdian tea (A), Organic herbal tea blend (B), Hibiskus (C), obtained by HPLC-ICP-MS procedure recorded at m/z 50, 52 and 53. All tea infusions are doubly spiked with 10 ng mL^{-1} ^{50}Cr(VI) and 10 ng mL^{-1} ^{53}Cr(III)

In Fig. 2 three typical chromatograms of analyzed teas are shown. We analyzed 13 teas and observed 3 typical patterns of Cr speciation. ^{nat}Cr(VI) was not detected in any of the tea infusions investigated . The added ^{50}Cr(VI) was either partially reduced (Fig. 2A) or completely reduced (Fig. 2B,C). The added ^{50}Cr(VI) was reduced to ^{50}Cr(III) species that are adsorbed on the column (2A,C) or reduced to ionic $Cr^{3+}$and negatively charged ^{50}Cr(III) complexes that are eluted (Fig 2B), depending on the type of tea examined. This confirmed our hypothesis that Cr(VI) cannot exist in tea due to the presence of antioxidants. The added ^{53}Cr(III) was not oxidized and was eluted either as ionic Cr^{3+} (Fig. 2A, 2C) or as negatively charged Cr(III) complex (Fig. 2B).

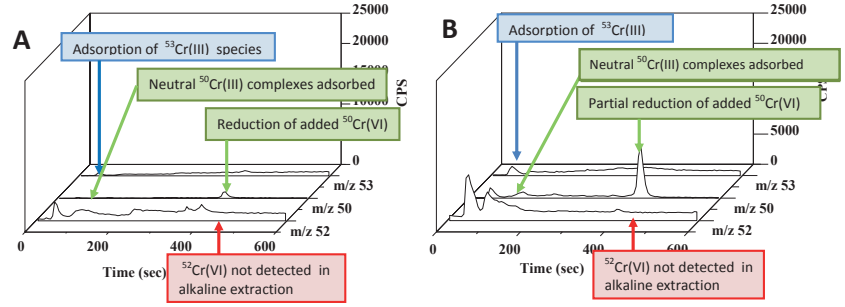

In Fig. 3 alkaline extraction of tea leaves (Fig. 3A) and whole grain bread (Fig. 3B) is presented. In the extracts ^{53}Cr(III) is present mainly as $Cr(OH)_3$ and is adsorbed on the column. The added ^{50}Cr(VI) was, despite the high pH, either partially (bread) or completely (tea leaves) reduced to Cr(III) and adsorbed on the column resin, indicating the strong reduction potential of organic ligands present in the sample extracts. In the alkaline extract of tea leaves and bread no ^{nat}Cr(VI) was detected.

Fig. 3 Chromatograms of alkaline extract (0.1 mol L^{-1} Na_2CO_3) of tea (A) ; alkaline extracts (0.01 mol L^{-1} NaOH) of whole grain bread (B)obtained by HPLC-ICP-MS procedure recorded at m/z 50, 52 and 53.

Conclusions: Speciation analyses have proven that ^{nat}Cr(VI) does not exist in tea infusions or in alkaline extracts of tea and bread samples. In tea infusions the added ^{53}Cr(III) was not oxidized, while added ^{50}Cr(VI) was readily reduced due to the presence of antioxidants. In alkaline extracts of tea and bread complete or partial reduction of ^{50}Cr(VI) was observed despite the high pH, indicating highly reductive nature of these organic ligands rich matrices. Based on our analytical data we have proven that ^{nat}Cr(VI) cannot exist in bread and tea due to the high content of organic ligands and antioxidants.

References:
1) K.L. Mandiwana, N. Panichev, S. Panichev, *Food Chem.*, 2011, **129**, 1839-1843. 2) M.E. Soares, E. Vieira, M. de Ludres Bastos, *J. Agric. Food Chem.*, 2010, **58**, 1366-1370. 3) B. Novotnik, T. Zuliani, A. Martinčič, J. Ščančar, R. Milačič, *Talanta*, 2012, **99,** 83–90.

Behaviour of Benzophenones under the Influence of Natural Sunlight

Kristina Pestotnik[1,2,3], **Tina Kosjek**[1], **Uroš Kranjc**[3], **Ester Heath**[1,2]

[1] Department of Environmental Sciences, Jožef Stefan Institute, Ljubljana, Slovenia

[2] Jožef Stefan International Postgraduate School, Ljubljana, Slovenia

[3] Ecological Engineering Institute Ltd, Maribor, Slovenia

kristina.pestotnik@ijs.si

Pharmaceuticals and personal care products (PPCPs) are a diverse group of compounds used as therapeutic drugs or consumer products for use on the human body (e.g. skin care, dental care and hair care products, sunscreen agents, soaps and cleaners, insect repellents, fragrances and flame retardants). They are produced in large quantities throughout the world and their consumption continues to rise. Consequently, these compounds enter the environment globally. In recent years there has been an increasing concern regarding the presence and effects of PPCP residues in the environment. Among numerous PPCPs this study is focused on benzophenone based compounds that include a pharmaceutical (ketoprofen), its phototransformation products and UV filters. Since photodegradation of PPCPs caused by solar irradiation is an important natural elimination process, we evaluated the behaviour of the selected benzophenones exposed to natural sunlight. Results confirmed low photostability of ketoprofen, while UV filters are more stable, which is in agreement with their use in sunscreens and other products. The results of photodegradation will provide a better understanding of the cycling and fate of these compounds in the environment.

MEDNARODNA PODIPLOMSKA ŠOLA JOŽEFA STEFANA

JOŽEF STEFAN INTERNATIONAL POSTGRADUATE SCHOOL

BEHAVIOUR OF BENZOPHENONES UNDER THE INFLUENCE OF NATURAL SUNLIGHT

Kristina Pestotnik, mag. farm.

Supervisor: Assoc. Prof. Dr. Ester Heath
Co-supervisor: Dr. Tina Kosjek

Jožef Stefan International Postgraduate School (Ecotechnology)
Jožef Stefan Institute, Department of Environmental Sciences, Ljubljana, Slovenia

INTRODUCTION

This study evaluates photolytic behaviour of benzophenone derived pharmaceuticals and personal care products (PPCPs) including a pharmaceutical ketoprofen (KP), its phototransformation products (EtBP, AcBP) and UV filters (BP, H-BP, HM-BP, DH-BP, DHM-BP). Since photodegradation may be of great significance in the natural elimination process of organic compounds, we have evaluated the behaviour of these compounds under the influence of natural sunlight.

METHODS and MATERIALS

spiked aqueous sample
↓
solar irradiation
↓
Solid Phase Extraction (SPE)
↓
derivatization
↓
GC/MSD

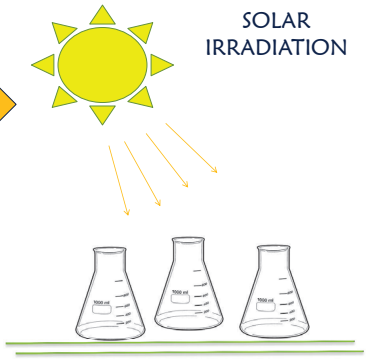

CHEMICAL STRUCTURES OF THE STUDIED BENZOPHENONES

Compound	Abbreviation	Chemical structure
benzophenone	BP	
3-ethyl-benzophenone	EtBP	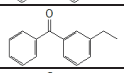
3-acetyl-benzophenone	AcBP	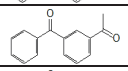
ketoprofen	KP	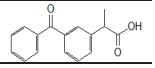
4-hydroxy-benzophenone	H-BP	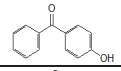
2,4-dihydroxy-benzophenone	DH-BP	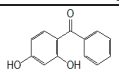
2-hydroxy-4-methoxy-benzophenone	HM-BP	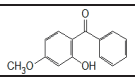
2,2'-dihydroxy-4-methoxy- benzophenone	DHM-BP	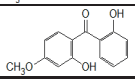

RESULTS

- **photostability:**
  DHM-BP > H-BP > HM-BP > BP > DH-BP > AcBP > EtBP > KP

- **KP:**
  1 day of irradiation:
  > 99.9 % degradation

- **EtBP:**
  1 week of irradiation:
  > 99.9 % degradation

- **H-BP, HM-BP, DHM-BP:**
  2 weeks of irradiation: no degradation
  4 weeks of irradiation: removal –
  41 % (H-BP),
  43 % (HM-BP),
  38 % (DHM-BP)

- **BP, AcBP, DH-BP:**
  pseudo-first-order kinetics
  BP: $k=0.0523\ days^{-1}$, $t_{1/2}= 13.25$ days
  AcBP: $k=0.0534\ days^{-1}$, $t_{1/2}= 12.98$ days
  DH-BP: $k=0.0561\ days^{-1}$, $t_{1/2}= 12.36$ days

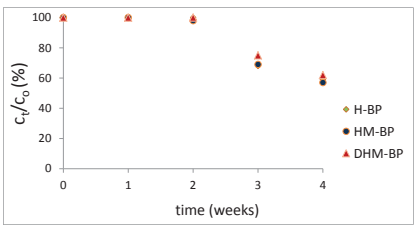

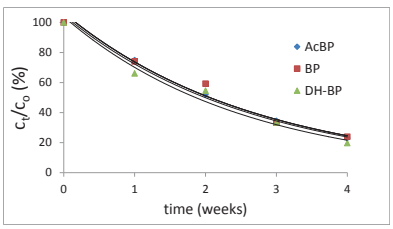

FURHER WORK

- Evaluation of the influence of different matrices on photodegradation of benzophenones
- Evaluation of various environmental processes (e.g. adsorption and biological degradation) that determine the fate and behaviour of benzophenone based PPCPs in the environment

Acknowledgements

The work was financially supported by the European Union (European Social Fund) and by the Slovenian Research Agency (Program Group P1-0143).

Investing in your future
Operation part financed by the European Union
European Social Fund

Stability of mercury compounds at high temperatures

Matej Sedlar[1,3], Majda Pavlin[2,3], Sani Bašič[1], Milena Horvat[2,3]

[1] Esotech, d.d.

[2] Department of Environmental Sciences, Jožef Stefan Institute, Ljubljana, Slovenia

[3] Jožef Stefan International Postgraduate School, Ljubljana, Slovenia

milena.horvat@ijs.si

The aim of this study was to calibrate a method for temperature fractionation which would provide an understanding of the chemical reactions of different mercury compounds at elevated temperatures. This would serve as a comparison to other solid samples that contain different mercury compounds, and be applicable to pyrolysis processes involving flue gases and release and trapping of mercury at high temperatures.

The experiments conducted showed that many factors, such as the type of carrier gas, the substrate and the heating rate, affect the release of mercury. These effects can be seen in the temperature of mercury release and in the number of peaks. Our findings raise questions about the decomposition of complex matrices releasing mercury and their temperature comparability with pure mercury compounds.

Further fractionation experiments will include mixtures of mercury compounds with different substrates, designed to resemble complex matrices for which temperature fractionation may provide useful information (for example coal, gypsum, limestone, and materials used for adsorption at higher temperatures). We shall also further investigate the potential of the method for separation and quantification of different mercury compounds (or fractions) present in solid materials, especially coal.

Stability of mercury compounds at high temperatures

Matej Sedlar, Majda Pavlin, Sani Bašič, Milena Horvat
Study programme: Ecotechnology
Supervision: prof. dr. Milena Horvat
Jožef Stefan Institute, Jamova 39, 1000 Ljubljana
Jožef Stefan International postgraduate school, Jamova 39, 1000 Ljubljana

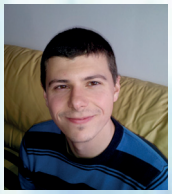

INTRODUCTION

What is the temperature fractionation of different mercury species applicable for?

- **to determine the release temperatures of different mercury compounds in solid samples (e.g. coal),**
- **to develop more efficient mercury removal technologies at high temperatures,**
- **to understand the complexity of mercury reactions in cement-producing industry.**

For developing the method of temperature fractionation, a home-made apparatus was used, in which known mercury compounds, pure or mixed with SiO_2, were heated by a slow increase of temperature (approximately 2.2 °C min^{-1}) to 800 °C in a flow of either nitrogen or air. Released elemental mercury was detected by an atomic absorption spectrometry technique. The results showed that not only the type of carrier gas, but also the substrate affected the number and size of the peaks and the temperature at which elemental mercury was released.

Method – Pyrolytic technique:

- Measuring apparatus: Lumex Pyro RA-915+ detection by cold vapour atomic absorption spectrometer (CVAAS) with Zeeman background correction,
- Temperature range: From room temperature to 800 °C,
- Heating rate: ~ 2.2 °C min^{-1},
- Carrier gas: Nitrogen or Air,
- Gas flow rate: 1 L min^{-1},

Sample:

- 9 mercury substances were used (**Hg_2Cl_2, $HgCl_2$, HgS, Hg_2SO_4, $HgSO_4$, HgF_2, HgSe, HgO-red and HgO-yellow**),
- Pure compounds,
- Compounds mixed with SiO_2 powder,
- Sample mass: 9 – 30 mg.

Fig. 1: HgS, pure and mixed with substrate in nitrogen

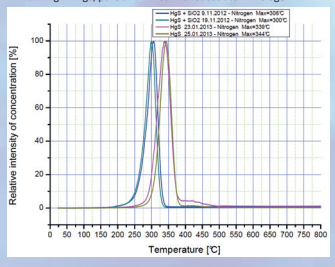

Fig. 2: HgF_2 pure and mixed with substrate in nitrogen

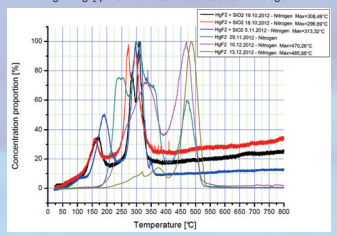

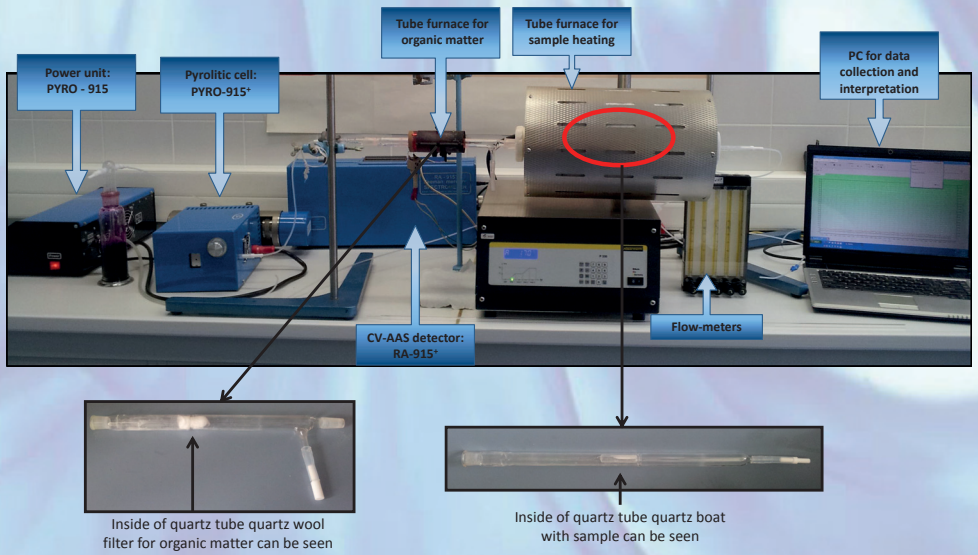

Inside of quartz tube quartz wool filter for organic matter can be seen

Inside of quartz tube quartz boat with sample can be seen

Fig. 4: HgSe pure and mixed with substrate in air

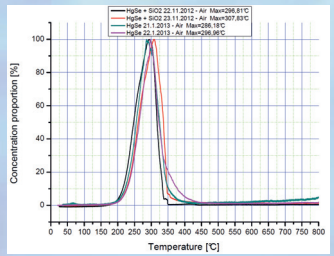

Fig. 3: HgSe pure and mixed with substrate in nitrogen

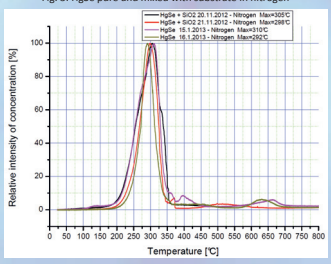

Results:

- Thermograms with one peak: HgS, Hg_2Cl_2, $HgCl_2$, HgO-red and HgO-yellow (Fig. 1),
- Thermograms with multiple peaks: HgF_2, Hg_2SO_4 and $HgSO_4$(Fig. 2),
- Thermogram of $HgSO_4$ is a single peak compound when used as a pure substance, but shows multiple peaks, when it is mixed with substrate SiO_2,
- Carrier gas effects the number of peaks and the temperature at which maximums occur,
- Substrate effects the mercury release for all compounds except for HgSe (Fig. 3, 4),
- The achieved repeatability of the maximum peak is below 15 degrees range.

Future work:

- Other substrates will be used such as: $CaSO_4$, Al_2O_3, charcoal and coal.
- Other pure mercury compounds as well as mixtures of them will be examined.

References:

- H. Biester and C. Scholz. Determination of Mercury Binding Forms in Contaminated Soils: Mercury Pyrolysis versus Sequential Extractions. Environ. Sci. Technol., 31:233–239, 1997,
- G. Luo, et al.. Identifying modes of occurrence of mercury in coal by temperature programmed pyrolysis. Proceedings of the Combustion Institute, 33:2763–2769, 2011,
- M. A. Lopez-Anton, et al.. Analysis of mercury species present during coal combustion by thermal desorption. Fuel, 89:629–634, 2010.

Molybdenum coordination compounds as precursors for the preparation of MoS_2

Gleb Veryasov[1], **Adolf Jesih**[1]

[1] Department of Inorganic Chemistry and Technology, Jožef Stefan Institute, Ljubljana, Slovenia

gleb.veryasov@ijs.si

Molybdenum materials and especially molybdenum disulphide, MoS_2, are widely applied in petroleum refraction and as lubricants in machines. The main advantage of this material is its stability against sulphur poisoning which diminish catalysts activity and is a serious industrial problem. However, just a small part in MoS_2 structure (it has layered structure) has catalytic activity, which results in low activity due to small amount of active sites.

Current work aims improvement of the catalytic activity of MoS_2 within new approaches of preparation.

MEDNARODNA PODIPLOMSKA ŠOLA JOŽEFA STEFANA

JOŽEF STEFAN INTERNATIONAL POSTGRADUATE SCHOOL

Molybdenum coordination compounds as precursors for preparation of MoS_2

Gleb Veryasov, univ. dipl. kem.
Študijski program: EKO-3,
Mednarodna podiplomska šola Jožefa Stefana
MENTOR: doc. dr. Adolf Jesih
SOMENTOR: doc. dr. Maja Ponikvar-Svet
Inštitut Jožef Stefan, Jamova cesta 39, 1000 Ljubljana

Abstract. New approach for preparation of molybdenum sulphides was explored. Application of coordination molybdenum compounds, e.g. $Mo(CO)_4$bipy, $Mo(CO)_3$Toluene, $Mo(CO)_5$pyrrolidine, $[Mo(CO)_5]_2$piperazine and $Mo(CO)_4$piperidine$_2$ for synthesis of MoS_2 provides active materials with different morphologies and surface areas. Sulphidization under different temperatures allowed to obtain sulphides with surface area up to 40 m^2/g, which is very high value in comparison to literature data on unsupported MoS_2 catalysts. Sulphides with highest surface areas were chosen for catalytic activity tests in methanation and hydrogenation reactions.

Table 1. Specific surface areas of sulphides obtained

Starting material	Specific surface area/ m^2g^{-1}
$Mo(CO)_3$Toluene	4
$[Mo(CO)_5]$piperazine	39
$Mo(CO)_4$piperidine$_2$	7
$Mo(CO)_4$bipy (800°C)	38

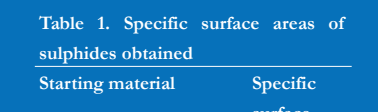

$Mo(CO)_4$piperidine$_2$

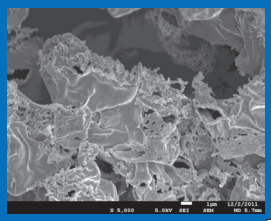

$Mo(CO)_4$piperidine$_2$ gives layered structure with a number of empty space in-between of layers

$Mo(CO)_4$bipy

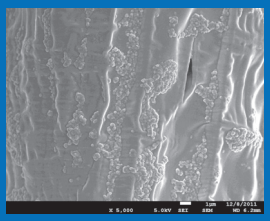

$Mo(CO)_4$bipy formed a very strong interconnected fibers of MoS_2, however, the sample prepared at 800° contained carbon

$[Mo(CO)_5]_2$piperazine

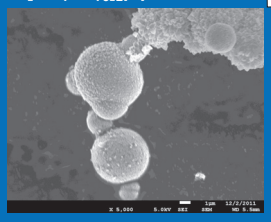

$[Mo(CO)_5]$piperazine form ball-like structure with empty space inside the spheres

$Mo(CO)_5$pyrrolidine

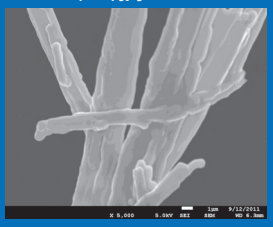

$Mo(CO)_5$pyrrolidine is an extremely sensitive compound, yield of sulphidization was very low, so that we were not able to measure surface area on the sample obtained

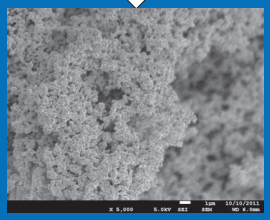

$Mo(CO)_3$Toluene

Sulphide, obtained from $Mo(CO)_3$Toluene form developed and rough structure with surface area of 4 m^2/g. Sulphidization of $[Mo(CO)_5]_2$piperazine leads to formation of ball-like MoS_2 with a micron size and with the biggest surface area out of the group of sulphides investigated

Simulation of *mer*-[$MoBr_3Py_3$] Raman spectrum by DFT method

Gleb Veryasov[1], **Dmitry Morozov**[2], **Adolf Jesih**[1]

[1] Department of Inorganic Chemistry and Technology, Jožef Stefan Institute, Ljubljana, Slovenia

[2] University of Jyväskylä, Department of Chemistry & Nanoscience Center, Finland, Jyväskylä

gleb.veryasov@ijs.si

Molybdenum materials and especially molybdenum disulphide, MoS_2, are widely applied in petroleum refraction and as lubricants in machines. The main advantage of this material is its stability against sulphur poisoning which diminish catalysts activity and is a serious industrial problem. However, just a small part in MoS_2 structure (it has layered structure) has catalytic activity, which results in low activity due to small amount of active sites.

Current work aims improvement of the catalytic activity of MoS_2 within new approaches of preparation.

MEDNARODNA PODIPLOMSKA ŠOLA JOŽEFA STEFANA

JOŽEF STEFAN INTERNATIONAL POSTGRADUATE SCHOOL

Simulation of *mer*-[$MoBr_3Py_3$] Raman spectrum by DFT method

Gleb Veryasov, univ. dipl. kem.
Študijski program: EKO-3,
Mednarodna podiplomska šola Jožefa Stefana
MENTOR: doc. dr. Adolf Jesih
SOMENTOR: doc. dr. Maja Ponikvar-Svet
Inštitut Jožef Stefan, Jamova cesta 39, 1000 Ljubljana

Abstract. We applied DFT method to simulate *mer*-[$MoBr_3Py_3$] Raman spectrum, using B3LYP functional, cc-PVDZ basis set and pseudo potentials for bromine and molybdenum atoms to take into consideration relativistic effects of heavy atoms; simulated Raman spectrum is compared to the recorded spectrum

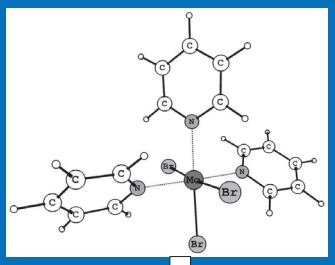

GAMESS(US) program packgage was used. Computation was done within DFT/B3LYP/cc-PVDZ method.

Step 1. Geometry optimization

Step 2. Hessian calculation

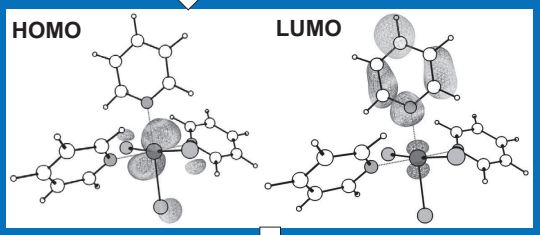

Step 3. Raman activities calculation & recalculation of activities to intensities

Table 1. Bands appeared in spectra below 500 cm^{-1} with assignments

Computed		Experimental		
Raman shift, cm^{-1}	I, rel.	Raman shift, cm^{-1}	I, rel.	Assignments
102	0.15	104	0.03	Py wagging
106	0.03	119	0.19	Py wagging
149	0.08	149	0.01	Py wagging
152	0.01			Py wagging
154	0.07			Py wagging
162	0.11	163	0.07	Py wagging
165	0.07			Mo-N stretching
171	0.03			Mo-Br stretch & Py wagging
176	0.14	176	0.03	Mo-N breathing
184	0.07	188	0.07	Py wagging
195	0.04	194	0.09	Py wagging
264	0.17	258	0.04	Mo-N stretching
276	0.08			Mo-Br stretching
388	0.01			oop ring deformation
393	0.01	396	0.01	oop ring deformation
438	0.00			oop ring deformation
439	0.01	440	0.01	oop ring deformation

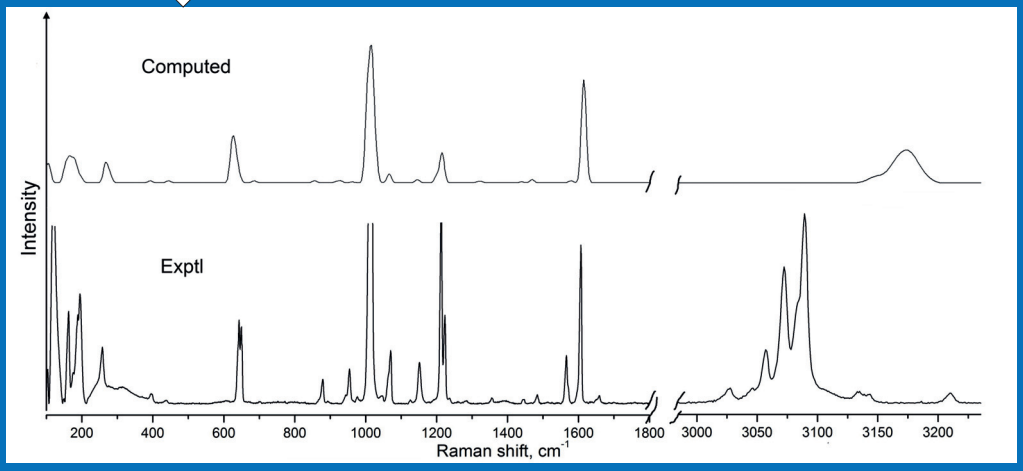

Conclusions. We simulated Raman spectrum of mer-[$MoBr_3Py_3$] using DFT/B3LYP/cc-PVDZ method with pseudo potentials on molybdenum and bromine atoms. Computed spectrum was found to be in good corellation with experimental one. Band assignment was performed.

Karakterizacija mleka in sira z uporabo stabilnih izotopov lahkih elementov (C, N in O) v Sloveniji

(prispevek dodiplomske študentke)

Urša Vezjak, Kanduč Tjaša[1], Nives Ogrinc[1]

[1] Odsek za znanosti o okolju, Institut "Jožef Stefan", Ljubljana, Slovenija

nives.ogrinc@ijs.si

Rezultati raziskav podpirajo razvoj sistema za monitoring prehrambenih proizvodov in razvoj metod za izvajanje kontrole živil. Z možnostjo dokazovanja avtentičnosti mleka in mlečnih izdelkov v prehrambenih izdelkih bodo pristojni organi zaščitili in zavarovali kakovost teh proizvodov hkrati pa tudi zaščitili potrošnika pred morebitnimi potvorbami.

Karakterizacija mleka in sira z uporabo stabilnih izotopov lahkih elementov (C, N in O) v Sloveniji

Urša Vezjak, Kanduč Tjaša, Nives Ogrinc
Odsek za znanosti o okolju, Institut "Jožef Stefan", Ljubljana, Slovenija

Mleko in mlečni izdelki predstavljajo pomemben del vsakdanje prehrane. V Sloveniji uživamo predvsem kravje mleko in sir, v manjši meri pa tudi kozje in ovčje mleko in proizvode iz njih, vendar so ti cenovno dražji in bolj podvrženi različnim potvorbam. Masna spektrometrija za analizo izotopov lahkih elementov (IRMS), ki temelji na meritvah vsebnosti stabilnih izotopov proizvoda ali specifične komponente proizvoda, je ena izmed najbolj inovativnih tehnik za opisovanje in nadzor kakovosti in pristnosti proizvodov, hrane in tudi mleka in mlečnih izdelkov. Z analizo relativne izotopske sestave ogljika, dušika in kisika v mleku in mlečnih izdelkih lahko sklepamo na prehrano živali [1, 2], okoljske pogoje [3, 4] in geografsko poreklo [1, 5].

Glavni namen predlaganega dela je vzpostaviti bazo podatkov o izotopski sestavi pristnega, slovenskega mleka, s pomočjo katere bomo lahko določili potvorjenost mleka in s tem zaščitili potrošnika in dobro ime slovenske mlekarske industrije. Pri tem smo se osredotočili na vzorce kravjega, ovčjega in kozjega mleka in sirov iz različnih geografskih področij v Sloveniji in ugotavljali vpliv klimatskih in področnih razlik na izotopsko sestavo mleka.

Vzorčevanje:

Mesečno zbiranje vzorce nehomogeniziranega mleka.
Analizirali smo 31 vzorcev kravjega mleka iz meseca marca, junija, septembra ter 43 decembrskih vzorcev v letu 2012. Obdobje laktacije pri ovcah in kozah je sezonsko, zato je analiza potekala na 75 vzorcih v maju, juniju in juliju ter na 25 vzorcih sira iz maja 2012.

Analize:

- meritve izotopske sestave kisika v mleku in vodi
- meritve izotopske sestave C in N v kazeinu v mleku in siru

Meritve so bile izveden na masnem spektrometru za analitiko stabilnih izotopov lahkih elementov s preparacijskim nastavkom ANCA-SL za trdne in tekoče vzorce.

Izotopsko sestavo oziroma razmerje med težjim in lažjim izotopom v spojini izražamo z vrednostjo-δ, ki predstavlja relativno razliko izotopske sestave raziskovanega vzorca (vz) glede na izbrani standard (st), in jo izražamo v promilih (‰):

$$\delta A = [(R_{vz} - R_{st})/R_{st}] \cdot 1000$$

A težji izotop elementa (^{13}C, ^{15}N, ^{18}O)
R razmerje med izotopi ($^{13}C/^{12}C$, $^{15}N/^{14}N$, $^{18}O/^{16}O$) v vzorcu (vz) in standardu (st).

Za ogljik je privzet karbonatni standard fosila Belemnitelle Americana iz kredne formacije PeeDee v Južni Karolini (PDB - Pee Dee Belemnite), za dušik zračni dušik (AIR), za kisik pa je privzet standard povprečne morske vode (SMOW - Standard Mean Ocean Water) na globini enega metra pri temperaturi 25 ° C.

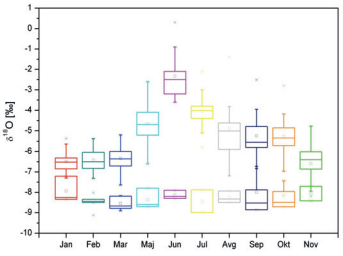

Spreminjanje izotopske sestave kisika v podzemni vodi in v mleku. Izotopska sestava mleka je v povprečju za 2 ‰ višja od sestave podzemne vode. Velikost obogatitve s težjim ^{18}O izotopom glede na podzemno vodo je posledica metabolizma krave, ki se sezonsko spreminja in prehranjevalnih navad. Podrobnejša razlaga rezultatov bo možna, po daljšem vzorčevalnem obdobju.

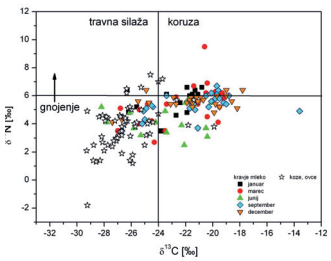

Spreminjanje izotopske sestave ogljika in dušika v kazeinu izoliranem iz mleka. $\delta^{13}C$ vrednosti, ki so višje od -24 ‰ nakazujejo pretežni del prehranjevanja s koruzo. $\delta^{15}N$ vrednosti, ki so višje od 6 ‰ nakazujejo uporabo organskih gnojil pri pridelavi hrane oziroma pri gnojenju pašnika.

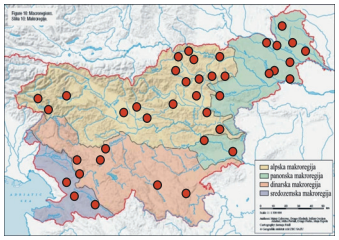

Vzorčevalna mesta

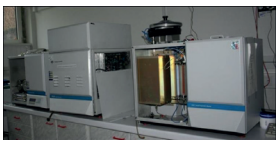

IRMS z ANCA-SL preparacijskim sistemom

Rezultati raziskav podpirajo razvoj sistema za monitoring prehrambenih proizvodov in razvoj metod za izvajanje kontrole živil. Z možnostjo dokazovanja avtentičnosti mleka in mlečnih izdelkov v prehrambenih izdelkih bodo pristojni organi zaščitili in zavarovali kakovost teh proizvodov hkrati pa tudi zaščitili potrošnika pred morebitnimi potvorbami.

Delo poteka v okviru CRP projekta V4-1108 z naslovom »Uporaba specifičnih metod za ugotavljanje in preprečevanje potvorb mleka in mlečnih izdelkov«, ki ga financirata Slovenska raziskovalna agencija (ARRS) in Ministrstvo za kmetijstvo in okolje (MKO).

Zahvaljujemo se Ljubljanskim mlekarnam, d.d., Pomurskim mlekarnam, d.d., Mlekarni Vipava d.d. in Mlekarna Planika predelava mleka d.o.o. in mlekarni Celeia za redno, mesečno dostavo vzorcev slovenskega mleka in podzemnih vod. Prav tako se zahvaljujemo Kmetijskemu gozdarskemu zavodu Nova Gorica za vzorčevanje kozjega in ovčjega mleka.

Literatura
[1] L. Bontempo in sod. *International Dairy Journal*, 23: 99-104, 2012.
[2] F. Camin in sod. *Rapid communications in mass spectrometry*, 22: 1690-1696, 2008.
[3] F. Camin in sod. *Journal of Agricultural and Food Chemistry*, 52: 6592-6601, 2004.
[4] R. Crittenden in sod. *International Dairy Journal*, 17: 421-428, 2007.
[5] L.A. Chesson in sod. *Journal of Agricultural and Food Chemistry*, 58: 2358-2363, 2010.
[6] F. Camin in sod. *Analytica Chimica Acta*, 711: 54-59, 2012.

Fatty acid composition as a tool for determination of geographical origin and authenticity of milk and dairy products

(undergraduate student contribution)

Adrián Vicent[1], Marinka Petrišič[1], Marijan Nečemer[2], Nives Ogrinc[1,*]

[1] Department of Environmental Sciences and [2]Department of Low and Medium Energy Physics, Jožef Stefan Institute, Ljubljana, Slovenia

* nives.ogrinc@ijs.si

Food authenticity and traceability of origin have been given high priority in the recent years. Due to their high nutrient content milk and dairy products represent an important part in the healthy balanced diet. As they are in considerable demand and relatively expensive, they are vulnerable to adulteration or false denomination. Strategies to detect adulteration include also fatty acid composition. Information available through this research should be used to increase the transparency of milk and dairy products supply chain and provide information related to authenticity.

MEDNARODNA PODIPLOMSKA ŠOLA JOŽEFA STEFANA

JOŽEF STEFAN INTERNATIONAL POSTGRADUATE SCHOOL

Fatty Acid composition as a tool for determination of geographical origin and authenticity of milk and dairy products

Adrián Vicent[1], Marinka Petrišič[1], Marijan Nečemer[2], Nives Ogrinc[1,*]
[1] Department of Environmental Sciences
[2]Department of Low and Medium Energy Physics, Jožef Stefan Institute, Ljubljana, Slovenia
*nives.ogrinc@ijs.si

Dairy products are in considerable high demand; therefore, there is a temptation to economic adulteration on these products. Authenticity and determination of geographical origin of these products are becoming an important issue for providers and consumers [1, 2]. The composition of fatty acids in ruminant's milk depends on the season following the changes in rumen's food [3]

The aim of this work is to determine fatty acid composition of milk and cheese from cow, sheep and goat provided from several farms from different regions of Slovenia, with the purpose to identify patterns that allow us to find differences according to geographical origin for cow's milk; difference between goat, sheep and cow milk; as well as the determination of goat or sheep milk adulteration with cow's milk.

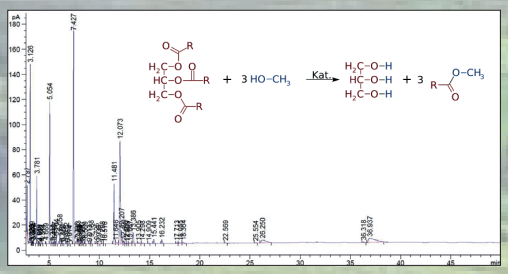

Figure 1: Chromatogram of fatty acids from a milk sample.

Geographical Origin

It was possible to differentiate milk from different geographical origin based on fatty acid composition using LDA (linear discriminant analysis). The separation was high up to 99.7%. The calculation showed that parameters that mainly contributed to the separation were C20:4n-6; C20:3n-6; C17 and C18:3n-3.

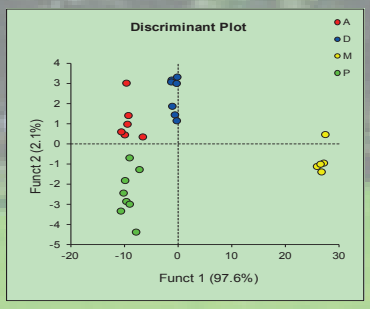

Figure 2: The fatty acid content in cow's milk with respect to geographical origin: A - Alpine, D - Dinaric, M – Mediterranean, P – Pannonia.

Differences between goat, sheep and cow's milk

For the fatty acid content in milk with respect to different animal origin function 1 explained 99.6% of the total variance and function 2 the rest, 0.4%. The calculation showed that parameters that mainly contributed to the separation were C20:0; C10:0; C22:1n9.

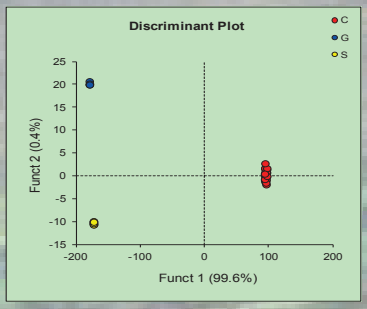

Figure 3: Linear discriminant score plots of fatty acid content in sheep's, goat's and cow's milk with respect to animal origin. (C-cow, G-goat, S-sheep).

Adulteration

The preliminary results of sheep and goat milk with addition of 10, 5, 2,5, 1 and 0,5% of cow milk were analysed with ANOVA and Kruskal–Wallis. In the case of sheep milk only C16:1 (ANOVA) was statistically significant (P - 0,0058) to discriminate adulteration. But other statistical analysis of variance (Levene test) indicated that variance was not homogeneous. In the case of goat milk C11:0 (P - 0.0348), C12:0 (P - 0.0348) and C18:1n9 (P - 0.0348) were statistically significant by Kruskal–Wallis test to discriminate adulteration with cow milk down to 1%. Further investigation is needed.

Conclusions

The present study represents the first report on the fatty acid composition with respect to the geographical origin. It was found that the month of production also influenced the composition of fatty acids in cow milk. Thus, it is important to determine fatty acid composition at least two times per year in summer and winter. The adulteration of sheep and goat milk with cow milk needs to be further investigated.

Information available through this research should be used to increase the transparency of milk and dairy products supply chain and provide information related to authenticity.

Acknowledgements
The work was performed within the project V4-1108 entitled "The use of specific methods for determination and prevention of adulteration of milk and dairy products" financially supported by Slovenian Research Agency and Ministry of Agriculture and the Environment. We thank Ljubljanske mlekarne, d.d., Pomurske mlekarne, d.d., Mlekarna Vipava d.d., Mlekarna Planika predelava mleka d.o.o. and Mlekarna Celeia for supplying monthly cow samples and Kmetijski gozdarski zavod Nova Gorica for supplying goat and sheep milk.The research was additionally supported by Leonardo da Vinci ADEIT program by the grant given to A. Vicent.

References.
[1] M.J. DENNIS; *Recent developments in food authentication*. Analyst 123 (1998) 151R-156R
[2] D.C.E. ROBERTS; *Food Authenticity*. British Food Journal, Vol.96 No.9 (1994) pp.33-35
[3] V. STIBILJ, M. K. RAJŠP; *Determination of fatty acids composition of winter consumer and UHT milk samples in Slovenia*.Biotehniškefak.V Ljubljani.Kmetijstvo.Zootehnika, 70 (1997)

Uporaba izotopov pri raziskavah podzemnih vod

Janja Vrzel[1,3], **Nives Ogrinc**[2,3]

[1] Institut za ekološki inženiring d.o.o., Maribor, Slovenija

[2] Odsek za znanosti o okolju, Institut Jožef Stefan, Ljubljana, Slovenija

[3] Mednarodna podiplomska šola Jožefa Stefana, Ljubljana, Slovenija

janja.vrzel@iei.si, nives.ogrinc@ijs.si

V naravi obstajata dve vrsti izotopov, stabilni in radioaktivni. V hidrologiji največ uporabljamo stabilne izotope lahkih elementov H, O, C, N in S, od radioaktivnih pa ^{3}H, ^{14}C, ^{36}Cl in ^{81}Kr. Vrednosti $\delta^{2}H$ in $\delta^{18}O$ v padavinah so namreč karakteristične glede na zemljepisno širino, oddaljenost od morja, nadmorsko višino in letni čas [5]. Na drugi strani nam izotopska sestava dušika ($\delta^{15}N$) in žvepla ($\delta^{34}S$) omogoča določevanje izvorov onesnaženja vodnih virov z nitrati in sulfati [4], ker se izotopske sestave posameznih virov med seboj razlikujejo. Izotopska sestava ogljika ($\delta^{13}C$) pa nam pomaga pri raziskavah kroženja ogljika, določanja njegovih izvorov in nastanka metana.

Pri proučevanju vodnih sistemov so prav tako nepogrešljivi podatki, ki jih dobimo z analizo radioaktivnih izotopov. Ti nosijo informacije o starosti vode, kar pa omogoči oceno ranljivosti vodonosnika.

Z raziskavami na Ljubljanskem polju, smo določili izotopsko sestavo in starost podzemnih in površinskih voda, kar je omogočilo locirane napajalnega območja tega vodonosnika. S tem smo pripomogli k boljšemu razumevanju nastanka podzemne vode, njene dinamike in ranljivosti zaradi onesnaženja.

UPORABA IZOTOPOV PRI RAZISKAVAH PODZEMNIH VOD

Janja VRZEL[1,2], Nives OGRINC[2,3]

[1]Institut za ekološki inženiring d.o.o., 2000 Maribor
[2]Mednarodna podiplomska šola Jožefa Stefana, študijski program Ekotehnologija
[3]Institut "Jožef Stefan", 1000 Ljubljana

TEORIJA

Na Zemlji je 70 % vode.

2,5 % pitne vode za več kot 7 milijard ljudi.

Slika1 in 2: Vira: http://www.123rf.com/ (levo) in http://www.deltadentalarblog.com/ (desno).

Vsakodnevna skrb za pitno vodo!

IZOTOPI omogočajo reševanje hidrogeoloških problemov.

RADIOAKTIVNI IZOTOPI

^{3}H, $^{3}H/^{3}He$, ^{14}C, ^{81}Kr, ^{36}Cl

Določanje starosti vode.

STABILNI IZOTOPI

FRAKCIONACIJA

Je proces, tekom katerega se spremeni izotopska sestava neke snovi (npr.: vode).

$\delta^{15}N$ (v NO_3^-), **$\delta^{34}S$** (v SO_4^{2-}) in **$\delta^{13}C$** (v CH_4) analize se uporabljajo predvsem za določevanje onesnaženja vodnih virov.

$\delta^{2}H$ in **$\delta^{18}O$** vrednosti so karakteristične glede na:
-zemljepisno širino,
-oddaljenost od morja,
-nadmorsko višino,
-letni čas.

Zato omogočajo določevanje:
-izvora vode,
-napajalnega območja,
-hidrodinamike,
-odnosa podzemne vode in površinske vode ter
-ranljivosti vodonosnika.

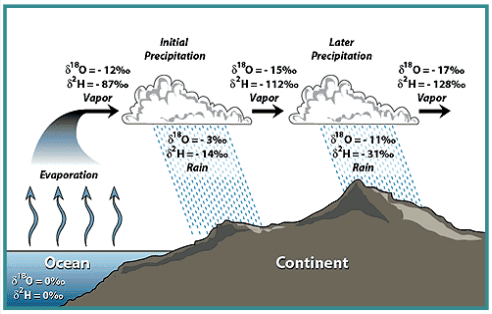

Slika 3: Skica spreminjanja izotopske sestave atmosferske vlage in padavin na poti proti notranjosti kontinenta (Vir: http://www.gns.cri.nz).

PRIMER TOVRSTNIH ANALIZ – Ljubljansko polje

Predmet raziskav: ugotoviti odnos med površinskimi in podzemnimi vodami. Zato smo določili:
- izotopsko sestavo podzemne vode, padavin in vode v reki Savi ter
- starost vode.

VZORČENJE IN ANALIZA

Vzorčenja so potekala na štirih lokacijah (Kleče, Hrastje, Jarški prod in Brest) v obdobju 2010–2011 (Slika 6).

Narejene so bile naslednje izotopske analize: $\delta^{2}H$ in $\delta^{18}O$ v vodi, $\delta^{15}N$ in $\delta^{18}O$ v nitratu ter ^{3}H in $^{3}H/^{3}He$.

REZULTATI IN INTERPRETACIJA

$\delta^{2}H$ in $\delta^{18}O$ analize so pokazale, da vodonosnik napajata dva različna vira, največji delež vode prispevajo padavinske, nekoliko manj pa je prisotno vode iz reke Save.

Rezultati $\delta^{15}N$ in $\delta^{18}O$ v nitratih (Slika 5):
- Najbolj onesnažena podzemna voda je v Hrastju.
- Najbolj ranljivo območje je Jarški Prod.

Rezultati $^{3}H/^{3}He$ analiz dajejo starost vode:
- Kleče → 10 % vode je stare 1.000–10.000 let;
- Hrastje → 8–7 let;
- Jarški Prod → 2–7 let (najbolj ranljivo območje);
- Brest → 40 let (najmanj ranljivo območje).

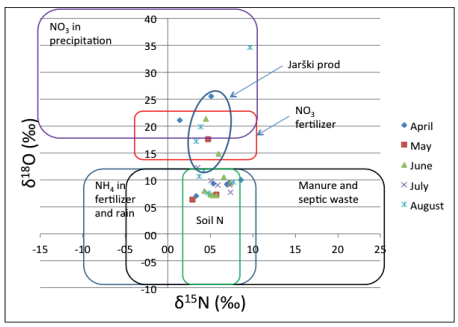

Slika 5: Odnos med izotopsko sestavo $\delta^{18}O$ in $\delta^{15}N$ v nitratu.

Slika 6: Karta Ljubljanskih vodarn z vzorčnimi lokacijami.

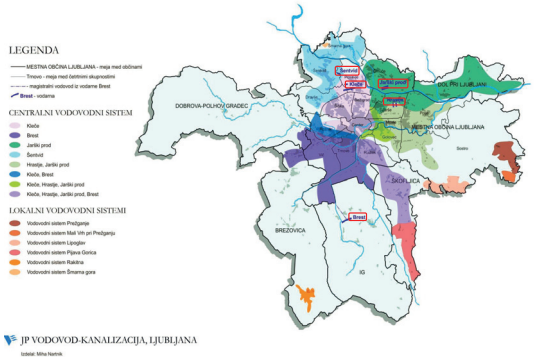

Informacijske in komunikacijske tehnologije (Information and Communication Technologies)

Sensor as a Service using the VESNA Sensor Platform

Adnan Bekan[1,2], **Carolina Fortuna**[1], **Matevž Vučnik**[1,2], **Mihael Mohorčič**[1,2]
[1] Department of E6, Jožef Stefan Institute, Ljubljana, Slovenia
[2] Jožef Stefan International Postgraduate School, Ljubljana, Slovenia
adnan.bekan@ijs.si, carolina.fortuna@ijs.si,
matevz.vucnik@ijs.si, miha.mohorcic@ijs.si

A wireless sensor platform is the basic building block of sensor network and it typically hosts a microprocessor, one or more sensors and a communication module. A sensor platform is thus capable to measure a physical quantity, perform some processing and communicate with other nodes in the network and with remote servers in the Internet using wireless technologies.

In our system, we are using a sensor platform called VESNA. VESNA is a modular platform for wireless sensor networks developed at the SensorLab, Jožef Stefan Institute, Slovenia. It is suitable both as a development environment as well as a final solution for a large variety of application areas.

Using VESNA in combination with ContikiOS and CoAP allows easy control and invocation of services in the sensor network over the Internet by calling RESTful handlers. The advantage of the CoAP protocol is that it is similar to the HTTP protocol, which allows simple translation and communication between these two protocols.

One advantage of this system architecture is that every node in sensor network has a unique IPv6 address which can be used for interconnection with platforms and sensors. Another advantage of this architecture is that such network can simultaneously handle more users than more primitive types of sensor networks.

MEDNARODNA PODIPLOMSKA ŠOLA JOŽEFA STEFANA

JOŽEF STEFAN INTERNATIONAL POSTGRADUATE SCHOOL

Sensor as a Service using the VESNA Sensor Platform

Adnan Bekan[1,2], Carolina Fortuna[2], Matevž Vučnik[1,2], Mihael Mohorčič[1,2]
ADVISOR: doc. dr. MIHAEL MOHORČIČ
[1]Jožef Stefan International Postgraduate School
Study program: Information and Communication Technologies
[2]Department of Communication Systems, Jožef Stefan Institute, Jamova cesta 39, 1000 Ljubljana

SYSTEM ARCHITECTURE

- This poster introduces system architecture for wireless sensor network supporting direct access to rich meta-data and data.
- The system provides an easy way for discovering, controlling and invoking services from the sensor network.
- Users can interact with the system at high level of abstraction using standards based communication protocols that blends with the existing stack used by the Internet (HTTP/TCP/IP).
- The reference implmentation was built based on a fully modular VESNA sensor node.
- The Internet's protocol stack is converted to the equivalent sensor network stack by low power gateways.

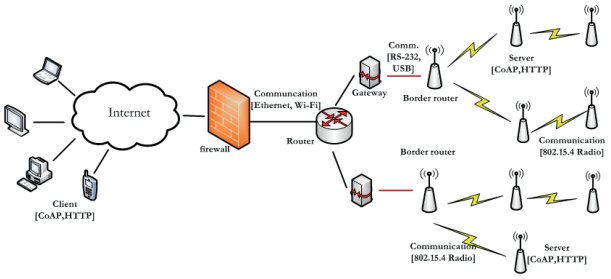

HARDWARE

- Sensor node - VESNA
  - ARM Cortex-M3 32 bit microcontroller with clock up to 72 MHz ,1 MB flash and 96 kB SRAM
  - VESNA supports a variety of interfaces: USB, RS232, UART, IrDA, SPI, I2C, micro SD, 12 bit ADC, DAC.
  - Power supply: Mains, Batteries, Solar cells.

Expansion connectors :

- One designed for radio modules (sub-gigahertz and 2.4 GHz-band transceivers) .
- Other for various purposes.

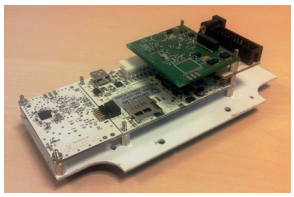

- Gateway – Raspberry Pi
  - 700 MHz ARM processor, 512 MB of RAM
  - Various interfaces: USB, GPIO ,LAN, HDMI, SD card slot
  - Power rating: 700 mA (3.5 W)
  - Power supply: 5volt via MicroUSB or GPIO header

SOFTWARE

Sensor node – VESNA :

- Contiki OS which is a minimalistic operating system intended for low power devices.
- Network stack uIP TCP/IP that supports IPv6 network with the 6LoWPAN and low-power transfer protocol CoAP.

Gateway– Raspberry Pi :

- Raspbian OS is optimized Debian for the Raspberry Pi
- To enable tunneling of IPv6 packets through RS-232 we used tunslip application.

INITIAL EVALUATION OF THE SENSOR NETWORK

- Experimental set-up contains 5 sensor platforms connected in a network that was flooded with 1000 packets per platform, each packet consisting of 32 bytes.

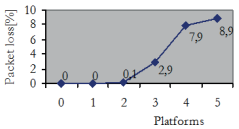

(a) Packet loss

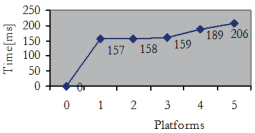

(b) Average time response

- As can be seen, the packet loss grows exponentially with the number of sensor platforms that are added to the experiments while the average response time seems to have a more linear growth.

The authors would like to thank SensorLab for its support.
sensorlab.ijs.si

Estimation of Human Energy Expenditure Using Inertial Sensors and Heart Rate Sensor

Božidara Cvetković[1,2], **Mitja Luštrek**[1,2]

[1] Department of Intelligent Systems, Jožef Stefan Institute, Ljubljana, Slovenia

[2] Jožef Stefan International Postgraduate School, Ljubljana, Slovenia

boza.cvetkovic@ijs.si, mitja.lustrek@ijs.si

Mobile devices are used for almost everything these days from talking and texting to event scheduling, daily life monitoring, finding direction, etc. Two of the reasons for such a fast success of the mobile devices and mobile applications are the embedded sensor and their significant improvement with each new model that appears on the market and availability and ease of development. Average smart phone has a rather powerful processing unit and it comes with variety of sensors, for example global positioning system (GPS), camera, proximity sensor, ambient light sensor, gyroscopic sensor and accelerometer, being the most interesting in terms of analysis of human physical activity, more precisely human energy expenditure which is a focus of this paper.

Over the years, research in medical field has shown that a sufficient amount of physical activity can have a positive impact on one's health and well-being regardless of age and that the physical inactivity is one of the leading causes of death worldwide. Although this is widely accepted as a fact, only small amount of population has regular or sufficient exercise. Key reason for this is the limited time, due to the fast pace of life. If one was able to measure amount of performed physical activity during the regular day and present the difference according to the sufficient physical activity, than this could serve as a motivation for the person to do additional exercise and reach the daily goal. Most importantly, the amount of physical activity can be also used to monitor one's diet, either being healthy individual or someone who suffers from dietary disease. This raises a question; How can we measure the amount of physical activity.

This paper presents a method for estimation of human energy expenditure during normal daily activities as well as sports activities using wearable inertial sensor attached to the person's thigh and chest as well as feasibility analysis of this method to be used as an application on an average smartphone.

MEDNARODNA PODIPLOMSKA ŠOLA JOŽEFA STEFANA

JOŽEF STEFAN INTERNATIONAL POSTGRADUATE SCHOOL

ESTIMATION OF HUMAN ENERGY EXPENDITURE USING INERTIAL SENSORS AND HEART RATE

BOŽIDARA CVETKOVIĆ, B.Sc.
Study Program: Information and Communication Technologies,
Jožef Stefan International Postgraduate School
SUPERVISOR: dr. MITJA LUŠTREK
Jožef Stefan Institute, Jamova cesta 39, 1000 Ljubljana

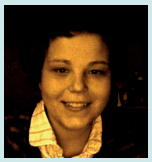

MOTIVATION

- Sufficient amount of physical activity can have a positive impact on one's health and well-being regardless of age
- Lack of regular or sufficient exercise due to limited time because of the fast pace of life

IF ONE COULD MEASURE DAILY PHYSICAL ACTIVITY ONE COULD:

- Know if todays physical activity reached the satisfactory level
- Monitor diet and maintain lifestyle
- Keep disease under control
- ...

HOW CAN WE MEASURE PHYSICAL ACTIVITY WITHOUT COSTLY DEVICES?

- Mobile device such as smartphone + chest-strap (optional)
- ML estimation using regression model

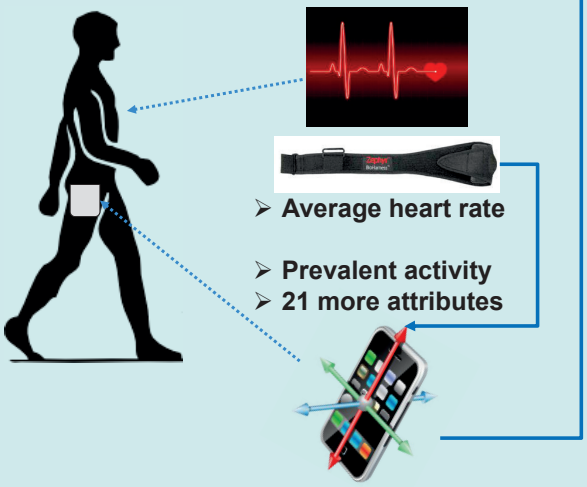

ENERGY EXPENDITURE ESTIMATION

- Train three regression models (23 attributes)

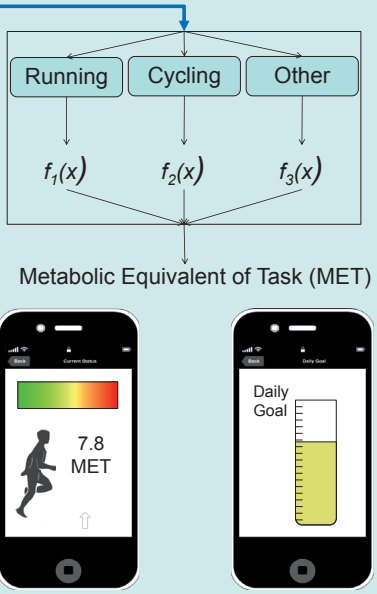

RESULTS (MEAN ABSOLUTE ERROR)

	M5PRules	M5P	REPTree	Linear Regression	MLP	SMOReg
Other activities	0.55	0.54	0.55	0.58	0.86	**0.52**
Running activity	0.94	0.96	1.02	0.98	**0.78**	0.99
Cycling activity	0.78	0.99	0.74	0.98	**0.66**	0.87

CONCLUSION

The paper presents low computational complexity method for estimation of human energy expenditure.
Presented method uses three regression models. Separate model is used for running activity, separate is used for cycling activity; and separate is used for all other activities. The regression models evaluated using leave-one-person-out approach.
Accurate estimation of energy expenditure and its integration into the device that can interact with the user, can have positive impact on quality of life.

Potential Usage of Smartphone Inertial Sensors in Healthcare Applications

Hristijan Gjoreski[1,2], Simon Kozina[1,2], Matjaž Gams[1,2], Mitja Luštrek[1,2]

[1] Department of Intelligent Systems, Jožef Stefan Institute, Ljubljana, Slovenia

[2] Jožef Stefan International Postgraduate School, Ljubljana, Slovenia

hristijan.gjoreski@ijs.si

Production of mobile phones is in constant increase. Currently, more than 85% of the world population owns a mobile phone. This shows that in a very short time, mobile devices will become easily accessible to virtually everybody. In recent years, the number of smartphones, which are a new generation of mobile phones, is in constant increase. In 2012, 1 billion smartphones were in use and this number is expected to be doubled in the next 3 years. Smartphones, in contrast to the basic telephony, are offering many features such as multitasking and the deployment of a variety of sensors: inertial, compass, GPS, light, pressure etc. The intelligent use of these sensors is allowing many potential applications. Recent studies have shown that the body-worn inertial sensors give rich information about the user, which can be used in many healthcare applications: automatic recognition of daily activities, detection of alarming situations (fall), step counters, energy expenditure estimation, etc. The early studies in this area were made using intrusive body-worn sensors and were not applicable for everyday usage. When these sensors were introduced in the smartphones, a whole new era for practical usage was has started. By applying intelligent techniques such as the ones described in this study, any smartphone user can benefit from the rich information that his/hers smartphone sensors can provide. In this paper an idea of transforming the smartphone into a healthcare device capable of recognizing everyday activities and detection of fall events is presented. This approach firstly use inertial sensors data as an input, then the data is preprocessed and segmented and finally, artificial intelligence methods are applied which recognize the user's activity and detect a fall event. If a fall is detected, an appropriate alarm notification can be triggered e.g. an SMS is sent to the user's predefined contacts. This is especially useful for elderly persons who live alone and could be, in the case of fall, stranded for a longer time. In the case of the activity recognition, the recognized activities are logged during the whole day and can be later analyzed. The analysis may contain daily activity statistics, comparison between different days and therefore, detection of health-related anomalies.

MEDNARODNA PODIPLOMSKA ŠOLA JOŽEFA STEFANA

JOŽEF STEFAN INTERNATIONAL POSTGRADUATE SCHOOL

Potential Usage of Smartphone Inertial Sensors in Healthcare Applications

Hristijan Gjoreski, mag. inf. kom. tehnol.

Simon Kozina, univ. dipl. inž. rač. mat.

Study Programme: Information and Communication Technologies,
Jozef Stefan International Postgraduate School
SUPERVISOR: prof. dr. MATJAŽ GAMS
RESEARCH SUPERVISOR: dr. MITJA LUŠTREK
Jozef Stefan Institute, Jamova cesta 39, 1000 Ljubljana

MOTIVATION

Smartphones

- More than 1 billion smartphones are in use.
- Smartphones are equipped with multiple sensors: **inertial**, compass, GPS, light, etc.

Healthcare applications

- Many studies have shown that body-worn inertial sensors give rich information about the user.
- This information can be used in many healthcare applications.

Use the smartphone as a healthcare device for:
recognition of everyday activities & detection of fall events

SMARTPHONE IMPLEMENTATION

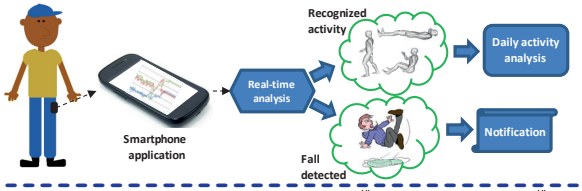

- **Smartphone application**
  - **Input**: inertial sensor data
  - **Data preprocessing**: synchronization, filtering, segmentation
  - **Methodology**: machine learning, context-reasoning, domain rules
  - **Output**: activity, fall detection (notification)

INERTIAL SENSORS

- 3-axis Accelerometer
- 3-axis Gyroscope

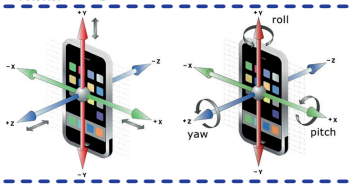

PREPROCESSING

- Sensor data fusion
- Synchronization
- Segmentation
- Filters
  - Low-pass
  - Band-pass

METHODOLOGY

Activity Recognition

- Three layer activity recognition **TriLAR**

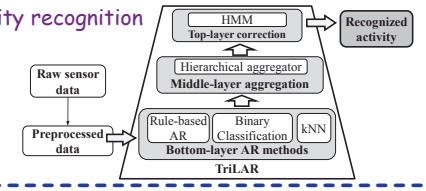

Fall Detection

- **CoFDILS**

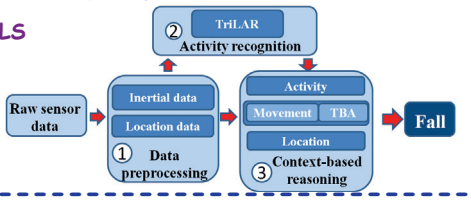

EXPERIMENTS

Activity Recognition

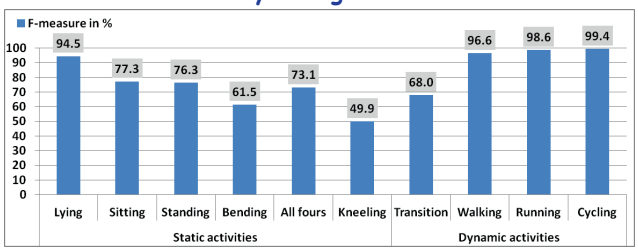

Fall Detection

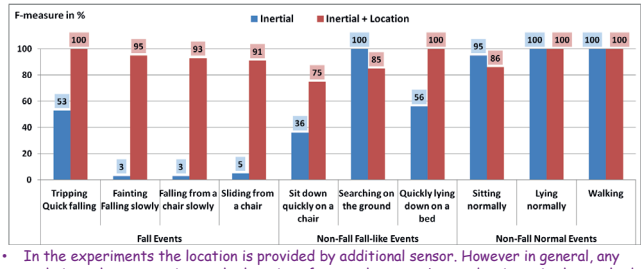

- In the experiments the location is provided by additional sensor. However in general, any technique that can estimate the location of smartphone can be used as input in the method

CONCLUSIONS

- Using the smartphone as a healthcare device: recognizing activities and fall detection.
- The methodology was evaluated on two comprehensive experimental scenarios.
- The results showed that it is possible to achieve satisfactory performance for the activity recognition task using only one inertial sensor, i.e. smartphone. For the fall detection, the location of the smartphone is required for improved performance.

Business simulation game – an innovative pedagogical approach in business environment

Andrej Jerman Blažič[1], **Tanja Arh** [1]

[1] Laboratory for Open Systems and Network, Jožef Stefan Institute, Ljubljana, Slovenia

andrejcek@5.ijs.si, tanja@e5.ijs.si

My research is based on serious games and their innovative approach in lifelong learning processes. As a matter of fact, people tend to absorb more easily information they acquire through interactive channels and while they respond to a challenge in a competitive and entertaining environment. From that viewpoint, game technology can give enhance existing learning approaches and training methodologies. The gaming technology is a vast area and has numerous challenges to be explored in order to support efficient learning and training.

MEDNARODNA PODIPLOMSKA ŠOLA JOŽEFA STEFANA

JOŽEF STEFAN INTERNATIONAL POSTGRADUATE SCHOOL

BUSINESS SIMULATION GAMES

An innovative pedagogical approach in business environment

Mag. Andrej Jerman Blažič
Study programme: Information and communication technologies, Jožef Stefan international postgraduate school
MENTOR: doc. dr. Tanja Arh
Laboratory for Open Systems and Networks, Jožef Stefan Institute, Ljubljana, Slovenia

1. SERIOUS GAMES - BUSINESS SIMULATION GAMES

Serious games are generally held to be applications developed with game technology and design principles having training, situation simulation or education while entertaining the user as a prime purpose. **Business Simulation Games** are games that support training and learning that is focused on management of economic processes. They help to model the realities of the business world by simulating basic – and in some cases advanced – business theories and practices in controlled game environments.
J. P. Gee (2003) stated that business simulation games include a lot of fundamental gaming principles which, combined with a scientific approach from the field of Computer-Supported Collaborative Learning (CSCL), can systematically increase the motivation to learn and teach knowledge of specific subjects.

2. INNOV8 - IBM BUSINESS PROCES MANAGEMENT SIMULATION

The INNOV8 is a role-playing game that simulates Business Process Management (BPM) in a 3D virtual environment. It is used to teach and train business skills to IT people and business professionals. The IBM Self-oriented architecture (SOA) team originally created the game to help educate potential SOA clients dealing with project team leaders. It takes players through the entire lifecycle of discovery, collaboration, optimization, and innovation of a fictional company's business processes.

The INNOV8 v.2 game uses "Second-Life-Like" graphic and virtual characters.

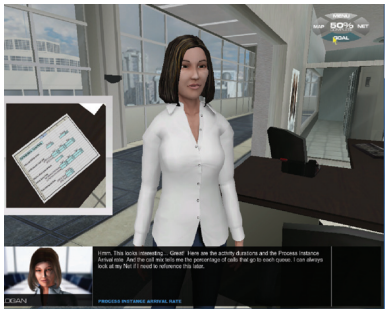

Players collaborate to map out business processes, identify process bottlenecks and explore what-if scenarios.

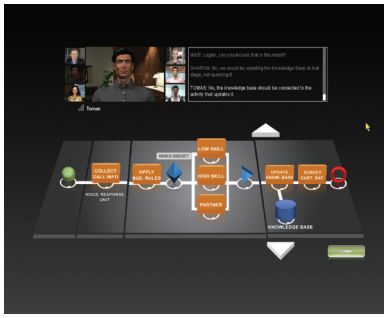

Players use drag-and-drop graphics to advance through the game. Here, players make decisions as they seek more efficient ways to manage a call center and respond to customers.

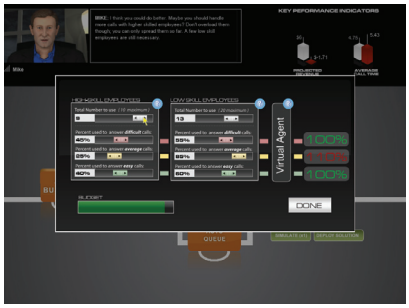

INNOV8 v.2 is available on line:
http://www-01.ibm.com/software/solutions/soa/innov8/index.html

3. WHY BUSINESS SIMULATION GAMES?

Business Simulation Games are tools, they can help us explore and understand issues, and train for various circumstances. They based on the use of the Computer and Internet capabilities and are a reality, they are expected to be the default tool in many areas in the future. They:

- Allow situated learning while offering entertainment of value,
- Merge high engagement and powerful content,
- Trigger profound reflections and permit a rapid understanding of complex environments,
- Allow the users have an active role, thus making them take credit for success, avoiding at the same time a sense of "failure" as they turn mistakes into precious learning elements,
- Help the users accomplish certain goals avoiding the repetitiveness and boredom of a dry, uninspired execution pattern or exercise,
- Show how actions affect context.

4. USAGE IN PRACTICE

According The Apply Group, a research firm, by 2014, between 100 and 135 of the Global Fortune 500 will have adopted gaming for learning, with the US, UK and Germany leading the way.

Several major U.S. companies and IBM business partners are already using the INNOV8 system.

more than 100 universities, including Duquesne University and the University of Southern California, have worked with IBM to add Innov8 to their business school curricula.

Time-window selection for optimal generalization with noise variance reduction in ecological data

Vladimir Kuzmanovski[1,2], **Marko Debeljak**[1,2], **Sašo Džeroski**[1,2,3]

[1] Department of Knowledge Technologies, Jožef Stefan Institute, Ljubljana, Slovenia

[2] Jožef Stefan International Postgraduate School, Ljubljana, Slovenia

[3] Centre of Excellence for Integrated Approaches in Chemistry and Biology of Proteins, Ljubljana, Slovenia

vladimir.kuzmanovski@ijs.si

In this paper we demonstrated an approach for noise reduction implemented in the domain of ecological data. The described approach employed stochastic optimization algorithm, Genetic Algorithm (GA), in order to delimit dataset into subsets by defining time-window that is representative for a time period under consideration. The optimization means finding most optimal solution regarding the defined fitness function. In addition, the term stochastic describes that the process of optimization takes in account the uncertainty by including randomness. The results of case study of La Jaillière (France) experimental site shows that defining time-window and optimizing its length increases the performance of the learned model, which can be used for prediction or classification, by reducing the noise caused by some non-systematic and non-measured variable that influence the value of the target variable over time. Finally, this approach has additional advantages when lazy learning methods for classification and regression will be applied since they are instance-based and don't build a model. Namely, these methods consider the whole training set during prediction. Therefore, the bigger the train dataset is, the longer it lasts.

MEDNARODNA PODIPLOMSKA ŠOLA JOŽEFA STEFANA

JOŽEF STEFAN INTERNATIONAL POSTGRADUATE SCHOOL

Time-window selection for optimal generalization with noise variance reduction in ecological data

Vladimir Kuzmanovski, MSc.

Knowledge Technologies

International Postgraduate School

Jozef Stefan Institute, Jamova cesta 39, 1000 Ljubljana

Mentor: Marko Debeljak

Co-mentor: Sašo Džeroski

Abstract

Due to the imperfect human ability for observing a real world processes, the raw measured environmental data contains unobservable systematic errors that are further transferred as noise in the observed data. In addition, the raw environmental data are never exactly representative of the real world processes that have been observed. On the other hand, for obtaining a quality performance of the analyses of those data, such systematic anomalies or noise need to be explored and considered in a proper way. This poster demonstrats an approach for noise (non-measured systematic error) reduction implemented.

Case-Study

The data we used in our analyses are from the experimental site La Jaillière, run by the technical institute ARVALIS - Institut du Végétal.The site has been dedicated to the study of the influence of agricultural management practices on water quality since 1987. The data were collected for each plot separately for 24 campaigns (1987-2011) All these data are collected in the PCQE (Pratiques Culturales et Qualité des Eaux) database.

	Feature	Description
Input	Field	*Name of the field*
	Campaign	*A campaign is the period from September 1st, and finishes August 31st, following year.*
	Metrological data	*Meteorological data including Rainfall, Evapotranspiration and Temperature*
	Landscape	*Landscape data including Slope and Soil properties*
	Agricultural practices	*Crop rotation, Tillage, Irrigation, Crop protection and Crop development coefficient*
Target	Outflow	*Runoff and Drainage*

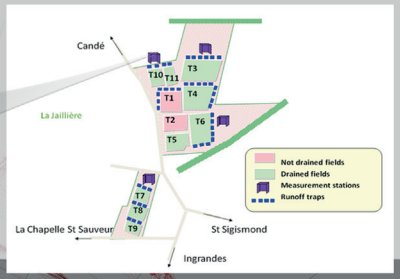

Methodology

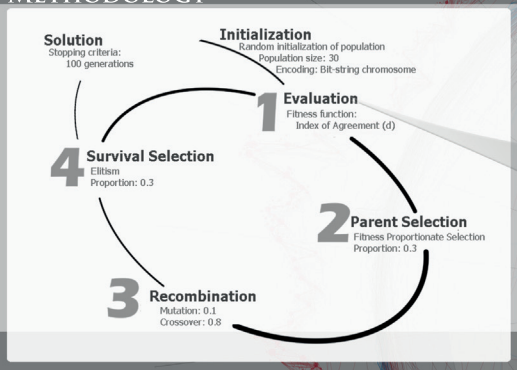

The described approach employed stochastic optimization algorithm for time-window length optimization using Genetic Algorithms.

The evaluation of chromosomes, from the population, converges in solving machine learning problem for accurately predicting outflow of drained water, on a field level, based on input data. The models are learned with M5P algorithm for inducing model trees and evaluated on a test sets.

Results & discussion

The results shows that defining time-window and optimizing its length increases the performance of the data analyses by reducing the noise caused by non-measured systematic variables that influence the value of the observed variable over time. In La Jailliere case study, time-window length of 11 years showed that is the most optimal solution.

	8 years	11 years	All data
Min. number of instances	610-612	618-619	1580-1850
Index of Agreement *(d)*	0.870	0.879	0.865
Std. Deviation of *d*	0.27	0.23	0.27

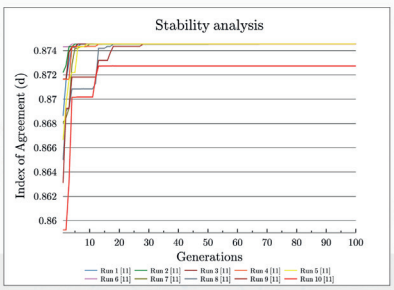

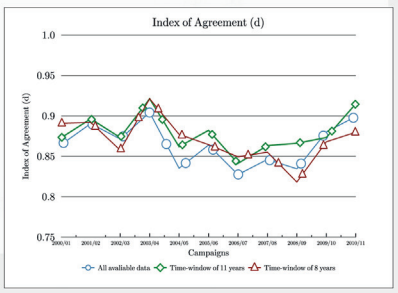

Acknowledgment

We ackowledge ARVALIS for financial support of project EVADIFF (Evaluation et développement de modèles et outils d'aide à la décision utilisés pour la prévention des pollutions diffuses par les produits phytopharmaceutiques)

Gene function prediction for *Solanum tuberosum* from time-series gene expression data

Jurica Levatić[1,2], **Živa Ramšak**[1,3], **Tjaša Stare**[3], **Dragi Kocev**[1], **Kristina Gruden**[3], **Sašo Džeroski**[1,2]

[1] Department of Knowledge Technologies, Jožef Stefan Institute, Ljubljana, Slovenia

[2] Jožef Stefan International Postgraduate School, Ljubljana, Slovenia

[3] Department of Biotechnology and Systems Biology, National Institute of Biology, Ljubljana, Slovenia

jurica.levatic@ijs.si

Deoxyribonucleic acid or DNA can be considered as a book of life, where all the information needed for the development and functioning of living beings is written. The smallest meaningful sentences of this book are called genes. Genes are the blueprints for building essential ingredients of life and hold the genetic traits passed to offspring.

One of the central challenges of modern biology is to understand the biological roles of particular genes in the organism. For example, certain genes determine the colour of our eyes, while some of them are included in the immunological response to viral infection. Such functions can be determined experimentally, but this is time-consuming, laborious and expensive task. However, on the other hand, machine learning techniques can be used to guide laboratory experiments. Such methods can learn from experimental biological data and predict the biological functions of genes. We used measurements of expression levels for 17,318 potato genes, following response of plants to viral attack, to build computational model for potato gene function prediction. With the learned model, we generated predictions for 20,547 potato genes with previously unknown biological function.

Preliminary inspection of the predictions by a domain experts showed that we were able to correctly predict certain biological functions, mainly the ones which change the most after viral infection. We can conclude that machine learning approaches have the potential to improve the knowledge about potato defence against pathogens and plant genetics in general.

MEDNARODNA PODIPLOMSKA ŠOLA JOŽEFA STEFANA

JOŽEF STEFAN INTERNATIONAL POSTGRADUATE SCHOOL

Gene function prediction for *Solanum tuberosum* from time-series gene expression data

Jurica Levatić
Study programme: Information and communication technologies,
Jožef Stefan International Postgraduate School
Supervisor: prof. dr. Sašo Džeroski
Jožef Stefan Institute, Jamova cesta 39, 1000 Ljubljana

Gene function annotation
- among key challenges of modern biology
- experimental procedures are slow and expensive

Can we use machine learning to predict the functions of genes?

Microarray gene expression data

Measurements of expression levels during several points in time following a response of plant to viral infection

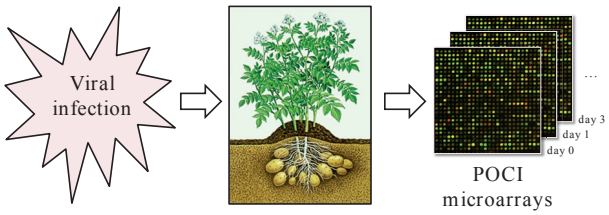

- 37,865 *Solanum tuberosum* (potao) genes
- two varieties of potato: *desiree* and *nahg*

Gene functions
- organized in hierarchy
- one gene → multiple functions

} Hierarchical multi-label classification problem

Machine learning methods

Ensemble of decision trees for hierarchical multi-label classification
- implemented in CLUS learning system

Training set: 17,318 genes with known function
Attributes: 42 numerical features
Target: 838 possible classes

Results

Heterogeneous class wise performance
- more frequent biological functions are modelled better
- large number of less frequent classes could not be modelled correctly
- we can make considerable selection of smaller classes where the predictive model was successful

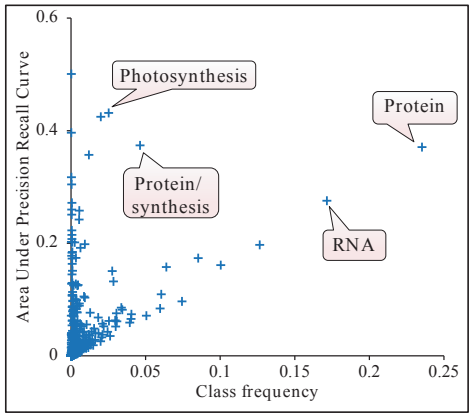

Application

We applied the developed model to predict the biological function for 20,547 potato genes for which this was otherwise unknown.
The preliminary inspection of de-novo predicted functions shows that the model works well for certain functions, namely *biotic stress* and *photosynthesis*.

Acknowledgments: We would like to thank to the biologists at National Institute for Biology, Kristina Gruden, Tjaša Stare and Živa Ramšak, for providing us with the potato dataset, as well as for many useful discussions and comments.
Author's information: E-mail: jurica.levatic@ijs.si, Tel.: +386 1 477 3639

Network Coding Aware Routing for Performance Boost in Wireless-Mesh-Networks

Erik Pertovt[1,2], **Kemal Alič**[1,2], **Aleš Švigelj**[1,2], **Mihael Mohorčič**[1,2]

[1] Department of Communication Systems, Jožef Stefan Institute, Ljubljana, Slovenia

[2] Jožef Stefan International Postgraduate School, Ljubljana, Slovenia

erik.pertovt@ijs.si

Wireless mesh networks are typical representatives of wireless access/backbone networks, where nodes such as wireless (WiFi) routers, are highly connected to each other through multi-hop wireless links enabling access to the Internet. Various mechanisms exist to improve the performance in multi-hop wireless mesh networks. Among the promising mechanisms, which have gained an increased attention in the past years, is wireless network coding. Network coding enabled node combines multiple packets from the same or from different traffic flows into one encoded packet and forwards it to the next node along the way to the destination, where original packets are recovered making use of several encoded packets, thus increasing the network capacity. In wireless networks, network coding exploits the broadcast nature of the wireless medium, where nodes can overhear packets which are not destined to them, resulting in new coding opportunities, which enable combining even more packets together. Further benefits and therefore the true potential of network coding in the network layer can be achieved with routing metrics and algorithms that are aware of coding opportunities that arise when an individual path is selected as a route. Applying network coding aware routing, paths with more coding opportunities can be discovered resulting in modified routes where more packets are being coded together, thus using even less bandwidth compared to network coding unaware routing for transferring the same amount of traffic from source to destination. On the other hand, the information on node's coding successfulness can be used to prevent the congestion at the bottleneck nodes in the network as more coding does not necessarily result in better network throughput. Therefore, we propose a novel congestion-avoidance coding-aware routing metric. It routes packets so as to avoid congested nodes based on the information of measured node coding gain, assuming that higher coding gain may indicate that traffic on that node is too high and node should be avoided. Using computer simulation we show that the proposed metric with network coding performs better than the existing (conventional) coding-unaware ETX routing metric with network coding.

MEDNARODNA PODIPLOMSKA ŠOLA JOŽEFA STEFANA

JOŽEF STEFAN INTERNATIONAL POSTGRADUATE SCHOOL

NETWORK CODING AWARE ROUTING FOR PERFORMANCE BOOST IN WIRELESS-MESH-NETWORKS

Erik Pertovt, Kemal Alič, Aleš Švigelj, Mihael Mohorčič

Study program : Information and Communication Technologies

Jožef Stefan International Postgraduate School

ADVISOR: doc. dr. Mihael Mohorčič

Department of Communication Systems, Jožef Stefan Institute, Jamova cesta 39, 1000 Ljubljana

Wireless Mesh Network (WMN)

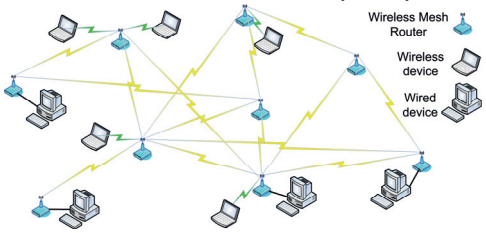

Increasing the network capacity through network coding!

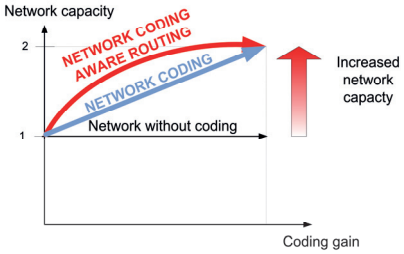

NETWORK CODING (NC)

- Combines multiple packets either from the same or from different traffic flows into one encoded packet for saving bandwidth
  - → **increases the network throughput**

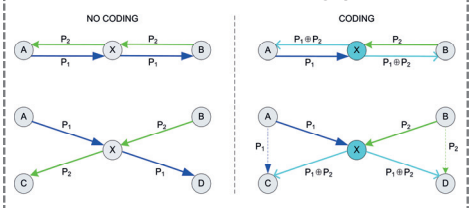

►NETWORK CODING AWARE ROUTING

- Routing metrics and algorithms that are aware of coding opportunities that arise when an individual path is selected as a route: **enables achieving further benefits and the true potential of NC**

→ paths with more coding opportunities are discovered

→ more packets are being coded together on modified routes thus using less bandwidth

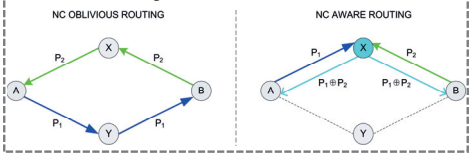

CONGESTION-AVOIDANCE CODING-AWARE ROUTING METRIC

- **The idea:** More coding does not necessarily result in better network throughput:

→ the information on node's coding successfulness can be also used to prevent the congestion at the bottleneck nodes in the network

→ the traffic on the red node is too high and the node should be avoided being selected as the route for packets P_1 and P_2

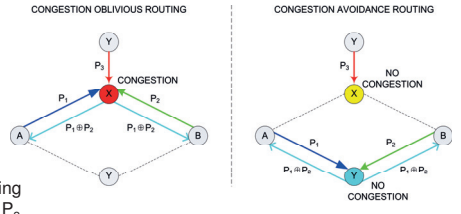

►THE PROPOSED NOVEL METRIC

→ routes packets so as to avoid congested nodes based on the information of measured node coding gain (CG): higher CG may indicate that traffic on that node is too high

→ ETX based metric enhanced with the link CG and node CG information:

$$Cost_{ij} = \begin{cases} ETX_{ij} + \left(\frac{g_{ij} + g_{ji}}{2} \cdot G_{thr}\right), & G_j \geq G_{thr} \\ ETX_{ij}, & G_j < G_{thr} \end{cases}$$

THE METRIC IS USED BY THE SHORTEST PATH ROUTING ALGORITHM AS DIJKSTRA

Measured CG of a node j (G_j):

$$G_j = \frac{N_{S,j}}{N_{C,j}}$$

$N_{S,j}$: number of source packets, routed by the node j without coding

$N_{C,j}$: number of packets required to send source packets with coding

Expected transmission count (ETX):

$$ETX_{ij} = \frac{1}{d_{ij} \cdot d_{ji}}$$

d_{ij}: probability that acknowledgement for the received packet (from the receiver j) has been successfully received at node i

d_{ji}: probability of successful packet transmission from the sender i to the receiver j

CG for a link ij (g_{ij}):

$$g_{ij} = \frac{n_{S,ij}}{n_{C,ij}}$$

$n_{S,ij}$: number of source packets which are transmitted from the sender i to the receiver j

$n_{C,ij}$: number of packets required to transmit all the source packets from the sender i to the receiver j using NC

G_{thr} → Parameter: a constant („threshold") value

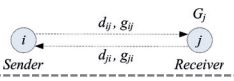

PERFORMANCE EVALUATION OF THE PROPOSED METRIC

Network:

- 40 same configured wireless nodes placed on 1 km x 1 km
- Each node transmits at 2 Mbit/s
- Packet delivery probabilities of wireless links: between 70% and 100%

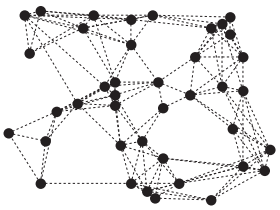

Parameters:

- Traffic load is generated on all nodes with the same intensity using exponential distribution of inter-arrival times and constant packet lengths (i.e., 10 kbit)
- Traffic load is increased through simulation runs
- Every simulation run took 330 seconds and results were collected during 250 seconds of steady traffic conditions

Quality of Service measurements:

- Delay for COPE with NC-aware ETX, COPE with ETX, and reference scenario without coding (ETX)

Quantity of Service measurements:

- Network goodput for COPE with NC-aware ETX, COPE with ETX, and ETX

Coding gain (CG) measurements:

- Nodes CG

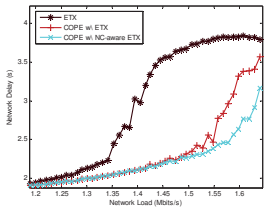

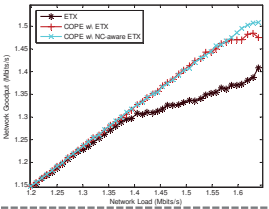

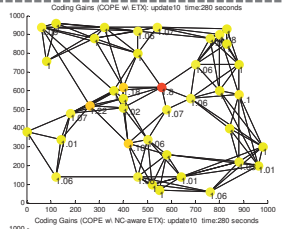

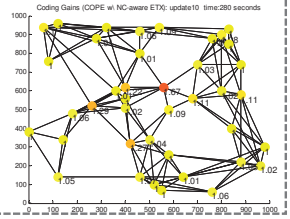

Learning bagged models of dynamic systems

Nikola Simidjievski[1,2] **, Ljupco Todorovski**[3] **, Sašo Džeroski**[1,2]

[1] Department of Knowledge Technologies, Jožef Stefan Institute, Ljubljana, Slovenia

[2] Jožef Stefan International Postgraduate School, Ljubljana, Slovenia

[3] Faculty of Administration, University of Ljubljana, Slovenia

nikola.simidjievski@ijs.si

"A model of a system is a tool used to answer questions about the real systems without having to do an experiment" – Lennart Ljung

Engineers and mathematicians construct mathematical model to describe and predict the behavior of real dynamic systems under various conditions. These kinds of models normally are formulated with ordinary differential equations (ODEs), which represent a change of the state of the system over time. This process can either be theoretical or empirical. In the theoretical approach, experts use their knowledge of the domain to derive a mathematical equation of some process in the nature. On the other hand, the empirical paradigm uses measured data and tries to find the model that best fits the observed data in a trial and error process. This paradigm has been recently used to develop machine learning approaches to constructing ODE models from observed data. The state-of-the-art approaches have emerged that combine both the domain-knowledge and measured data to identify both the model structure and the values of the models parameters.

Our research is concerned with extending the existing machine leaning paradigms of automated modeling towards learning ensembles of ODE models. Our primary objective is adapting the existing and developing new techniques for combing ODE models, thus improving the descriptive and predictive performance of nonlinear and chaotic dynamic systems.

DEPARTMENT OF KNOWLEDGE TECHNOLOGIES
Jožef Stefan Institute

MEDNARODNA PODIPLOMSKA ŠOLA JOŽEFA STEFANA

JOŽEF STEFAN INTERNATIONAL POSTGRADUATE SCHOOL

Learning Bagged Models of Dynamic Systems

Nikola Simidjievski[1,2], Ljupco Todorovski[3], Sašo Džeroski[1,2]

1 Department of Knowledge Technologies, Jozef Stefan Institute, Ljubljana, Slovenia
2 Jozef Stefan International Postgraduate School, Ljubljana, Slovenia
3 Faculty of Administration, University of Ljubljana, Slovenia
nikola.simidjievski@ijs.si

Introduction

*Equation Discovery (ED) is the process of inducing scientific laws and models in form of equations from observations (measured data)

*Inductive Process Modeling (IPM) based on ED uses combination of domain knowledge and observations (measurements) to induce explanatory process-based models of dynamic systems

*Ensemble learning methods (ensembles) consider combinations of multiple predictive models to maximize the predictive performance of the system

Motivation

*Ensembles of dynamic models has not yet been considered in the machine learning community.

*Adapting the traditional Bagging approach, in the context of learning ensembles of ODE models

Aim : Evaluate the performance of ensemble of ODE models compared to classical ODE models with automated process based modeling approach

ProBMoT (Čerepnalkoski et. al.)

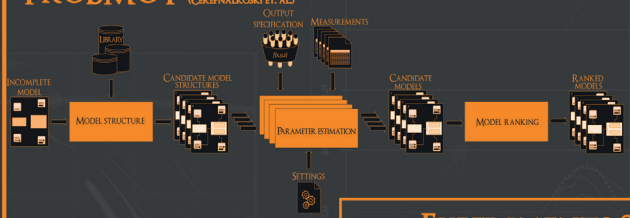

*ProBMoT - tool for complete modeling, parameter estimation and simulation of process-based models

*Conceptual (high-level) representation of a model
- Rules which indicate how the model structures are generated

*Models are formulated as ODEs

*Knowledge is represented as library of entities and processes

*Entities are state/variable of the system

*Processes represent the interaction between the entities

*Parameter estimation is based on meta-heuristic optimization

*ProBMoT implements custom quantitative objective functions

*Modification of ProBMoT to meet the criteria for generating ensembles of ODE models

Ensembles of ODE models

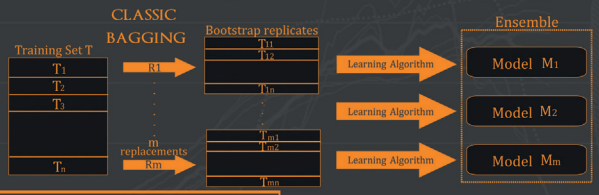

Experiments & Conclusion

Lake Bled , Slovenia

Modeling phytoplanckton concentration

Train Set : 6 datasets containing measurements by year (1996-2001)

Test Set : 1 dataset with measurements of year 2002

Adapted Bagging for ODE models

Evaluation scenario : Learning Curve

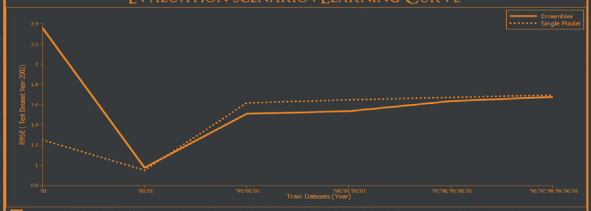

The ensemble model only slightly improves the overall performance of the ODE models

Adding too many preceding data sets to the training data doesnt improve the predictive performance

These results uncover important characteristics of the ensembles approach. Moreover, they clearly point to important directions for future improvement of the performance of this methodology

Our approach chooses uniformly random time points from the time series & assigns weights to each of them.

By penalizing (encouraging) different time points from each boot-

Adapted bagging

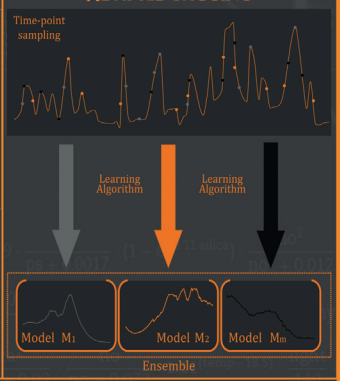

Food-web dynamics in Aquatic Ecosystems

Example model

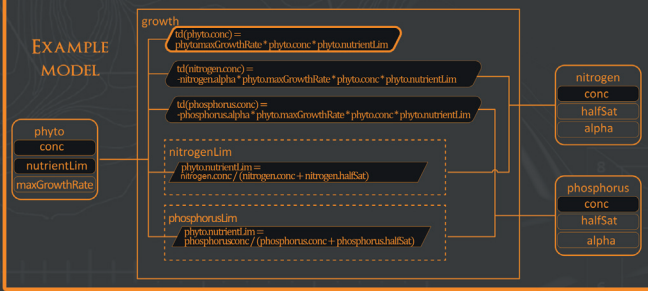

Conceptual model

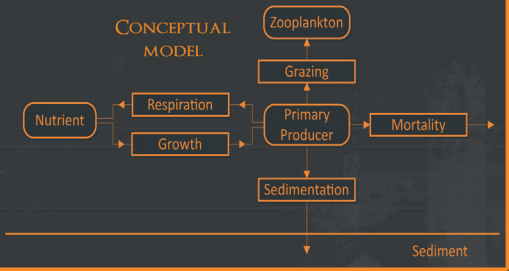

Pharmacokinetic model for the evaluation of a proposed drug delivery system

(undergraduate student contribution)

Maja Somrak[1], **Miha Moškon**[1], **Dušan Vučko**[1], **Boštjan Pirš**[2], **Miha Mraz**[1], **Roman Jerala**[3,4]

[1] Faculty of Computer and Information Science, University of Ljubljana, Slovenia

[2] Faculty of Medicine, University of Ljubljana, Slovenia

[3] National Institute of Chemistry, Ljubljana, Slovenia

[4] Centre of excellence ENFIST, Ljubljana, Slovenia.

maja.somrak@gmail.com

Typical pharmacological therapy comprises regular applications of drugs into the body, which cause high fluctuations of drug concentration and wide distribution of drug throughout the body. An advanced therapy based on synthetic biology would consist of the localized continuous production of biological drugs which should lead to reduced systemic side effects and lower total amount of required drug. In order to evaluate the efficacy of new type of therapy, we utilized pharmacokinetic modeling for comparison of different therapeutic regimens.

Mathematical model relies on experimentaly determined parameters and physiological mechanisms affecting drugs inside the human body. In simulation, the outcomes of the key drug processes, through which every drug passes inside the body, are calculated. The result of modeling is the concentration time course for each of the selected organs and tissues, which determines the efficacy and side effects of the therapy.

Simulation results serve as a basis for therapy evaluation and comparison. It is possible to use the model for calculation of additional parameters, e.g. necessary dose adjustments for patients with renal disfunction or the required amount of implanted microcapsules for the new cell-based therapy.

We obtained very informative and encouraging results, regardless of the fact, that computer model is only an approximation of the real and complex processes. While simulation cannot substitute clinical trials, it can definitely benefit and improve drug development process, save time, expenses and other resources.

MEDNARODNA PODIPLOMSKA ŠOLA JOŽEFA STEFANA

JOŽEF STEFAN INTERNATIONAL POSTGRADUATE SCHOOL

Pharmacokinetic model for the evaluation of a proposed drug delivery system

Maja Somrak[1], Miha Moškon[1], Dušan Vučko[1], Boštjan Pirš[2], Miha Mraz[1], Roman Jerala[3,4]

[1] Faculty of Computer and Information Science, University of Ljubljana, [2] Faculty of Medicine, University of Ljubljana, [3] National Institute of Chemistry, [4] Centre of excellence ENFIST.

Drug discovery and development is a very expensive and time consuming process that could be aided with the utilization of computer simulation. It is possible to provide insight into the potential therapy by calculating the outcomes of drug processes in the body by implementing a corresponding mathematical model.

For the purpose of therapy evaluation, computer modeling represents a simpler and faster option than clinical testing. However, computer simulation cannot substitute drug trials, but it can accelerate trials by reducing the number of required tests and support further development.

Results of such pharmacokinetic simulations could be used for:

- evaluation and comparison of therapies
- predicting the degree of side effect occurrence
- calculating unknown parameters (*e.g.* required drug production or adjusted dose)

The model

MULTI-COMPARTMENT
Compartments represent bodily organs and tissues.

PHYSIOLOGICALLY BASED
Relies on actual physiological mechanisms.

PHARMACOKINETIC MODEL
Model simulates four key processes, which the drug goes through inside the body:

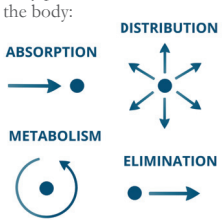

Study case – a cell-based drug delivery system

We implemented the model for therapeutic treatment based on synthetic biology and evaluated its effectiveness. The proposed therapy incorporates **implanted microencapsulated** engineered **cells, that would constantly produce** small amounts of the **drug inside the diseased organ**.
We conducted tests for two biological drugs, interferon and anakinra, for the treatment of hepatitis C and myocardial infarction, respectively.

Results & Conclusion

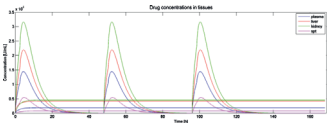

Figure: Simulation results for biological drug interferon – conventional subcutaneous therapy graph (visible high peaks of concentration) overlapped with proposed local drug production therapy graph (steady and low concentration levels).

When comparing results, we can see that the proposed therapy has the following **predicted advantages** over conventional therapies:

- stable concentration levels
- drug is more localized
- reduced side effects
- more effective treatment

Model enabled us to **calculate the required amount** of implanted cells to achieve the desired **drug production**.

Although the model is only an approximation of the real, complex pharmacokinetic mechanisms, we obtained very informative results.

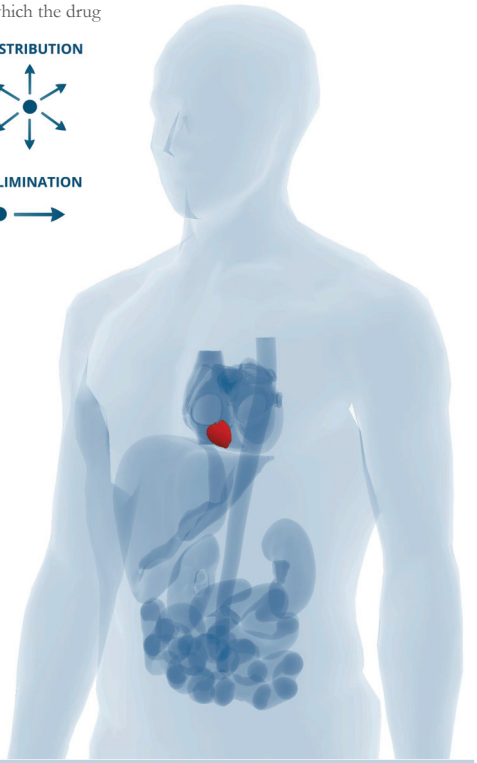

Figure: Simulation of potential therapy with a cell-based drug production and delivery system reveals that local production of the biological drug (anakinra) inside the infarcted tissue would cause the drug concentration to remain high in the affected area, but very low throughout the rest of the system. This would result in higher therapy effectiveness at lower doses and reduced systemic side-effects.

Acknowledgements

Presented work is a part of the project "**Switch IT: Inducible Therapeutics**" which team Slovenia presented at International Genetically Engineered Machine (iGEM) 2012 synthetic biology competition.

Semi-automatic construction of pattern rules for translation of natural language into semantic representation

Janez Starc[1,2], **Dunja Mladenić**[1,2]

[1]Artificial Intelligence Laboratory, Jožef Stefan Institute, Ljubljana, Slovenia

[2] Jožef Stefan International Postgraduate School, Ljubljana, Slovenia

janez.starc@ijs.si

Imagine computers being able to read understand and memorize a large encyclopedia like Wikipedia. This means that they would be able to answer any question regarding the read text and provide explanation for it. This is the goal of a subfield of artificial intelligence called machine reading. By the definition, it is automatic, unsupervised understanding of text [1]. The aim of our research is to make progress towards machine reading.

To be able to fulfill machine reading, computers must store the read data in a language they understand. We will call it semantic language. An example sentence in semantic language would be *(placeOfBirth TigerWoods CypressCalifornia)*, which in our language means that Tiger Woods was born in Cypress, California. Computers need to know all the components of a semantic language sentence before memorizing it. This is called the background knowledge.

Text is translated into semantic language with pattern rules. These rules consist of textual and semantic pattern. Textual pattern connects with different portions of text that have similar meaning. Semantic pattern becomes a semantic sentence after applying the rule. There are two ways to acquire pattern rules. Either have them constructed manually or learn them with machine-learning methods. The first way is very expensive in terms of human labor. There are an enormous number of rules to be produced, and it takes time for a human to learn producing rules. On the other hand, machine-learning methods need less human involvement, but suffer from inaccuracy.

We built an interface, which allows a human to develop good rules in a fast way. This is done by suggesting him frequent and coherent textual patterns. Additionally, it suggests concepts from background knowledge that are likely to form the semantic pattern. The user constructs a rule on a selected document. When a new rule is constructed, the system searches all the documents for possible applications of the rule. In the future, we will add machine-learning methods to our system and make it simpler to use, thus it will be available for wider audience.

MEDNARODNA PODIPLOMSKA ŠOLA JOŽEFA STEFANA

JOŽEF STEFAN INTERNATIONAL POSTGRADUATE SCHOOL

SEMI-AUTOMATIC CONSTRUCTION OF PATTERN RULES FOR TRANSLATION OF NATURAL LANGUAGE INTO SEMANTIC REPRESENTATION

JANEZ STARC
Artificial Intelligence Laboratory
Jožef Stefan International Postgraduate School
Program: Information and Communication Technologies
Mentor: prof. dr. Dunja Mladenić
Jožef Stefan Institute

The goal of our work is to store the information in **natural language** into structured **computer-readable representation**. We argue that **manual construction** is **more precise and less rigid** than machine learning methods. Our system allows the user to construct **pattern rules** and applies them on the underlying corpus. To make the translation **faster and more productive**, the system **suggests** different parts of rules.

PATTERN RULE consists of

- **lexical pattern**, which matches with **text**
- **logical pattern**, which converts into semantic expression in a target **ontology** when the rule is applied
- **argument mappings**, which connect arguments in lexical pattern with arguments in logical pattern

Lexical pattern	Logical pattern
primer ministro , Person1 ,	(isa %Person1% PrimeMinister-HeadOfGovernment)

Expressions
(isa [Mariano_Rajoy] PrimeMinister-HeadOfGovernment)
(isa [Recep_Tayyip_Erdogan] PrimeMinister-HeadOfGovernment)
(isa [David_Cameron] PrimeMinister-HeadOfGovernment)
(isa [Shinzo_Abe] PrimeMinister-HeadOfGovernment)

Pattern rule representing relation "is a prime minister" in Spanish

GENERALIZATION

To obtain lexical patterns from text, the underlying set of documents needs to be processed with **natural language processing tools** and **generalized**.

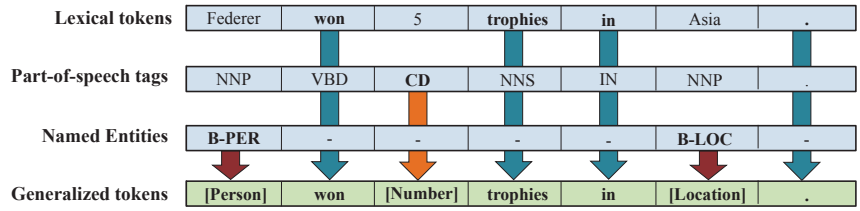

The user selects the language and document number; the document appears in the document panel

The user clicks on the suggested pattern in document panel or selects and drags a fraction of text; the pattern will appear in the lexical pattern area

In this box the user constructs the logical pattern; the system prepares an initial generic expression

The system suggests a few concepts from the ontology that are denoted by the words from the lexical pattern

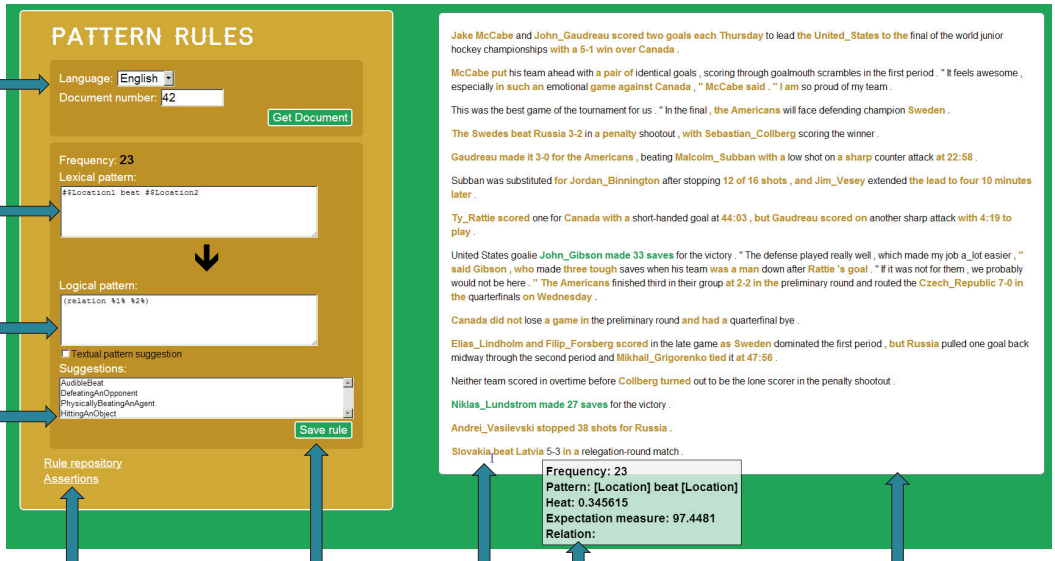

By clicking on these links, the user gets the list of rules and list of logical expression for each rule

When the user clicks the button, the system stores the rule and looks for its applications in every document

If the user moves the mouse over a colored text; the pattern and a few of its statistics will appear in a hint box nearby

In this panel the selected document is presented; if the part of text is **orange** it represents an suggested pattern; if it is **green** the rule for it has already been made

Automated modeling of Rab5–Rab7 conversion in endocytosis

Jovan Tanevski[1,2], **Ljupčo Todorovski**[3], **Sašo Džeroski** [1,2]

[1] Department of Knowledge Technologies, Jožef Stefan Institute, Ljubljana, Slovenia

[2] Jožef Stefan International Postgraduate School, Ljubljana, Slovenia

[3] Faculty of Administration, University of Ljubljana, Slovenia

jovan.tanevski@ijs.si, ljupco.todorovski@fu.uni-lj.si, saso.dzeroski@ijs.si

Our work focuses on artificial intelligence approaches to modeling dynamical systems. In particular, we work on development and application of tools for inductive-process modeling. These tools take at input knowledge formalized as library of model components for modeling dynamical systems in a particular domain of interest and time-series data about the behavior of the observed system. They integrate knowledge transformation methods from artificial intelligence with standard simulation and parameter estimation methods from system identification to automate the process of establishing a model of the dynamical system at hand.

While most of the inductive-process modeling applications have been in the domain of ecology, our interests are towards using them in context of system and synthetic biology. The work presented in this paper is an application of the IPM approach to the domain of systems biology. It describes the entire process of automating a manual experiment from the literature. The challenges and the findings to which we come across during the various application scenarios, like the one presented in this work, provide us with directions towards the further development of the approaches and towards the goal of providing tools that improve the ease and the efficiency of the task of modeling.

MEDNARODNA PODIPLOMSKA ŠOLA JOŽEFA STEFANA

JOŽEF STEFAN INTERNATIONAL POSTGRADUATE SCHOOL

Automated modeling of Rab5–Rab7 conversion in endocytosis

Jovan Tanevski[1], Ljupčo Todorovski, Sašo Džeroski

[1]Study programme: Information and communication technologies,

[1]Jožef Stefan International Postgraduate School

[1]Supervisor: prof. dr. Sašo Džeroski

Institute Jožef Stefan, Jamova cesta 39, 1000 Ljubljana

Introduction

Inductive process modeling (IPM) is knowledge and data driven approach based on equation discovery principles.
We apply the IPM approach to modeling dynamical systems in the domain of systems biology.
We automate the modeling process of the dynamics of the Rab5–Rab7 interaction, which is a part of the endocytic pathway.

Process-Based Knowledge

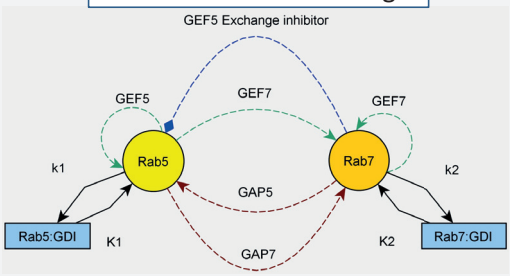

Using the knowledge obtained from a manual experiment from the literature, we formulate a process-based library of knowledge, which we use to describe all hypothetical processes which give rise to possible candidate models for this interaction.

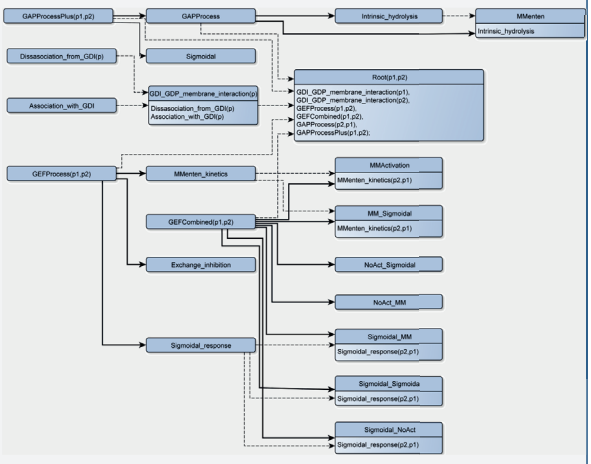

High level conceptual model is developed as a guideline which determines which parts of the library and in which way are to be used during the structure generation process. Following the conceptual model, ProBMoT enumerated 126 possible candidate structures using all possible combinations of alternatives for the GEF and GAP processes.

Results

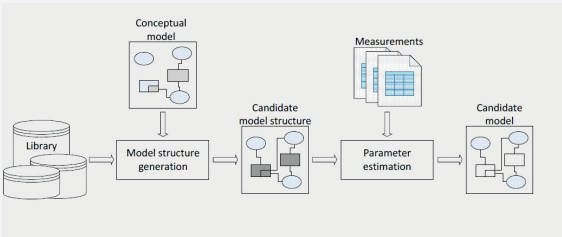

We fitted the candidate structures to the measured time-course data.

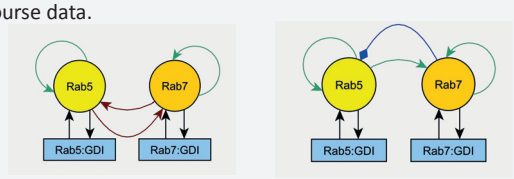

(a) (b)

The range of errors for the obtained models is narrow. Many models have errors only slightly higher than the best model.
The structure of the model with the lowest error given the data (a), and the model reported in the literature (b) have different error values, different structures and type of interactions.
Both structures have good fit to the data.

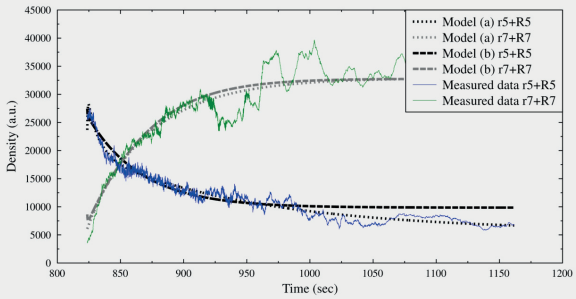

Conclusion

The experiment resulted in structurally different models which have similarly good fit to the measured data.
We found out that, an objective based on the model error given the data is not sufficient. In order to discriminate between models we need an additional criteria. Integrating other information about the properties of the system can improve the method and its performance.

Analysing Financial Vocabulary Using a New Semantic Subgroup Discovery System Hedwig

Anže Vavpetič[1,2], **Petra Kralj Novak**[1,2], **Nada Lavrač**[1,2]

[1] Dept. of Knowledge Technologies, Jožef Stefan Institute, Ljubljana, Slovenia

[2] Jožef Stefan International Postgraduate School, Ljubljana, Slovenia

anze.vavpetic@ijs.si

Our work was stimulated by our collaboration in the Forecasting Financial Crises (FOC) EU project. The topic of the FOC project is to understand and possibly forecast systemic risk and global financial instabilities.

In our work we started from a large collection of web news articles from a variety of internet sources and focused on answering the following question: what is the main vocabulary (e.g., countries, persons, companies) that is used in the news when certain financial events occur? More specifically, we focused on a troubled Eurozone country, Portugal, and the trend changes in its Credit Default Swap (CDS) prices which reflect the risks to the lending of money to the country in question. The higher the CDS prices, the higher the chances of the country failing to repay its debts.

In the paper, we introduce a novel system Hedwig that was used for the previously described task. We report the main vocabulary occurring in news together with Portugal at the time when its CDS price reached a global extreme (a local minimum or maximum). In the long term, we intend to induce models for actually predicting the future CDS trend changes based on the contents of the current news articles.

MEDNARODNA PODIPLOMSKA ŠOLA JOŽEFA STEFANA

JOŽEF STEFAN INTERNATIONAL POSTGRADUATE SCHOOL

ANALYSING FINANCIAL VOCABULARY USING A NEW SEMANTIC SUBGROUP DISCOVERY SYSTEM HEDWIG

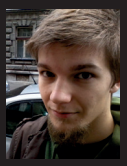

Anže Vavpetič, Petra Kralj Novak, Nada Lavrač

Jožef Stefan Institute, Ljubljana, Slovenia
Jožef Stefan International Postgraduate School, ICT programme

KEYWORDS

semantic data mining, subgroup discovery, ontology, text mining, credit default swap, financial crisis

INTRODUCTION

- Subgroup discovery (SD) is a data mining technique lying between classification and association discovery
- SD is most commonly used for descriptive tasks and is used to find descriptions of statistically interesting subgroups of individuals
- We present the results of applying a newly developed system Hedwig

- In this work Hedwig was used to analyze news articles and is stimulated by our participation in the FIRST and FOC EU projects
- Within the projects a vast amount of articles (~8 million) were collected
- We focus on articles about Portugal, a domain ontology and a history of its Credit Default Swap (CDS) prices
- CDS is insurance for country bonds and indicates the probability that the country will default

Task:
- What is the relationship between the financial market perception (CDS price) of a financial entity and the articles mentioning the entity?

Main contributions:
- A new semantic data mining system Hedwig with its premiere application
- The first insights into the relationship between the European sovereign debt crisis vocabulary and the CDS price trends

METHODOLOGY

- Notation: rules are a subset of first-order logic expressions (Horn clauses)

```
Max(X) <= Country(C), Before(X,Y), comp_NESTLE_S_A(Y). [50,10]
```

- We employ a beam search algorithm, with the best *N* found rules so far
- Each rule in the beam is specialized via three operations, until there is no improvement to the collection of rules:

1. Replace the rule's predicate with a predicate that is a sub-class of the previous one, e.g., `City(X)` is specialized to `Capital(X)`.

2. Append a new unary predicate to the rule, e.g., `Max(X) ← City(X)` is specialized to `Max(X) ← City(X), Company(X)`.

3. Append a new binary predicate, thus introducing a new existentially quantified variable, e.g.: `Max(X) ← City(X)` is specialized to `Max(X) ← City(X), Before(X,Y)`.

- A rule will not be specialized once its coverage falls bellow some pre-determined threshold or is 0
- Our system implements some popular scoring functions: *WRAcc*, *ChiSq* and *Z-score*
- Examples and ontologies can be loaded as a set of RDF triples

DATA PREPARATION

- We started with a database of annotated news articles (over 8 million)
- For each article we had the information about which entities appear in a given article (e.g., Angela Merkel or Portugal)
- These entities are part of a large domain ontology
- We focused on articles mentioning Portugal and our preparation consisted of two steps:

1. Counting the number of times Portugal appears together with every other entity for each day
2. Selecting only the significant co-occurrences as example features: those that appeared at least 1.5 times than on average

- Each example is described by the presence or absence of these entities and labeled as *max*, *min* or *steady*, indicating if a local extreme was reached
- 337 examples with on average 282 features

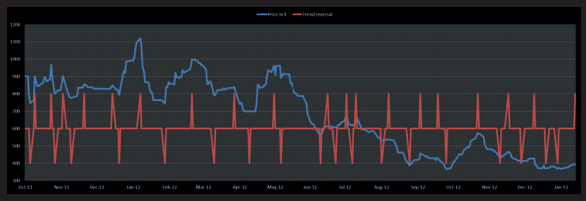

EXPERIMENTAL RESULTS

- Beam width 100, min coverage 5, number of predicates per rule 6
- Best rule for local maxima:

```
Max(X) <= reg_Western_Europe(X), Angela_Merkel(X),
    glo_austerity(X), glo_recession(X). [28, 7]
```

- Best rule for local minima:

```
Min(X) <= Index(X), comp_GALP_ENERGIA(X), Loan_Term(X),
        glo_fiscal_stimulus(X). [43, 8]
```

- The results show that the higher the CDS prices the more the sovereign debt vocabulary is used
- When CDS prices are low, a more general financial terminology is used

CONCLUSIONS

- We presented a new semantic SD system Hedwig
- Hedwig was applied for analyzing news articles about Portugal
- We used co-occurrence frequencies of vocabulary appearing with Portugal, a history of CDS prices and a domain ontology
- We induced subgroups describing prominent vocabulary appearing at times of CDS trend reversals
- The results indicate that the news content does indeed reflect the CDS prices
- We plan to proceed with actually predicting CDS trend changes by including additional information extracted from the text (TF-IDF and not only pre-defined vocabulary)
- We will employ several classification algorithms and compare them

DEPARTMENT OF KNOWLEDGE TECHNOLOGIES Jožef Stefan Institute

FIRST

foc forecasting financial crises

Nanoznanosti in nanotehnologije (Nanosciences and Nanotechnologies)

Hidrotermalna sinteza fotokatalitične prevleke iz TiO_2 na aluminiju

Anže Abram[1,2], **Goran Dražić**[1,2,3]

[1] Department for Nanostructured Materials, Jožef Stefan Institute, Ljubljana, Slovenia

[2] Jožef Stefan International Postgraduate School, Ljubljana, Slovenia

[3] National Institute of Chemistry, Laboratory for materials electrochemistry, Ljubljana, Slovenia

anze.abram@ijs.si

Eden največjih problemov trajnostnega razvoja je zagotovitev zadostne količine pitne vode v prihodnosti. Poraba vode raste proporcionalno s svetovno populacijo, medtem ko se zaloge hitro zmanjšujejo. V manj razvitih delih sveta dostop do čiste in pitne vode že danes predstavlja velik problem. Prav zato se velik poudarek daje tehnologijam čiščenja zraka in vode, med katerimi svoje mesto v zadnjih letih zasedajo tudi sistemi samočistilnih naprav na osnovi fotokatalize. Fotokatalitski materiali, ki so po navadi v obliki nanometerskih delcev, med obsevanjem z ultravijolično svetlobo (ki je prisotna tudi v sončni svetlobi) tvorijo radikale, ki razgrajajo organske snovi, ki pridejo v stik z organskimi delci. S pravilno pripravo lahko dosežemo samočistilni efekt na cenovno ugoden način, kar je še posebej pomembno za države v razvoju, kjer dostop do drugih tehnologij ni mogoč.

Nanodelci lahko že sami po sebi predstavljajo ekološki in zdravstveni izziv zaradi lahkega vnosa v telo skozi dihala ali kožo. Vpliv nanodelcev titanovega dioksida na zdravje je v zadnjih letih še posebno raziskan zaradi njegove množične uporabe v kozmetiki (sončne kreme). Zato je veliko raziskav usmerjenih v imobilizacijo titanovega dioksida v obliki trdno vezanih prevlek. Obstaja več možnosti priprave takih plasti (plazemsko nanašanje, potapljanje,…), ki pa bodisi ne dajo zadostnih fotokatalitskih učinkov ali pa so prešibko vezani na podlago. Postopek hidrotermalne sinteze predstavlja dobro rešitev za obrabno obstojne prevleke, ki bi zmanjšale vnos nano titanovega dioksida v okolje.

Gre za postopek, pri katerem raztopino s prekurzorjem in podlago postavimo v hermetično zaprto posodo in izpostavimo povišani temperaturi, kar posledično poveča tlak v reakcijski posodi. Zaradi istočasnega raztapljanja prekurzorja v vodi in obarjanja nanodelcev na površine, ki so v stiku z vodo, se na podlagi tvori tank sloj titanovega dioksida. Tako pripravljene obloge titanovega dioksida na aluminiju so se izkazale za fotokatalitsko učinkovite.

MEDNARODNA PODIPLOMSKA ŠOLA JOŽEFA STEFANA

JOŽEF STEFAN INTERNATIONAL POSTGRADUATE SCHOOL

HIDROTERMALNA SINTEZA FOTOKATALITIČNE PREVLEKE IZ TiO_2 NA ALUMINIJU

Anže Abram, univ. dipl. inž. metal. in mater.

Nanoznanosti in nanotehnologije, Mednarodna podiplomska šola Jožefa Stefana

Mentor: **doc. dr. Goran Dražić**

Institut ‚Jožef Stefan', Jamova cesta 39, 1000 Ljubljana

POVZETEK

Titanov dioksid je zaradi svojih fotokatalitičnih lastnosti postal pomemben material za čiščenja zraka in vode. Fotokatalitične lastnosti kaže samo v obliki delcev nanometerskih dimenzij. Večina nanomaterialov je zdravju škodljivih, zato se njihovi uporabi v obliki nanoprahov ter suspenzij izogibamo, saj tako najlažje vstopajo v telo. Raziskal sem možnost priprave trdno vezane obloge anataznega TiO_2 filma na aluminijevi podlagi, pripravljene po postopku hidrotermalne sinteze iz titanovega izopropoksida ($Ti(OCH(CH3)_2)_4$) v vodnem mediju. Izkazalo se je, da se poleg nanodelcev anataznega TiO_2 na površini pojavi predvsem bemit ((γ-AlO(OH)), med katerega so ujeti TiO_2 delci. Fotokatalitičnost oblog na aluminiju se je izkazala za primerljivo oblogam na titanovi podlagi.

SINTEZA

Hidro- oz. solvotermalna sinteza je metoda kristalizacije iz raztopine pri visokih tlakih in visoki temperaturi pri čemer je voda (v primeru hidro-) topilo.

$Ti(OCH(CH_3)_2)_4 : dH_2O$
1 : 10
+
Aluminij pločevina
Impol M13

→

Temperatura
100, 150, 200 °C

Čas
1, 3, 6, 12, 48 ur

→

Fotokatalitična TiO_2 trdo vezana prevleka na aluminiju (z bemitom)

REZULTATI

AFM

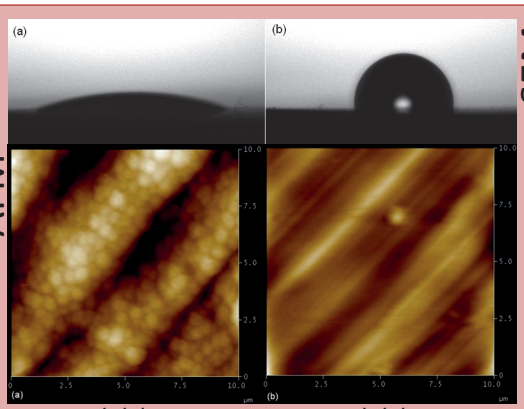

obdelan *neobdelan*

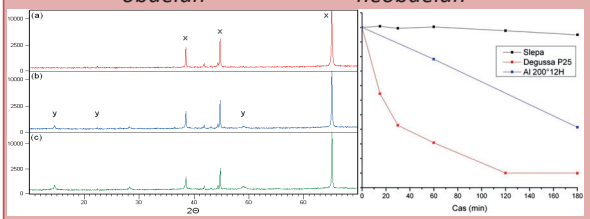

XRD,»x« - aluminij, »y« - bemit
(a) neobdelana podlaga
(b) HT, 150 °C, 12h
(c) HT, 200 °C, 12h

Fotodegradacija kofeina
(v primerjavi s P25)

SEM

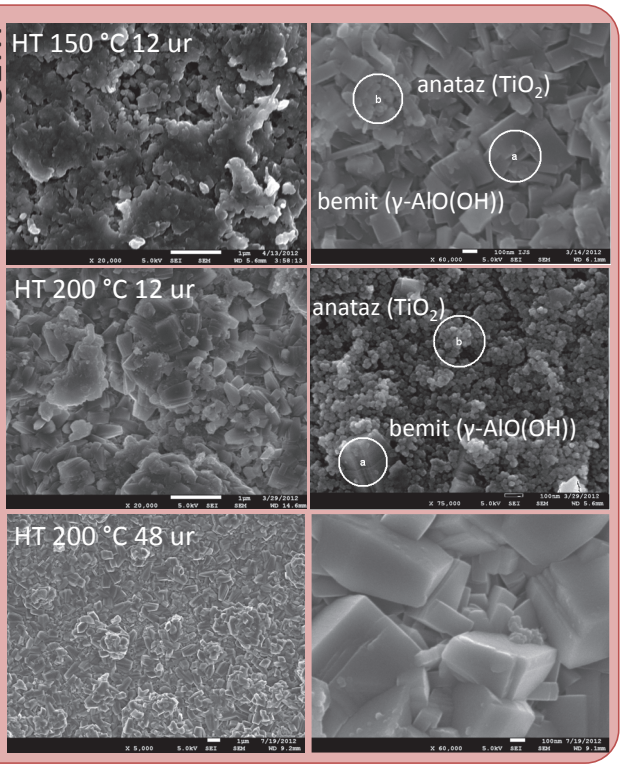

Transformations of alcohols mediated by *N*– halosuccinimides: reactions in solution or under solvent-free conditions

Njomza Ajvazi[1], **Stojan Stavber**[2,3]

[1] Jožef Stefan International Postgraduate School, Ljubljana, Slovenia

[2] Department of Organic and Bioorganic Chemistry, Jožef Stefan Institute, Ljubljana, Slovenia

[3] Centre of excellence for integrated approaches in chemistry and biology of proteins

njomzaajvazi@hotmail.com

Aim of this work is to achieve direct conversion of tertiary alcohols to vicinal halohydrins — chlorohydrins and bromohydrins — under green reaction conditions, i.e. to find a synthetic way that allows us a selective introduction of chlorine and bromine atom into organic molecule in only one step by using less hazardous reagents with lower impact on human health and environment. We showed that tertiary alcohols could be directly converted to vicinal halohydrins using *N*-halosuccinimides. These transformations were successfully performed in the following solvents: *cyclopentyl methyl ether, 2-methyl tetrahydrofuran, acetic acid, acetonitrile and water*. In all cases vicinal halohydrins were found to be the main products except in the case of the reaction in acetic acid, where the formation of haloalkene was the main process. Transformation of tertiary alcohols to vicinal halohydrin in aqueous media was considerably enhanced and yields improved in the presence of *sodium dodecyl sulphate* in the amounts around its critical micelle concentration. Additionally, we performed these transformations under alkyl alcohols high concentration reaction conditions. Furthermore, we have discovered and developed new method for direct conversion of secondary and tertiary alcohols to dimeric ethers using *N*-halosuccinimides in catalytic amount under solvent-free reaction conditions. Another new method of direct transformation of secondary and tertiary alcohols into alkyl aryl ethers was discovered and developed using *N*-halosuccinimides in catalytic amounts in the presence of another alkyl alcohol under high concentration reaction conditions or in solution. So far, we obtained benzyl alkyl ether and we are in a good way to get dialkyl ethers under the same conditions. These discoveries represent considerable contribution to the green chemical approach to transformations of alcohols into various valuable derivatives.

MEDNARODNA PODIPLOMSKA ŠOLA JOŽEFA STEFANA
JOŽEF STEFAN INTERNATIONAL POSTGRADUATE SCHOOL

Transformations of alcohols mediated by *N*-halosuccinimides: reactions in solution or under solvent-free conditions

Njomza Ajvazi[1] and Stojan Stavber[2,3]

Study program: Nanosciences and Nanotechnology
[1] Jožef Stefan International Postgraduate School, Ljubljana, Slovenia
[2] Jožef Stefan Intstitute, Ljubljana, Slovenia
[3] Centre of excellence for integrated approaches in chemistry and biology of proteins, Ljubljana, Slovenia

INTRODUCTION

Vicinal halohydrins are versatile building blocks in organic, medical and industrial chemistry, as they are widely used for transformation into epoxides[1] and ketones.[2] Halohydrins can be directly synthesized by functionalization of alkenes to *vic*-halohydrins with molecular halogens and water.[3] ***Alkyl aryl ethers*** are important solvents and synthetic building blocks for the production of fragrances, cosmetics, pharmaceuticals, and dyestuffs.[4] One of the most common methods for the preparation of ethers is the Williamson ether synthesis, which requires the conversion of an alcoholate with alkyl derivatives of Bronsted acids.[5]

Above mentioned methods for the synthesis of both *vicinal halohydrins* and alkyl aryl ethers have several disadvantages, *i.e.* multiple step synthesis, toxic and expensive reagents, problematic manipulation, and long reaction time.

Aim of this work: transformations of alcohols to vicinal halohydrins, alkyl aryl ethers and other derivatives mediated by *N*-halosuccinimides. Reactions are performed in ***solution***, under ***alkyl alcohol high concentration reaction conditions (HCR)*** or under ***solvent-free reaction conditions (SFR).***

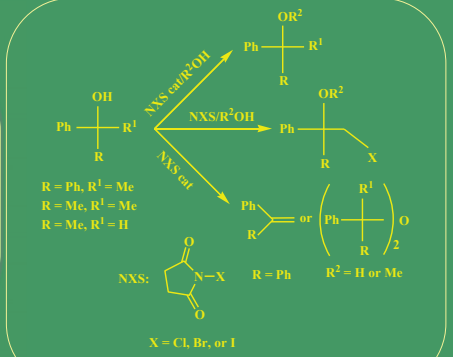

General concept and work-plan of the research

RESULTS

Table 1. The catalytic effect of NIS on conversion of 1-phenylethanol **13** under ***SFR*** or in ***solution***

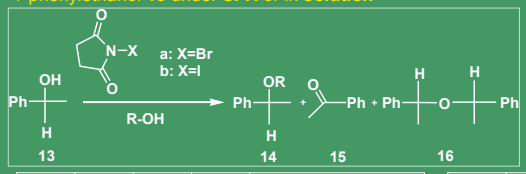

Entry	X[c]	R-OH	Conv. (%)	Relative distribution (%)		
				14	15	16
1	I	/	91	/	13	78
2	I	MeOH	100	82	/	18

[c] Catalytic amount: 3 mol %, R-OH (1ml), time 22-24h at temp. 49-75°C

Table 2. The catalytic effect of NXS on conversion of 2-phenyl-2-propanol **7** in ***solution***

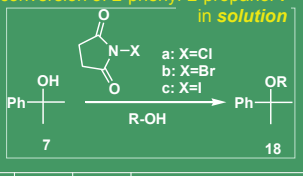

Entry	X[c]	R-OH	Conv. (%)	Relative distribution (%)
				18
1	Cl	MeOH	100	100
2	Br	MeOH	100	100
3	I	MeOH	94	94

[c] Catalytic amount: 0.5-6 mol %, R-OH (1-5 ml), time 22-24h at temp. 56-65°C

Table 3. The catalytic effect of NIS on conversion of 1,1-diphenylethanol **3** under ***alkyl alcohol HCR***

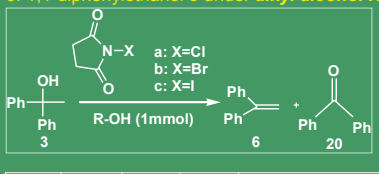

Entry	X[c]	R-OH	Conv. (%)	Relative distribution (%)	
				6	20
1	Br	PrOH	100	100	/
2		iPrOH	100	71	29
3	I	/	96	96	/

[c] Catalytic amount: 4-5 mol %, time 3[30]-24h at temp. 60-75°C

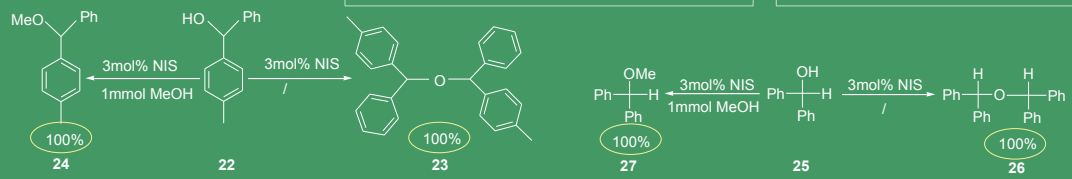

Transformation of 4-methylbenzhydrol **22** and diphenylmethanol **25** catalysed by NIS ***under alkyl alcohol HCR*** and under ***SFR***

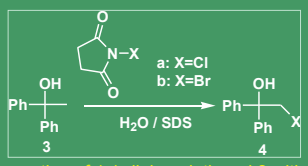

The reaction of 1,1-diphenylethanol **3** with NXS in aqueous media in the presence of SDS

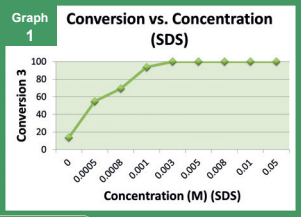

*The effect of added amount of SDS surfactant on the efficiency of the reaction of 1,1-diphenylethanol **3** with NCS (**Graph 1**) and NBS (**Graph 2**)*

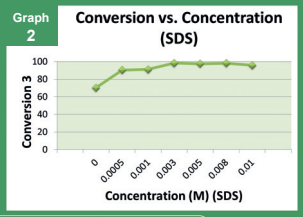

CONCLUSION

- Tertiary alcohols could be directly converted to vicinal halohydrins using *N*-halosuccinimides in one step. This transformation in aqueous media was considerably enhanced and yields improved in the presence of *sodium dodecyl sulphate (SDS).*
- Furthermore, we developed a new method for direct conversion of secondary and tertiary alcohols to dimeric ethers catalysed by *N*-halosuccinimides under ***solvent-free reaction conditions***. Direct transformation of secondary and tertiary alcohols into alkyl aryl ethers was discovered and developed using *N*-halosuccinimides in catalytic amounts under ***alkyl alcohol high concentration reaction conditions*** or in ***solution.***
- Newly developed methods present a significant contribution from a green chemistry viewpoint, economy of time and reagents.

REFERENCES

[1] M. B. Smith, J. March. *Advanced Organic Chemistry, 5th Edition*. Wiley-Interscience, New York, NY 2001
[2] D. Dolenc, M. J. Harej. *Org. Chem.* 67, 312, 2002
[3] J. H. Rolston, K. J. Yates. *Am. Chem. Soc.* 91, 469, 1969
[4] F. Edgar, T. Jörg. *Org. Process Res. Dev.* 9, 206-211, 2005
[5] S. Eğe. *Organic Chemistry structure and reactivity, 5th Edition*. Houghton Mifflin Co., Boston New York 2004

Electrical and thermal properties of polymer systems with coexisting ferroelectric and relaxor states

Goran Casar[1,2], Xinyu Li[3], Jurij Koruza[1,2], Qiming Zhang[3], Vid Bobnar[1,2]

[1] Jožef Stefan Institute, Ljubljana, Slovenia
[2] Jožef Stefan International Postgraduate School, Ljubljana, Slovenia
[3] Department of Electrical Engineering and Materials Research Institute, The Pennsylvania State University, University Park, Pennsylvania 16802, USA

goran.casar@ijs.si

Dielectric spectroscopy investigates electrically-induced properties of a material as a function of frequency and/or temperature. Dielectric properties are related to polarizability and thus depends on the structure and molecular properties of a material. That is why it is an useful tool for material characterization and is used in pharmacy, biotechnology and material science. The basic quantity in dielectric spectroscopy is complex dielectric constant ε^*, which consists of the real, ε', and imaginary, ε'', part. The real part is related to stored energy within the medium, whereas the imaginary part describes the losses. That is why the dielectric constant is very important in devices for storing electrical energy (capacitors).

Numerous materials are also able to convert the electrical energy into mechanical work (electromechanical effect) or into heat (electrocaloric effect) – note that electrical energy converted into heat in electrocalorics is not due to the electrical current running through it. Such properties of a material can be utilized in many devices such as actuators, sonars, integrated microelectromechanical systems or artificial muscles, which use the electromechanical effect, or in heating/cooling devices of new generation, which use the electrocaloric effect.

Our aim was to investigate P(VDF-TrFE), irradiated with lower doses, which was believed to be neither ferroelectric nor completely transformed into a relaxor. In our work we show, by means of dielectric spectroscopy and differential scanning calorimetry, that ferroelectric and relaxor states indeed coexist in P(VDF-TrFE), irradiated with low and moderate doses. In addition we demonstrate how such a coexistence influences some of the materials properties, particularly the electrocaloric response.

MEDNARODNA PODIPLOMSKA ŠOLA JOŽEFA STEFANA

JOŽEF STEFAN INTERNATIONAL POSTGRADUATE SCHOOL

ELECTRICAL AND THERMAL PROPERTIES OF POLYMER SYSTEMS WITH COEXISTING FERROELECTRIC AND RELAXOR STATES

Goran Casar,[1,2] Xinyu Li,[3] Jurij Koruza,[1] Qiming Zhang[3] and Vid Bobnar[1]

[1]*Jožef Stefan Institute and Jožef Stefan International Postgraduate School, Jamova 39, SI-1000 Ljubljana, Slovenia*

[2]*Study Programme: Nanosciences and Nanotechnology; Supervisor: Asst. Prof. Dr. Vid Bobnar*

[3]*Department of Electrical Engineering and Materials Reasearch Institute, The Pennsylvania State University, University Park, Pennsylvania 16802, USA*

Exciting properties of relaxors:

- Giant electromechanical response;
- Large electrocaloric effect;
- High electric energy density, fast response speeds.

Potential applications:

- Actuators, sonars, artificial muscles;
- Heating/cooling devices of new generation;
- Capacitors.

- **Ferroelectrics** ↔ Long-range dipolar order;
- **Inorganic relaxors** ↔ Compositionally disordered systems, short-range dipolar order;
- **Relaxor polymers** ↔ Disorder is introduced into a ferroelectric polymer by either high-energy electron irradiation or incorporation of additional monomers into the polymer chain.

Fundamental physical properties

Dielectric spectroscopy, particularly nonlinear dielectric investigations, and differential scanning calorimetry reveal the coexistence of ferroelectric and relaxor states.

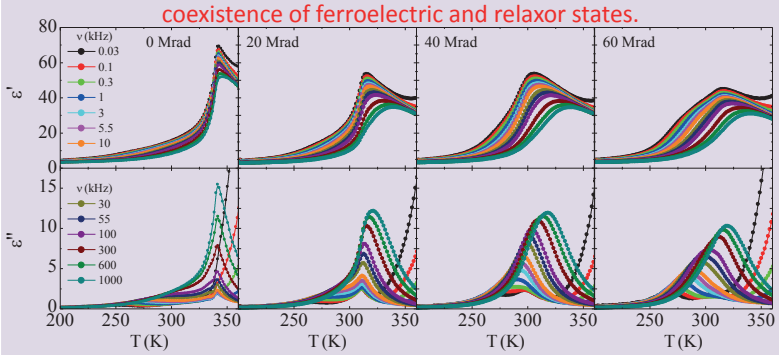

Figure 1: Dispersive maxima in the temperature dependences of the real and imaginary parts of the linear dielectric constant reveal the relaxor nature of irradiated samples. Complex linear dielectric constant was measured by HP4284A Precision LCR Meter during cooling runs with the rate of -0.5 K/min.

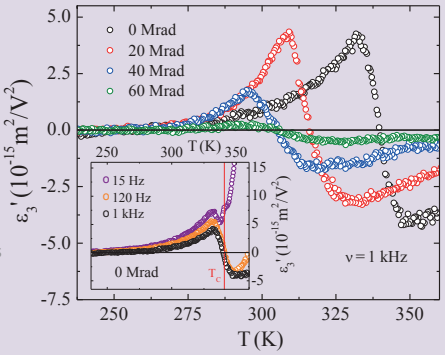

Figure 2: The nonlinear dielectric response, i.e. the third harmonic vs. temperature, which changes sign, reveals that the ferroelectric states remain persistent in the irradiated samples. The response was measured at various frequencies by using HP35665A Dynamic Signal Analyzer.

Applied-oriented research

Due to the coexistence of phases the electrocaloric effect is further enhanced.

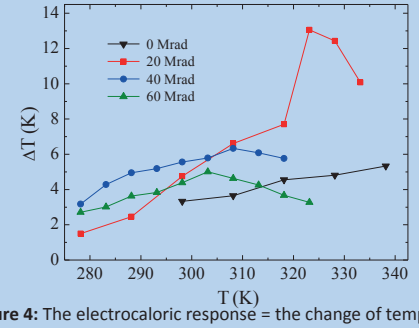

Figure 4: The electrocaloric response = the change of temperature when the electric field is adiabatically applied or removed. The response was measured using specially designed calorimeter.

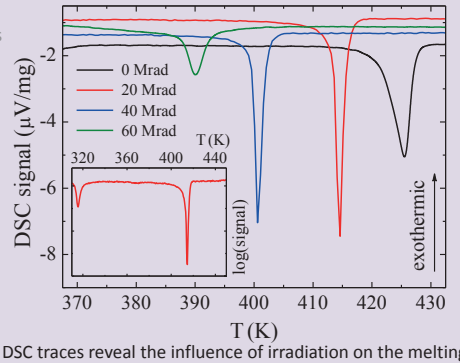

Figure 3: DSC traces reveal the influence of irradiation on the melting point (main frame) and confirm the coexistence of ferroelectric and relaxor states in irradiated samples (inset). The curves were recorded on a Netzsch DSC 204 F1 calorimeter. Temperatures at peaks maxima are phase transition temperatures and the area of peaks is proportional to the crystallinity of samples.

We report dielectric, thermal and electrocaloric investigations of P(VDF-TrFE) copolymer, irradiated with high-energy electrons. While up to now investigations have mainly focused either on non-irradiated ferroelectric P(VDF-TrFE) copolymer or P(VDF-TrFE), irradiated with high doses, which is completely transformed into a relaxor, we concentrate on samples, irradiated with low or moderate doses. We show that in these samples (i) ferroelectric and relaxor states coexist and that, consequently, (ii) large electrocaloric response of P(VDF-TrFE)-based systems is further enhanced.

Synthesis of superparamagnetic clusters as a carrier for wine fining agents

Peter Dušak[1,2], **Slavko Kralj**[1], **Darko Makovec**[1,2]

[1] Department of Materials Synthesis, Jožef Stefan Institute, Ljubljana, Slovenia

[2] Jožef Stefan International Postgraduate School, Ljubljana, Slovenia

peter.dusak@ijs.si

Magnetic particles are promising materials for magnetic carriers, because they can be guided or held on a certain point in a magnetic-field gradient. Magnetic carriers are used in biomedicine, e.g. for drug delivery systems, in biotechnology for separation of products from complex mixture, in food industry for cleaning products from unwanted ingredients, in remediation of water from heavy-metal pollution, etc. In mentioned applications, magnetic particles are dispersed into mixture containing targeted species, e.g. molecules, cells or microorganisms. After the attachment of targeted species onto the magnetic particle, the conjugate is separated from the mixture using an external magnetic field. To disperse magnetic particles it is beneficial if they are small enough to be in superparamagnetic state, which is usually less than 20nm. The use of superparamagnetic nanoparticles is beneficial, because they do not show spontaneous magnetic moments and in contrast to larger ferri/ferromagnetic particles, they do not agglomerate due to magnetic dipole-dipole interactions.For separation applications used in biotechnology, chemistry and especially in food industry the size of magnetic carriers is very important. In applications that involve guiding particles in a magnetic-field gradient, assembly of superparamagentic nanoparticles into clusters shows a distinct advantage over individual superparamagnetic nanoparticles, due to much larger the magnetic force acting on them in a magnetic field gradient. Besides the size, the carrier surface has an important role in the separation applications. The carriers' surfaces need to be specifically functionalized, i.e. appropriate functional groups have to be provided at their surfaces to enable specific interactions with the targeted species needed to be separated. The aim of our work was to study the controlled synthesis of superparamagnetic clusters, with heteroagglomeration, i.e. agglomeration between oppositely charged particles, in aqueous suspensions. These clusters would be further functionalized with a specific species, e.g. molecules, proteins, enzymes, which would interact with specific targeted species. As-prepared superparamagnetic clusters are developed to be used in food and beverage industry to separate allergen species.

MEDNARODNA PODIPLOMSKA ŠOLA JOŽEFA STEFANA

JOŽEF STEFAN INTERNATIONAL POSTGRADUATE SCHOOL

SYNTHESIS OF SUPERPARAMAGNETIC CLUSTERS AS A CARRIER FOR WINE FINING AGENTS

PETER DUŠAK, Slavko Kralj, Darko Makovec
Study programme: Nanoscience and nanotechnologies,
Jožef Stefan International Postgraduate School
SUPERVISOR: prof. dr. DARKO MAKOVEC
Jožef Stefan Institute, Jamova cesta 39, 1000 Ljubljana

INTRODUCTION

- phenolic and polyphenolic compounds cause haze formation, which presents a problem for wineries
- fining agents working on protein-polyphenol interaction are used to stabilize wine, BUT:
- some proteins, e.g. caseinate, can cause allergic reactions by consumers
- the removal of allergenic fining agents can be achieved by immobilization of fining agents to an appropriate carrier
- superparamagnetic nanoparticles can be used as a carrier in separation applications because of their ability to be manipulated with an external magnetic field
- in applications involving guiding particles in a magnetic-field gradient, assembly into superparamagnetic clusters show a adventage over the individual superparamagnetic nanoparticle
- controlled heteroagglomeration of maghemite superparamagnetic nanoparticles in aqueous suspension was used to prepare superparamagentic clusters (SCs)

APPLICATION

SUPERPARAMAGNETIC CLUSTERS

SEPARATION APPLICATIONS

PROTEIN CARRIER

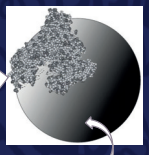

a **support** for immobilization of **protein** used as a fining agent

SCIENTIFIC

MODEL TYPE OF NANOPARTICLES

CARBOXYL- functionalized silica- coated superparamagnetic maghemite nanoparticles (cMNPs) and AMINO- functionalized silica nanoparticles (aSNPs) were used to study interactions between nanoparticles to form clusters with heteroagglomeration

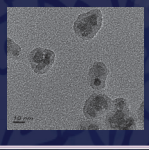

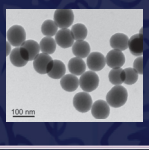

clusters =

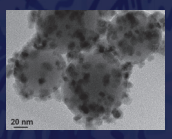

FORMED by:

a) ELECTROSTATIC INTERACTIONS;
at the biggest difference of zeta potential

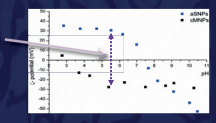

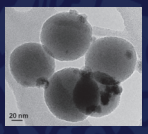

Increasing concentration

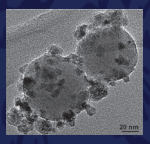

b) CHEMICAL INTERACTIONS;
by activation of carboxyl and amine surface groups

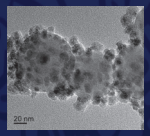

better coverage of aSNPs compared to electrostatic interactions

THE SYNTHESIS OF SUPERPARAMAGNETIC CLUSTERS

formed by different functionalized types of superparamagentic iron oxide nanoparticles

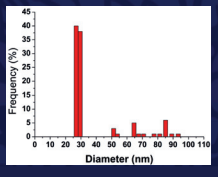

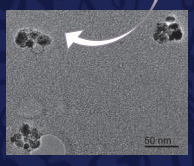

ACKNOWLEDGMENT: This work was financially supported by ARRS. The authors acknowledge the use of equipment in the CENN - Nanocenter

Investigation of the structural, optical and electrical properties of Ta_2O_5-rich thin films from solution

Raluca C. Frunză[1,2], Martin Strojnik[1], Marko Jankovec[3], Marko Topič[3], Barbara Malič[1]

[1] Jožef Stefan Institute, Ljubljana, Slovenia

[2] Jožef Stefan International Postgraduate School, Ljubljana, Slovenia

[3]Faculty of Electrical Engineering, University of Ljubljana, Tržaška cesta 25, Ljubljana, Slovenia

raluca.frunza@ijs.si

The trend in electronics nowadays is to produce transparent and flexible devices which could be used in applications such as flat panel displays, thin-film transistors (TFTs), solar cells, organic light emitting diodes (OLEDs), etc.. Since a lot of them are just concept devices, research is made for the development of industry oriented materials and technologies. Transparent materials, possibly with an amorphous structure, are of interest. Furthermore, one main requirement for transparent electronics is the low cost deposition onto substrates requiring low temperature processing, as glass or even plastic.Several different high-K (K= permittivity, dielectric constant) metal oxides are researched, and tantalum oxide (Ta_2O_5) is a promising candidate due to its high relative permittivity (about 25 for the amorphous state), good thermal and chemical stability. Still, its high leakage currents tend to limit the advantages of pure Ta_2O_5 as high-K dielectric. To improve its electrical properties, novel amorphous multicomponent dielectrics, resulting from mixing in a single phase Ta_2O_5 and low K oxides may be considered.

From the technological point of view, these materials can be fabricated using several methods, including atomic layer deposition, sputtering, chemical solution deposition, and various processes based on chemical vapour deposition. Physically deposited layers of pure or mixtures of Ta_2O_5 were processed at low temperatures to be used in transparent TFTs. However, little work has been done on the sol-gel preparation of such materials.

This study aims at the investigation of structural, optical and electrical properties of low temperature processed high-K thin films from solution. Samples of both the ternary composition $Ta_2O_5 – Al_2O_3 – SiO_2$ with the Ta:Al:Si = 8:1:1 atomic ratio and pure Ta_2O_5 were processed at 300 °C and 400 °C.

MEDNARODNA PODIPLOMSKA ŠOLA JOŽEFA STEFANA

JOŽEF STEFAN INTERNATIONAL POSTGRADUATE SCHOOL

Investigation of the structural, optical and electrical properties of Ta_2O_5-rich thin films from solution

Raluca C. Frunză[1,2], M. Strojnik[1], M. Jankovec[3], M. Topič[3], B. Malič[1]

[1] Jožef Stefan Institute, Ljubljana, Slovenia

[2] Jožef Stefan International Postgraduate School, Ljubljana, Slovenia

[3] Faculty of Electrical Engineering, University of Ljubljana, Tržaška cesta 25, Ljubljana, Slovenia

raluca.frunza@ijs.si

Introduction

In the last decades, transparent electronics became one of the most fascinating and fast growing research areas. It aims towards the realization of fully transparent devices, and thus it requires the low cost deposition of semiconducting or dielectric thin films with suitable properties onto the substrates requiring low temperature processing, as glass or even plastic. Among the dielectric materials, tantalum pentoxide (Ta_2O_5) has promising properties. Ta_2O_5-rich thin films on glass and platinized silicon substrates were processed by Chemical Solution Deposition (CSD) and processed at 300 °C – 400 °C. The samples were characterized from the structural, optical and electrical point of view.

Experimental

Solution synthesis

The precursors for Ta_2O_5–based thin films were prepared via the alkoxide-based sol gel synthesis.

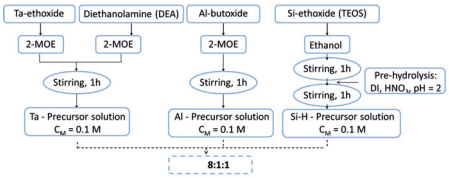

Thin film processing

- Substrates:
  - Borosilicate glass
  - Pt(111)/TiO_2/SiO_2/Si (Pt/Si)
- Compositions:
  - Ta_2O_5 (Ta)
  - Ta_2O_5–Al_2O_3–SiO_2 with the Ta:Al:Si = 8:1:1 (8:1:1)
- Spin coating: 30 s, 3000 rpm
- Drying: 2 min at 150°C
- Pyrolysis: 2 min at 300°C, 400°C,

Results

XRD

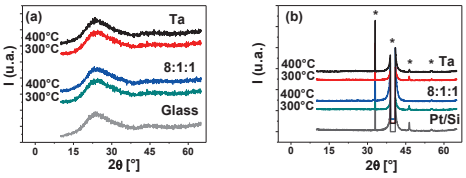

Diffractograms of Ta_2O_5-based thin films spin-coated on glass (a) and Pt/Si (b). The Pt/Si substrate peaks are denoted by *.

AFM

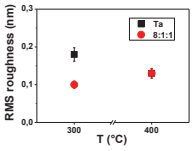

Root mean square (RMS) vertical surface roughness as determined from the AFM images of the Pt/Si samples.

Thickness of the samples

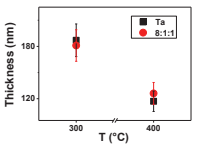

Thickness values as estimated from the FE-SEM cross-section images of the Ta_2O_5-based films on Pt/Si.

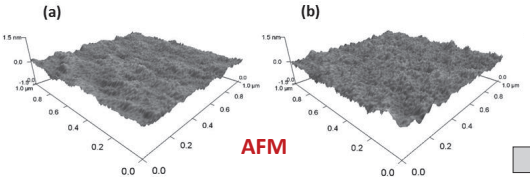

AFM 3D topography of the Ta (a) and 8:1:1 (b) samples deposited on Pt/Si and heated at 400 °C.

Electrical properties

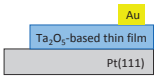

MIM configuration

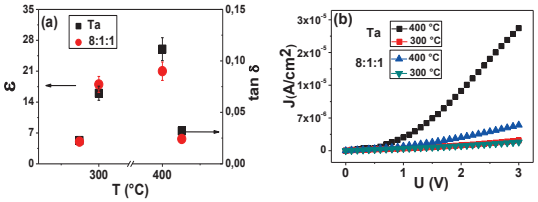

Room temperature dielectric properties (a) and I(V) characteristics (b) measured in a metal-insulator-metal (MIM) configuration.

Transmittance

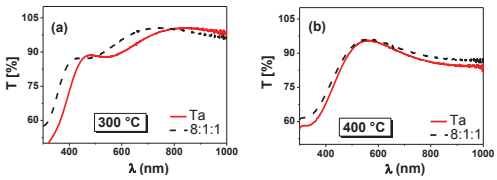

Optical transmittance spectra of the Ta_2O_5-based thin films deposited on glass.

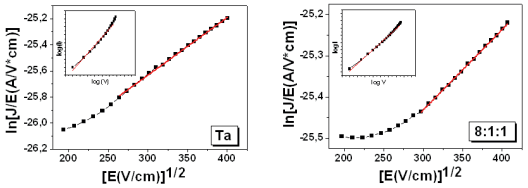

J-E characteristics of the MIM capacitors plotted as ln(J/E) vs $E^{1/2}$ for the thin films heated at 300 °C. The insets show the log V vs. log I plots.

Conclusions

Solution-derived Ta_2O_5 – Al_2O_3 – SiO_2 (Ta:Al:Si = 8:1:1 atomic ratio) and Ta_2O_5 thin films were processed at the temperatures 300 °C and 400 °C. All films were XRD-amorphous and showed high optical transparency in the visible range. The dielectric permittivity values of the thin films heated at 400 °C were 22 and 27 for the 8:1:1 and the Ta samples, respectively. The samples heated at 300 °C exhibited an ε value of about 18 for both compositions. As compared to the pure Ta_2O_5 thin films, the samples with the mixed composition showed lower leakage within the investigated temperature range. The current-voltage characteristics were ohmic at low applied electric fields and exhibited Poole-Frenkel behaviour at higher applied fields.

Co-sintering of magnetoelectric composites of Co-ferrite and selected ferroelectrics

Petra Jenuš[1,2], **Darja Lisjak**[1], **Danjela Kuščer**[3,4], **Darko Makovec**[1,2,5], **Miha Drofenik**[1,6]

[1] Department for Materials Synthesis, Jožef Stefan Institute, Ljubljana, Slovenia

[2] Jožef Stefan International Postgraduate School, Ljubljana, Slovenia

[3] Electronic Ceramics Department, Jožef Stefan Institute, Ljubljana, Slovenia

[4] Centre of Excellence NAMASTE, Ljubljana, Slovenia

[5] CENN Nanocenter, Ljubljana, Slovenia

[6] Faculty of Chemistry and Chemical Engineering, Maribor, Slovenia

petra.jenus@ijs.si

Magneto-electric (ME) ceramic composites of cobalt ferrite (CoF) and lead zirconate titanate (PZT) or barium titanate (BT) were prepared by mechanical mixing of the constituent powders followed by co-sintering at low temperatures (900-1000°C). It was found that the CoF powder needs to be pre-sintered at 700°C for 2h in order to minimize the differences in the sintering kinetics of the constituent powders. The optimization of the co-sintering conditions in order to prepare dense ceramic ME composites, which can display ME effect, was under investigation.

MEDNARODNA PODIPLOMSKA ŠOLA JOŽEFA STEFANA

JOŽEF STEFAN INTERNATIONAL POSTGRADUATE SCHOOL

PREPARATION OF MAGNETOELECTRIC COMPOSITES OF CO-FERRITE AND SELECTED FERROELECTRICS

Petra Jenuš[1,2], Darja Lisjak[1], Danjela Kuščer[3,4], Darko Makovec[1,2,5,*], Miha Drofenik [1,6]

[1] Department for Materials Synthesis, Jožef Stefan Institute, Ljubljana, Slovenia
[2] Jožef Stefan International Postgraduate School, Ljubljana, Slovenia, Programe Nanosciences and Nanotechnologies
[3] Electronic Ceramics Department, Jožef Stefan Institute, Ljubljana, Slovenia
[4] Centre of Excellence NAMASTE, Ljubljana, Slovenia
[5] CENN Nanocenter, Ljubljana, Slovenia
[6] Faculty of Chemistry and Chemical Engineering, 2000 Maribor, Slovenia
petra.jenus@ijs.si; * supervisor prof. dr. Darko Makovec

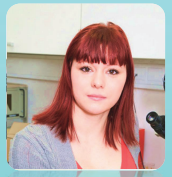

MAGNETOSTRICTIVE material + **PIEZOELECTRIC** material = **MAGNETOELECTRIC (ME)** composite

$CoFe_2O_4$ (CoF)

- Hydrothermal synthesis @ 200°C for 2h
- d ≈ 20 nm

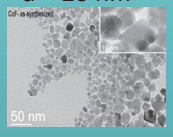

- Pre-fired @ 700°C for 2h

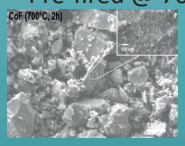

$Pb(Zr_{0.53}Ti_{0.47})O_3$ (PZT)

- Solid-state synthesis
- Milling
- Sub-micron size

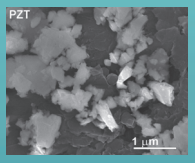

$BaTiO_3$ (BT)

- Inframat Advanced Materials
- d = 50 nm

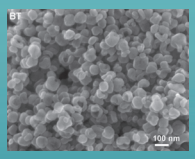

Converse ME effect = $\frac{\text{electric}}{\text{mechanical}} \times \frac{\text{mechanical}}{\text{magnetic}}$

Control of magnetic properties with electric field

Where to use this? ?

- Mechanical mixing of constituent powders (mass ratio 1:1)
- Uni-axial pressed into discs
- Co-sintered @ 900, 950 or 1000°C for 4h

SEM

CoF-BT

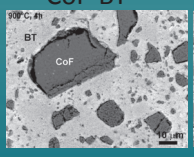

CoF-PZT

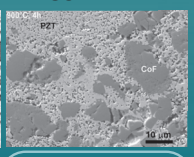

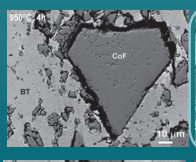

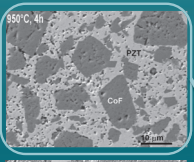

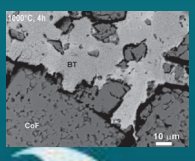

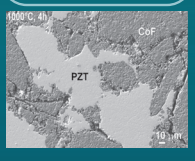

XRD (samples sintered @950°C for 4h)

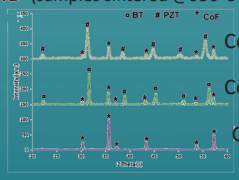

Magnetic properties

- Samples sintered @ 950°C for 4h

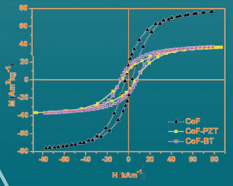

CONVERSE ME EFFECT

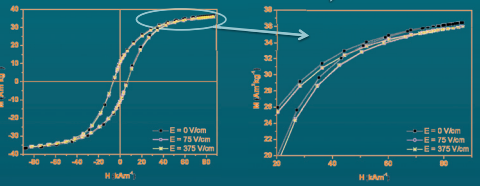

Potentially useful in novel multifunctional devices.

NOVEL MEMORY DEVICES

WHERE IS THE LIMIT?

SENSORS

The co-sintering of $CoFe_2O_4$-$PbZr_{0.53}Ti_{0.47}O_3$ and $CoFe_2O_4$-$BaTiO_3$ ceramic composites were investigated. The much higher sintering rate of the as-synthesized $CoFe_2O_4$ nanopowder was suppressed by pre-firing of the powder at 700°C for 2h. The optimum co-sintering conditions were determined to be 950°C for 4h. The converse magneto-electric (ME) effect was measured in terms of the influence of an applied electric field on the magnetization.

Acknowledgement: This work was financially supported by the Slovenian Research Agency. CENN Nanocenter for the use of the equipment.

The influence of oleic acid on the morphology and magnetic properties of $CoFe_2O_4$ nanoparticles

Sonja Jovanović[1,2], **Matjaž Spreitzer**[1], **Mojca Otoničar**[1,2], **Danilo Suvorov**[1,2]

[1] Advanced Materials Department, Jožef Stefan Institute, Ljubljana, Slovenia

[2] Jožef Stefan International Postgraduate School, Ljubljana, Slovenia

sonja.jovanovic@ijs.si

In the last couple of decades cobalt ferrite has become an interesting magnetic material as a result of its properties, such as a large magneto-crystalline anisotropy, moderate saturation magnetization, good chemical stability and mechanical hardness. On the basis of these properties it can be used in high-density information storage devices, spintronic devices, drug-delivery systems, sensors, etc. The presented results are obtained within a project that aims to enhance the applicability of cobalt ferrite nanoparticles by improving their size and shape uniformity as well as their dispersibility and magnetic properties.

MEDNARODNA PODIPLOMSKA ŠOLA JOŽEFA STEFANA

JOŽEF STEFAN INTERNATIONAL POSTGRADUATE SCHOOL

The influence of oleic acid on the morphology and magnetic properties of $CoFe_2O_4$ nanoparticles

Sonja Jovanović[1,2], Mojca Otoničar [1,2]

[1]Advanced Materials Department, Jožef Stefan Institute
[2] Jožef Stefan International Postgraduate School

Supervisors: Prof. Dr. Danilo Suvorov[1], Dr. Matjaž Spreitzer[1]

Introduction

Spinel cobalt ferrite ($CoFe_2O_4$, ***CFO***) is an outstanding magnetic material with a high Curie temperature, a large magnetization, a remarkable chemical stability and mechanical hardness [1–3]. Due to its magnetic properties, CFO can be used in high-density information-storage devices [4], spintronic devices [5,6], magnetoelectric transducers [7,8] and actuators [9,10].

The aim of this work was to investigate the influence of oleic acid on the formation of CFO nanoparticles obtained by a solvothermal synthesis method in order to improve their applicability by controlling the particle size and shape uniformity as well as the dispersibility and magnetic properties.

Experimental

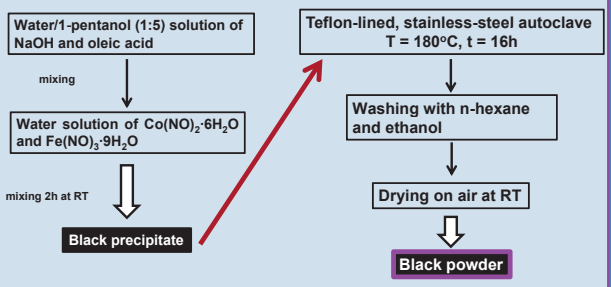

Results

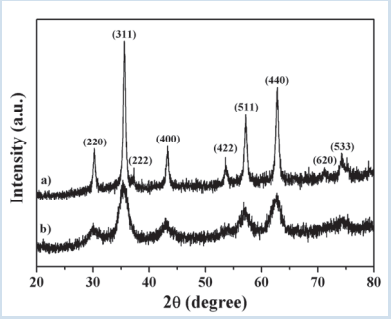

Figure 1. XRD patterns of the $CoFe_2O_4$ nanoparticles prepared a) without and b) with oleic acid.

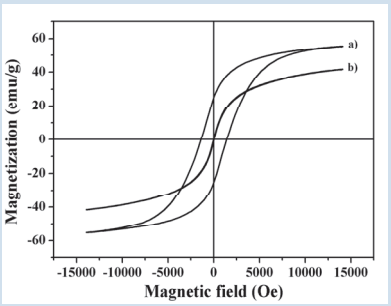

Figure 2. Hysteresis loops of the $CoFe_2O_4$ nanoparticles prepared a) without and b) with oleic acid.

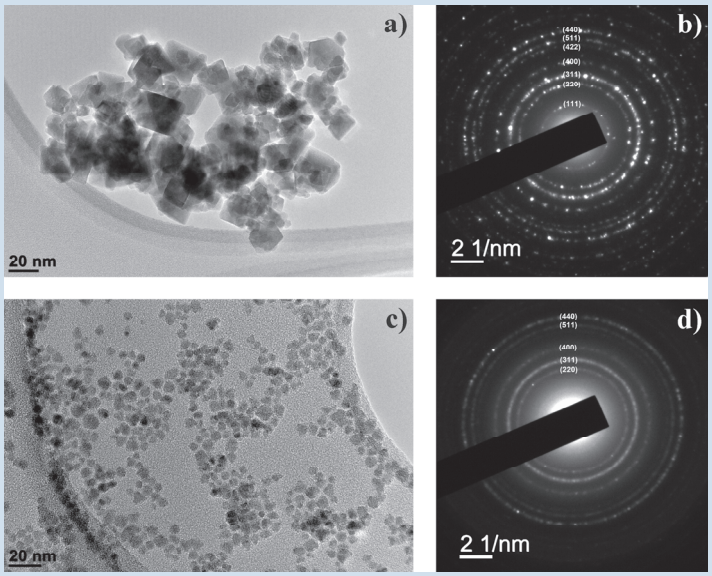

Figure 3. The TEM images and the selected-area electron diffraction (SAED) patterns of the $CoFe_2O_4$ nanoparticles prepared without oleic acid (a) and b)) and with oleic acid (c) and d)).

Conclusion

The obtained results indicate that oleic acid has a substantial influence on the crystallinity, morphology and dispersibility of CFO nanoparticles. Compared to the synthesis route in which the capping agent was absent, the size distribution of CFO nanoparticles become narrower and the shape uniformity was significantly improved. The layer of oleic acid that forms on the surface of nanoparticles is essential because it prevents the agglomeration and growth of the nanoparticles. As a result, CFO nanoparticles prepared with 1 M oleic acid are superparamagnetic in comparison to ferromagnetic nanoparticles prepared without oleic acid.

[1] D. Peddis, C. Cannas, G. Piccaluga, E. Agostinelli, D. Fiorani, Nanotechnology, 21(2010) 125705.
[2] R. Comes, H. Liu, M. Khokhlov, R. Kasica, J. Lu, S. A. Wolf, Nano Lett., 12 (2012) 2367.
[3] D. Peddis, N. Yaacoub, M. Ferretti, A. Martinelli, G. Piccaluga, A. Musinu, C. Cannas, G. Navarra, J. M. Greneche, D. Fiorani, J. Phys.:Condens. Matter., 23 (2011) 426004.
[4] E. Snoeck, C. Gatel, R. Serra, G. BenAssayag, J. B. Moussy, A. M. Bataille, M. Pannetier, M. Gautier-Soyer, Phys. Rev. B, 73 (2006) 104434.
[5] M. J. Carey, S. Maat, P. Rice, R. F. C. Farrow, R. F. Marks, A. Kellock, P. Nguyen, B. A. Gurney, Appl. Phys. Lett., 81 (2002) 1044.
[6] K. Inomata, N. Ikeda, N. Tezuka, R. Goto, S. Sugimoto, M. Wojcik, E. Jedryka, Sci. Technol. Adv. Mater., 9 (2008) 014101.
[7] H. Zheng, J. Wang, S. E. Lofland, Z. Ma, L. Mohaddes-Ardabili, T. Zhao, L. Salamanca-Riba, S. R. Shinde, S. B. Ogale, F. Bai, D. Viehland, Y. Jia, D. G. Schlom, M. Wuttig, A. Roytburd, R. Ramesh, Science , 303 (2004) 661.
[8] K. Srinivas, G. Prasad, T. Bhimasankaram, S. V. Suryanarayana, Mod. Phys. Lett. B, 14 (2000) 663.
[9] S. Monz, A. Tschope, R. Birringer, Phys. Rev. E, 78 (2008) 021404.
[10] F. Gazeau, C. Baravian, J. C. Bacri, R. Perzynski, M. I. Shilomis, Phys. Rev. E, 56 (1997) 614.

Microstructure, Yield Stress and Hardness in Weld Heat-Affected Zone of 9-12% Cr Steels

Fevzi Kafexhiu[1,2], **Franc Vodopivec**[1], **Jelena V. Tuma**[2]

[1] Department of Surface Engineering and Applied Surface Science, Institute of Metals and Technology, Ljubljana, Slovenia

[2] Jožef Stefan International Postgraduate School, Ljubljana, Slovenia

fevzi.kafexhiu@imt.si

The efficiency (electricity produced per unit of heat input) of power plants that use coal as an energy source, is obtained through higher temperatures and pressures of the steam that enters the turbine. Such conditions require materials with high creep resistance, i.e., the ability to withstand a long-term loading at high temperatures. This requires a careful material selection and a periodical checking of its properties and remaining lifetime after the certain period of operation in power plants. The checking of the creep strength is expensive and time-consuming. For this reason, simpler methods are being developed. Such methods use less expensive and faster tests and enable a quite reliable establishment of materials condition. One among these methods is to check the room-temperature mechanical properties and microstructure after a certain heat treatment, simulating changes of microstructure and properties that occur after a longer operation in a power plant (real conditions). The measured properties are then correlated with the creep rate, which is either measured using the standard creep test, or obtained through calculations using the most reliable models known up to date.

Welding, as the fundamental joining technique of vital parts of power plants, mainly made of steels with 9-12% Cr content, causes the creation of so-called heat affected zone (HAZ) consisting of few regions with different microstructures. This is because the welding process itself causes temperatures that are near the melting point of these steels. Two of these regions, namely coarse-grained (γ) and inter-critical ($\alpha+\gamma$) have been chosen for the present study, because the majority of failures in welded constructions made of 9-12% Cr steels occurred within these two regions.

MEDNARODNA PODIPLOMSKA ŠOLA JOŽEFA STEFANA

JOŽEF STEFAN INTERNATIONAL POSTGRADUATE SCHOOL

Microstructure, Yield Stress and Hardness in Weld Heat-Affected Zone of 9-12% Cr Steels

Fevzi Kafexhiu[1,2], Franc Vodopivec[2], Jelena Vojvodič-Tuma[1]

Study program: Nanosciences and Nanotechnology

[1]Jožef Stefan Internatinal Postgraduate School, Jamova 39, 1000 Ljubljana, Slovenia

Mentor: Prof. dr. Jelena Vojvodič - Tuma

[2]Institute of Metals and Technology, Lepi pot 11, 1000 Ljubljana, Slovenia

fevzi.kafexhiu@imt.si

INTRODUCTION

The key property of steels used at power plant operating conditions is their resistance to creep. The best choice for such application are the 9-12% Cr steels. It has been shown that there is a correlation between yield stress, hardness and stationary creep rate. Thus, the aim of this work was to study the effects of tempering on the microstructure, yield stress and hardness of two weld heat-affected zone (HAZ) regions, namely coarse grained (γ) and inter-critical (α+γ) for the X20CrMoV121 and P91 steels, simulating changes of microstructure and properties in real power plant conditions.

EXPERIMENTAL

I. Chemical analysis

Chemical composition, wt %

Elements	C	Si	Mn	P	S	Cr	Ni	Mo	V	Cu	Nb	Al	N
X20CrMoV121	0.2	0.29	0.52	0.019	0.011	11	0.64	0.94	0.31	0.059	0.024	0.032	0.017
P91	0.1	0.38	0.48	0.012	0.002	7.9	0.26	0.98	0.23	0.14	0.11	0.016	0.064

II. Welding

A multilayer tungsten inert gas (TIG) welding was performed.

III. Heat treatment

Tempering for 2, 4320, and 8760 h at 750°C, and up to 17520 h at 650°C.

IV. Room-temperature tensile tests and hardness measurements

Tensile tests - performed on the standard specimens (see the following figure).

Hardness measurements - on metallographic specimens used for SEM imaging.

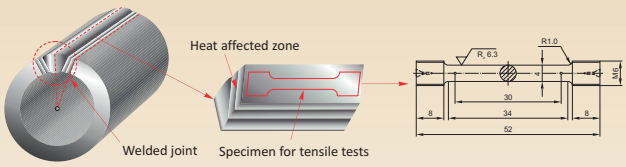

V. Scanning Electron Microscopy (SEM) imaging

The SEM specimens were prepared from the initial state of both HAZ regions, as well as after 2, 4320, and 8760 h of tempering at both 650°C and 750°C. Three images were acquired on each specimen at a magnification of 10 000×.

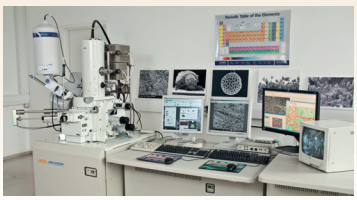

JEOL JSM-6500F FE-SEM at IMT

RESULTS

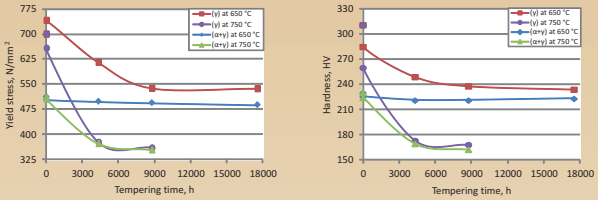

Changes of yield stress and hardness of the steel X20CrMoV121 due to the tempering

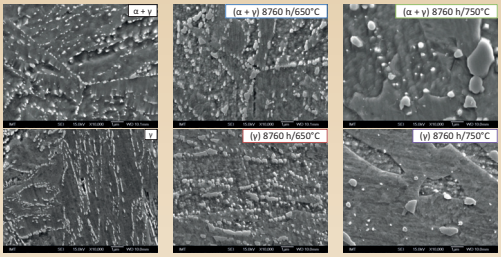

Microstructure evolution in the steel X20CrMoV121 due to the tempering

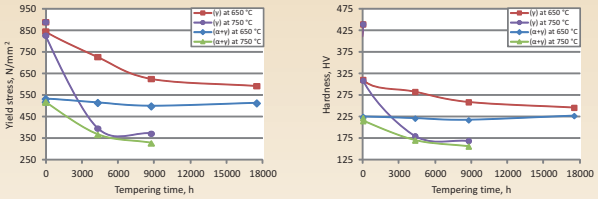

Changes of yield stress and hardness of the steel P91 due to the tempering

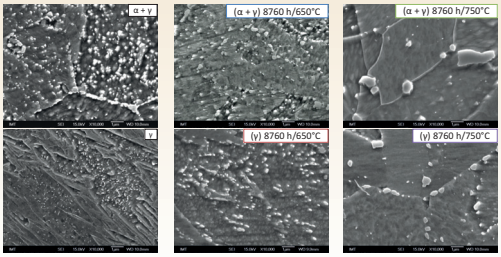

Microstructure evolution in the steel P91 due to the tempering

CONCLUSIONS

- Tempering at 650 °C causes relatively small changes of the microstructure and properties, unlike the tempering at 750 °C, where changes are more pronounced.
- Effect of tempering on the coarse-grained (γ) microstructure was greater for both steels and both tempering temperatures, in comparison to the inter-critical (α+γ) microstructure.
- The equalisation of the properties in the (γ) and (α+γ) after half year of tempering at 750°C, leads us to a conclusion of a greater role of stable precipitates compared to the role of the grain size in the microstructure of creep-resistant steels.

Single-step decoration of MoSI based nanowires with platinum nanoparticles

Andrej Kovič[1,2], Sumeet Kumar[3,4], Aleš Mrzel[1], Mojca Vilfan[1]

[1] Jožef Stefan Institute, Jamova 39, Ljubljana, Slovenia

[2] Jožef Stefan International Postgraduate School, Ljubljana, Slovenia

[3] Atoms Italia, Rossano Veneto, Italy

[4] Innovation Factory, AREA Science Park, Trieste, Italy.

andrej.kovic@ijs.si

We presented a simple step efficient self-decoration of $Mo_6S_yI_z$ ($8.2 \leq y+z \leq 10$) nanowires with platinum nanoparticles at room temperature without any additional reducing reagents. We were able to successfully decorate nanowires with platinum in the solution. The described procedure is one of the few examples of redox templating at room temperature without use of reducing agent to produce noble metal-decorated nanowires, which enables large scale production for different applications including sensors and platinum catalyzed reactions.

MEDNARODNA PODIPLOMSKA ŠOLA JOŽEFA STEFANA

JOŽEF STEFAN INTERNATIONAL POSTGRADUATE SCHOOL

Single-step decoration of MoSI based nanowires with platinum nanoparticles

Andrej Kovič, univ. dipl. kem.
Študijski program: Nanoznanosti in nanotehnologije,
Mednarodna podiplomska šola Jožefa Stefana
MENTOR: dr. ALEŠ MRZEL
SOMENTOR: Prof. dr. DRAGAN D. MIHAILOVIĆ
Inštitut Jožef Stefan, Jamova cesta 39, 1000 Ljubljana

Abstract

Solution based *in situ*, single step coatings with platinum nanoparticles of MoSI-based nanowires is presented in this communication. An average particle diameter of 2.25 nm (±0.66 nm) was obtained for Pt-coated MoSI nanowires, showing a narrow size distribution. Single-step *in situ* reduction method could be applied for large-scale applications, given the economic and environment viability of such synthesis process.

Experimental

Bundles of $Mo_6S_yI_z$ ($8.2 \leq y+z \leq 10$) nanowires were synthesized directly from the elements in a one-step procedure. The ampoule was left for 60 hours in a temperature gradient with lower temperature being 750 °C and higher temperature 850 °C. At the higher-temperature end, the remaining material was a dark-brown powder (Fig. 1a). We have shown previously that the obtained powder consists of bundles of nanowires, molybdenum grains and MoS_2 crystals [1](Fig 1b). After sonication, the supernatant was extracted (Fig. 2a) and separated by centrifugation (1250*g* for one hour) to remove heavier MoS_2 crystals, molybdenum grains and bundles with larger diameters. The supernatant was micro-filtrated and dried at 50 °C, with resulting yield around 10 wt% and the average diameter of the bundles was around 20-80 nm (Fig. 2b).

By using a 2.5 mM water solution of $Na_2[PtCl_4]$ as a source of Pt, the bundles were self-decorated in 20 mg/L MoSI water dispersion. The density of Pt nanoparticles on NWs was controlled simply by changing the amount of the added $Na_2[PtCl_4]$ solution (Fig 3a). A proof that the observed material are indeed $Mo_6S_yI_z$ ($8.2 \leq y+z \leq 10$) nanowires covered with platinum (Fig. 3a) is given by the energy-dispersive X-ray spectrum (EDS), shown in Fig. 3b.

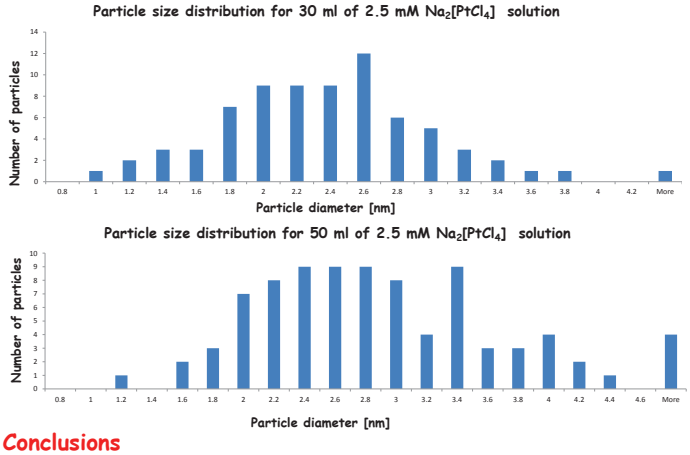

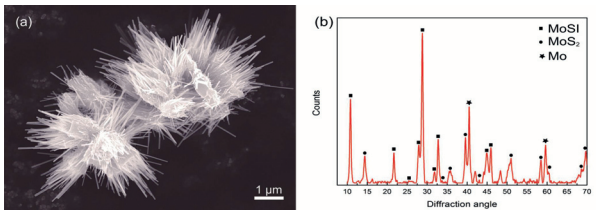

Fig 1: SEM image of the synthesized material obtained directly from the chemical transport reaction (a). XRD of the same material (b) showing its composition: $Mo_6S_yI_z$ ($8.2 \leq y+z \leq 10$) nanowires (squares), MoS_2 (circles), and Mo (asterisks)

sonication

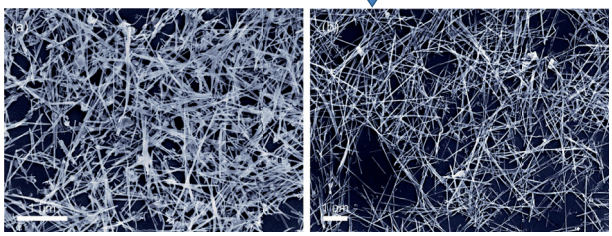

Fig 2: SEM images of $Mo_6S_yI_z$ ($8.2 \leq y+z \leq 10$) nanowire bundles before (a) and after (b) purification

$Na_2[PtCl_4]_{(aq)}$

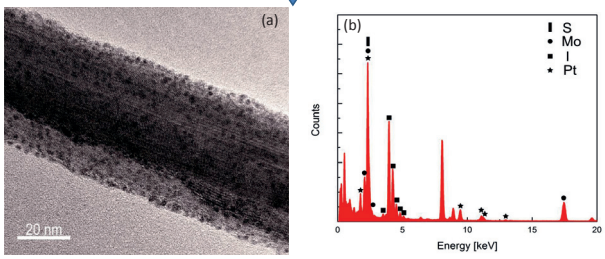

Fig. 3: (a)TEM image of MoSI nanowire decorated with platinum nanoparticles, (b) EDS spectrum confirming the composition of the obtained material

Conclusions

We presented a simple step efficient self-decoration of $Mo_6S_yI_z$ ($8.2 \leq y+z \leq 10$) nanowires with platinum nanoparticles at room temperature without any additional reducing reagents. We were able to successfully decorate nanowires with platinum in the solution. The described procedure is one of the few examples of redox templating at room temperature without use of reducing agent to produce noble metal-decorated nanowires, which enables large scale production for different applications including sensors and platinum catalyzed reactions.

References
[1] Kovič A., Žnidaršič A., Jesih A., Mrzel A., Gaberšček M., Hassanien A.: A novel facile synthesis and characterization of molybdenum nanowires. *Nanoscale research letters*, 2012, vol. 7, str. 567-1-567-7

Photocatalytic water treatment with TiO_2: slurry reactor vs. microreactor

Matic Krivec[1,2], Luka Suhadolnik[1], Kristina Žagar[1], Miran Čeh[1,2], Goran Dražić[1,2]

[1] Department for Nanostructured Materials, Jožef Stefan Institute, Ljubljana, Slovenia

[2] Jožef Stefan International Postgraduate School, Ljubljana, Slovenia

matic.krivec@ijs.si

Remediation and elimination of hazardous chemicals and wastes from contaminated waters is a growing concern of societies all over the world. Photocatalytic degradation with TiO_2 is a prospective solution to overcome this problem, although the procedure contains several engineering limitations which prevent the scale-up of the process. Photocatalytic degradation inside a microreactor with immobilized TiO_2 has several advantages in comparison to the conventional TiO_2-type reactors: the system works in the continuous operation mode, there is no need for an additional catalyst separation operation and the provided light is homogeneously distributed in the whole reactor depth. Moreover, the reactor can be optimized to its final version in a laboratory as the numbering-up process replaces the standard scale-up process in the industry. The parallel binding of these reactors results in higher flows and consequently higher efficiencies of this system without changing (reducing) the activity of the reactor during scale-up.

MEDNARODNA PODIPLOMSKA ŠOLA JOŽEFA STEFANA

JOŽEF STEFAN INTERNATIONAL POSTGRADUATE SCHOOL

Photocatalytic water treatment with TiO_2: slurry reactor vs. microreactor

Matic Krivec, univ. dipl. biok.
Study programme: Nanoscience and Nanotechnology
Jožef Stefan International Postgraduate School
Mentor: doc. dr. Goran Dražić
Jožef Stefan Institute, Jamova 39, 1000 Ljubljana, Slovenia

Motivation…

In recent years, the availability of a clean and non-polluted water sources is dropping rapidly, especially in third world countries. Aliphatic carboxylic acids, dyes, simple aromatics, halogenated alkanes, pesticides and other hazardous chemicals start to accumulate in water and present a huge environmental and health problem.

Solution…

Photocatalytic degradation of the pollutants with TiO_2:

- complete mineralization:

Pollutant (e.g. caffeine) $\xrightarrow{TiO_2}$ $CO_2 + H_2O$ (UV-light)

Techniques…

Slurry reactor (suspended TiO_2)

- (+) High surface-to-volume ratio
- (+) Catalyst replacement (fouling)
- (+) Uniform catalyst distribution
- (-) Post-process filtration
- (-) Low illuminated surface area

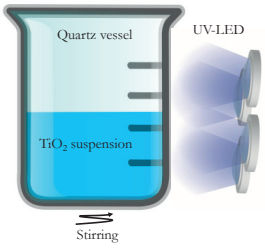

Microreactor (immobilized TiO_2)

- (+) High surface-to-volume ratio
- (+) No need for post-process filtration
- (+) High spatial illumination
- (+) Good light penetration
- (+) Continuous operation
- (-) Possible fouling effect

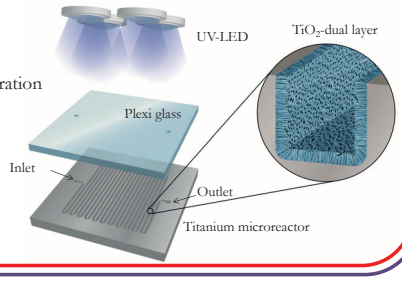

Results…

Characteristic	Surry reactor	Microreactor
State of TiO_2	Suspended (Degussa P25)	Immobilized (nanotubes + particles)
TiO_2 phase	Anatase, rutile	Anatase
Reactor volume [mL]	10	0.07
Surface-to-volume ratio [m^2/m^3]	2000-7000	6780
UV-LED intensity [mW/cm^2]	1.2	1.2

Langmuir-Hinshelwood (L-H) degradation mechanism:

$$R_i = -\frac{d[caffeine]}{dt} = \frac{k_a K c_i}{1 + K c_i}; \qquad \frac{1}{R_i} = \frac{1}{k_a} + \frac{1}{k_a K}\frac{1}{c_i}$$

linearization

c_i; initial caffeine concentration
k_a; reaction rate constant
K; adsorption coefficient

Reactor type	C_i [mg L^{-1}]	ξ [%]	ξ_{stand} [cm^{-2}]*10^{-3}
Slurry reactor	25	1.49	0.006
	10	0.10	0.008
	5	0.59	0.014
	2.5	0.42	0.021
Microreactor	25	0.30	0.62
	10	0.29	0.61
	5	0.20	0.42
	2.5	0.10	0.22

Photonic efficiency:

$$\xi = \frac{R_i}{I_0}$$

R_i; initial raction rate
I_0; incident monochromatic light intensity

Standardized photonic efficiency:

$$\xi_{stand} = \frac{\xi}{A}$$

A; photocatalytic surface area

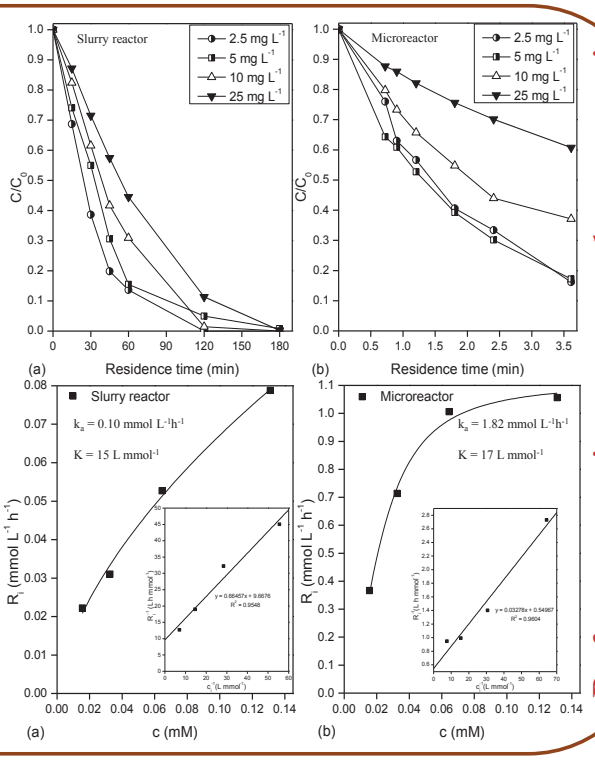

Performance: microreactor > slurry reactor!

Quasiparticle relaxation through the superconducting gap above T_c measured by multipulse femtosecond spectroscopy in $Bi_2Sr_2CaCu_2O_{8+d}$

Ivan Madan[1], Migaku Oda[2], Y. Toda[2], Tomaž Mertelj[1], Dragan Mihailović[1]

[1] Complex Matter Department, Jozef Stefan Institute, Ljubljana, Slovenia
[2] Department of Applied Physics, Hokkaido University, Sapporo, Japan

ivan.madan@ijs.si

In the conventional pump-probe experiments above T_c weak superconducting component of transient reflectivity signals cannot be distinguished from the strong pseudogap component. Novel three pulse technique allows us to measure recovery of the superconducting state after superconducting-to-normal state laser induced transition. In the low excitation regime this kind of phase transition occurs without perturbing the pseudogap subsystem thus allowing us to detect the recovery of weak superconducting component above Tc.

In the present work we investigated underdoped $Bi_2Sr_2CaCu_2O_{8+\delta}$ 2212 with T_c =81 K and show appearance of the superconducting quasiparticle response up to 102 K. This temperature is 11 K higher than T_c of optimally doped samples, so the effect cannot be attributed to local inhomogeneities.

complexmatter | Jožef Stefan Institute

Quasiparticle relaxation across the superconducting gap above T_c measured by multipulse femtosecond spectroscopy in underdoped $Bi_2Sr_2CaCu_2O_{8+d}$ (T_c=81 K)

I. Madan*, M. Oda**,Y. Toda**, T.Mertelj*, D. Mihailovic*
* Complex Matter Department, Jozef Stefan Institute, Jamova 39, 1000 Ljubljana, Slovenia
**Department of Applied Physics, Hokkaido University, Sapporo 060-8628, Japan

Abstract:

Using a novel 3-pulse technique we investigate the QP recombination across the superconducting gap and the psesudogap as the system evolves through the superconducting-to-normal transition induced by a strong laser pulse. In conventional pump-probe experiments above T_c a weak superconducting component of transient reflectivity signals cannot be distinguished from the strong pseudogap component. In the low excitation regime, this kind of phase transition occurs without perturbing the pseudogap subsystem thus allowing us to detect the recovery of the weak superconducting component above Tc.

In the present work we investigated underdoped $Bi_2Sr_2CaCu_2O_{8+\delta}$ 2212 with T_c =81 K and show the appearance of the superconducting quasiparticle response up to 102 K. This temperature is 11 K higher than T_c of optimally doped samples, so the effect cannot be attributed to local doping inhomogeneities.

Introduction:

Disentangling the superconducting (SC) response from the pseudogap (PG) in different experiments and understanding the connection between these states is an important issue in the physics of high-Tc superconductors. In the conventional pump-probe transient reflectivity measurements careful selection of wavelength and polarization of both pump and probe beams will give a different sign of the reflectivity change for quasiparticles relaxing through the SC gap and the PG[1]. This feature is crucial for separating superconducting fluctuations above T_c from the pseudo-gap.

Superconducting fluctuations above T_c were previously observed in cuprates in ARPES measurements[2], as a diamagnetic effect [3], a Nernst effect [4], in the specific heat [5] and in paraconductivity measurements[7]. The beauty of our experiment qualitatively is that we do not need to make any assumptions of the PG behavior to separate the SC component from the signal. We gain new information about the lifetime of the excitation of the fluctuating state and the lifetime of the state itself.

We emphasize that this state is distinct from the pseudogap which persists up to much higher temperature, up to T^*~200 K.

The 3 pulse technique:

1. A high energy pulse (D-pulse) destroys superconductivity in the surface layer of the sample.

2. Transient refelctivity is probed by a sequence of weaker pump-probe (P-p) pulses at different delay $t_{D,P}$ after the D pulse.

For this work we used a Ti:Saphire amplifier (250 kHz REGA) seeded by a Ti:Saphire laser. The pulse length was 50 fs and the photon energy was 1.55 eV

In the present study we limit ourselves to low fluences of the destruction pulse up to 11μJ/cm^2 which is 5 times lower than the threshold for PG destruction.

The main advantage of this approach is that it allows to separate recovery of the superconducting state from quasiparticle relaxation.

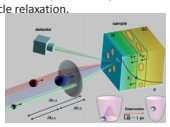

Fig.1 Schematic representation of 3 Pulse experiment. Colors are schematic.

The pump-probe response:

Below T_c the relaxation signal consists of three exponential components: the normal state component – which is temperature independent [1], the PG component which appears below T^*~200 K and the SC component which is dominant below T_c = 81 K.

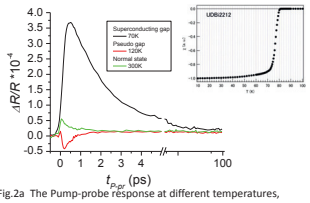

Fig.2a The Pump-probe response at different temperatures, revealing dominant signal in each temperature region.
Inset: Magnetic susceptibility measurements shows Tc = 81 K.

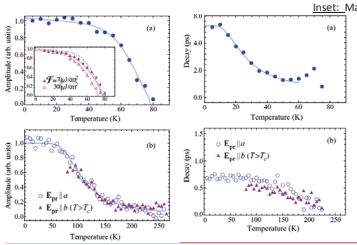

Fig.2b. Superconducting (a) and Pseudogap (b) amplitude and relaxation time temperature dependences measured separately using two-color spectroscopy (Data from [1] Tc = 78 K).
Relaxation time of superconducting component shows divergence at critical temperature.

Infrared two-color ultrafast spectroscopy was performed using OPA and signal is to weak for accurate detection of fluctuations contributions

Recovery dynamics of the superconducting state **below T_c**

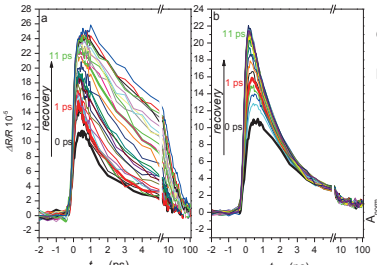

Fig.3 The raw pump-probe signal at different delays after the destruction pulse in the SC state at 15 K (a) and 65 K(b).

At the selected fluence below T_c destruction of the SC is incomplete.

Measured recovery of the SC state is presented in the Figure 3.

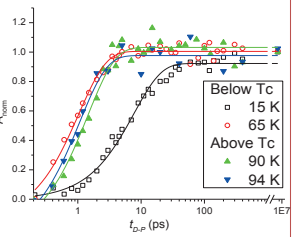

Fig.5 The amplitude of the pump-probe response from figures 3 and 4 as a function of the D-P delay fit by an exponential function.

Recovery dynamics of the superconducting state **above Tc**

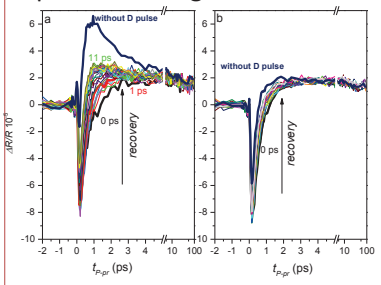

Fig.4 The pump-probe signal at different delays after the D pulse at 90 K (a) and 94 K(b).

Above T_c a recovery similar to that observed below T_c is also present (fig 5). The characteristic recovery time is close to that at 65 K(fig 4). The change in the signal above T_c cannot be attributed to the pseudogap as both heating and/or destruction of the PG state caused by D pulse would lead to decrease of PG signal i.e. different sign of the change.

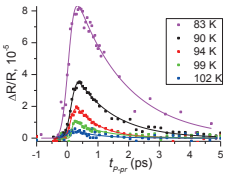

Fig.6 The SC component of the signal obtained by subtracting the signal at 0.2ps from the signal without the D pulse.

Further away from Tc (in the region 94 - 104 K) the signal is to weak for us to be able to measure the recovery curve, but, we are still able to detect the suppression of the SC response after the D pulse. The SC component (i.e. the difference between the signals without D and just after the D pulse arrived) is plotted in Figure 6.

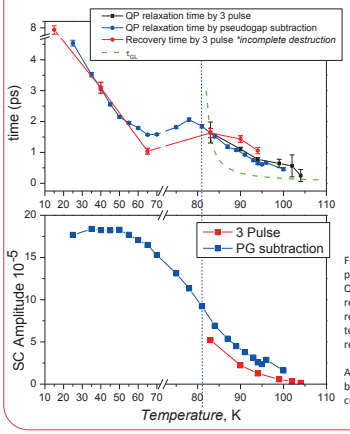

The temperature dependences of amplitude and relaxation time are plotted in fig.7. The recovery time above T_c is significantly larger than that expected from the time-dependent Ginzburg-Landau (TDGL) theory $\tau_{GL} \approx \pi\hbar[8k(T-T_c)]^{-1}$ [6] even though this is the region where TDGL is expected to be valid (as this is a truly gapless case). This implies that higher order correlation between electrons takes place (e.g. of the origin of Maky-Thompson correction to paraconductivity) with significant life-time (equal to recovery time for fluctuating state).

Fig 7. The QP relaxation time and SC recovery time are higher than predicted by TDGL (green dashed).
QP relaxation time obtained in 3 pulse experiment compared to relaxation time of the signal obtained by subtraction of the PG response(temperature dependence of the PG is fitted by temperature independent gap model [1] using 120K amplitude and relaxation time as input parameters).

Amplitude of the signal obtained by two different techniques differs because of CW heating effect in 3 pulse experiment(shifts the actual curve to the left) and some freedom in subtraction procedure.

References:

1.Toda Y. et al., PRB 84, 174516 (2011)
2.Kondo et al., Nat.Phys. 7, 21–25(2011)
3.Lu Li et al., PRB 81, 054510 (2010)
4.Yayu Wang, PRB 73, 024510 (2006)
5.Tallon et al., preprint at http://arxiv.org/abs/0908.4428 (2009).
6.Demsar et al., PRL 82, 24 (1999)
7.Laszlo Forro Fizika A (Zagreb) 8 (1999) 4

Conclusions:

For the first time we unambiguously separate the superconducting fluctuations above the critical temperature from the pseudogap response.

The temperature range where the fluctuations are present is surprisingly large and exceeds 20 K above T_c. The superconducting fluctuations cannot be described within the TDGL approach.

Raziskave tekočekristalnih elastomerov z jedrsko magnetno resonanco

Jerneja Milavec[1,2]

[1] Odsek F5, Inštitut Jožef Stefan, Ljubljana, Slovenija

[2] Mednarodna podiplomska šola Jožefa Stefana, Ljubljana, Slovenija

jerneja.milavec@ijs.si

Tekočekristalni elastomeri (TKE) so v zadnjih nekaj letih zbudili veliko zanimanja med raziskovalci, najverjetneje zaradi njihove potencialne uporabe v različnih tehnoloških napravah, kot so umetne mišice, pametne površine, mikrovalovi in drugo . Njihove makroskopske in fizikalne lastnosti so zelo povezane z elastičnostjo polimerne mreže in orientacijskimi lastnostmi mezogenov. Elastične lastnosti stranskoverižnih monodomenskih tekočekristalnih elastomerov smo določili s termo-mehanskimi meritvami, z devterijevo jedrsko magnetno resonančno (^{2}H JMR) spektroskopijo pa smo raziskali domensko urejanje selektivno devteriranih monodomenskih tekočekristalnih elastomerov. Dokazali smo, da je povprečna orientacijska urejenost krajših molekul mezogena M4 slabša, kot urejenost daljših molekul mezogena M11 in zamreževalca, ki je vpet na obeh koncih na polimerno verigo. S termo-mehanskimi meritvami pa smo dokazali, da so bili vsi trije vzorci enako dobro pripravljeni, da imajo okoli 40% raztezka in so zaradi teh lastnosti dobri kandidati za različne aplikacije.

MEDNARODNA PODIPLOMSKA ŠOLA JOŽEFA STEFANA

JOŽEF STEFAN INTERNATIONAL POSTGRADUATE SCHOOL

RAZISKAVE TEKOČEKRISTALNIH ELASTOMEROV Z JEDRSKO MAGNETNO RESONANCO

Jerneja Milavec
Mednarodna podiplomska šola Jožefa Stefana, Nanoznanost in nanotehnologije
MENTOR: prof.dr. Boštjan Zalar
Inštitut Jožefa Stefana, Jamova Cesta 39, 1000 Ljubljana

Tekočekristalni elastomeri (TKE) so v zadnjih nekaj letih zbudili veliko zanimanja med raziskovalci, najverjetneje zaradi njihove potencialne uporabe v različnih tehnoloških napravah, kot so umetne mišice, pametne površine, mikrovalovi in drugo.

Stransko-verižni tekočekristalni elastomeri

Tekočekristalni elastomeri kombinirajo orientacijsko urejenost tekočih kristalov in elastičnost polimerne mreže.

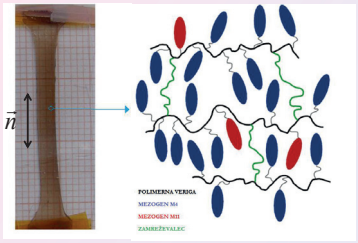

Kemijska struktura devteriranih molekul za pripravo TK elastomerov

Mezogen M4

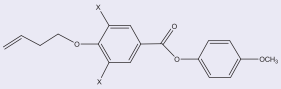

Zamreževalec

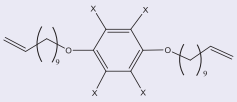

Mezogen M11

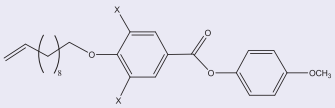

Polimerna veriga

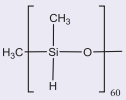

Termo-mehanske lastnosti

Orientacijsko urejenost molekul mezogena v TKE lahko dosežemo z mehanskim raztezanjem elastomera med pripravo.

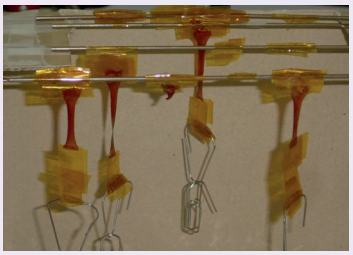

Pri 362K je viden prehod iz nematske v paranematsko fazo, raztezek L/L_0 pri minimalni masi 100g je 40%.

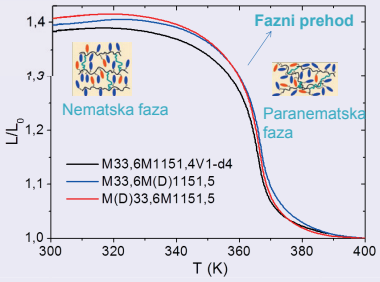

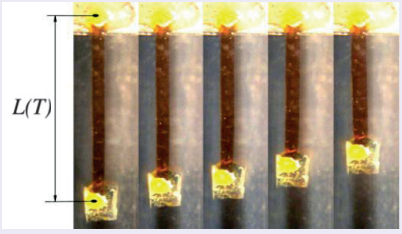

Nematska faza ⟵ gretje, hlajenje ⟶ izotropna faza

Ureditveni parameter

➔ **Fazni prehod iz paranematske v nematsko fazo**

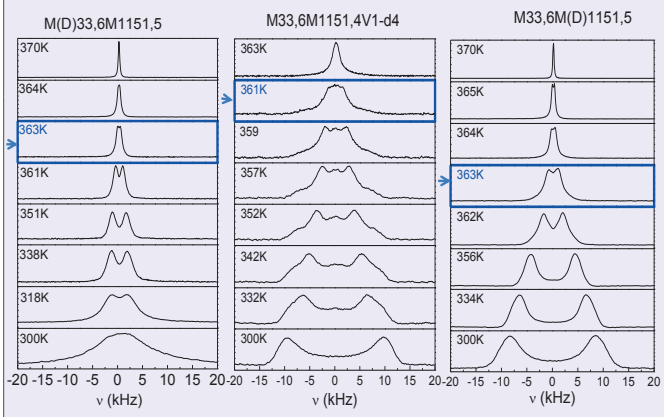

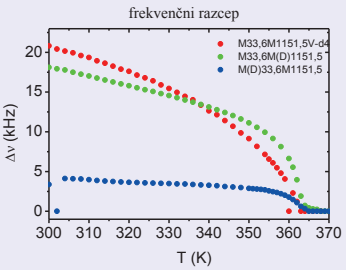

Frekvenčni razcep je v idealno orientiranem vzorcu sorazmeren z ureditvenim parametrom $\Delta\nu = 3\bar{\nu}_0 S(3\cos^2\theta - 1)/4$.

Ultrashield Advance III Bruker spektrometer s 500 MHz superprevodnim magnetom

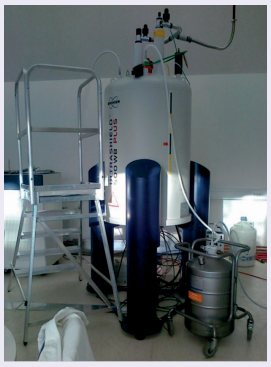

Zaključek

S pomočjo ^{2}H JMR spektroskopije smo lahko izmerili orientacijsko urejenost selektivno devteriranih molekul v tekočekristalnem elastomeru. Dokazali smo, da je povprečna orientacijska urejenost krajših molekul mezogena M4 slabša, kot urejenost daljših molekul mezogena M11 in zamreževalca, ki je vpet na obeh koncih na polimerno verigo. S termo-mehanskimi meritvami smo dokazali, da so bili vsi trije vzorci enako dobro pripravljeni, da imajo okoli 40% raztezka in so zaradi teh lastnosti dobri kandidati za različne aplikacije.

Synthesis of LaF_3 nanoparticles

Olivija Plohl[1,2], **Darja Lisjak**[1,2], **Darko Makovec**[1,2,4], **Miha Drofenik**[1,3]

[1] Department of K8, Jožef Stefan Institute, Ljubljana, Slovenia

[2] Jožef Stefan International Postgraduate School, Ljubljana, Slovenia

[3] Faculty of chemistry and chemical engineering, Maribor, Slovenia

[4] CENN Nanocenter, Ljubljana, Slovenia

olivija.plohl@ijs.si

In this paper the syntheses of LaF_3 nanoparticles with solvothermal method using different solvents (i.e., water, ethylene glycol) is described. LaF_3 nanoparticles were previously synthesized with different syntheses and superior properties were obtained by high-temperature organic-precursors decomposition method. Since this method uses toxic reagents (e.g., oleylamine, octadecene) our aim was to study more in details the synthesis of LaF_3 nanoparticles with an ecologically more acceptable solvothermal synthesis. Morphology and chemical composition of synthesized nanoparticles was characterized with transmission and scanning electron microscopies combined with energy-dispersive X-ray spectroscopy while their crystal structure was analysed with X-ray powder diffraction.

MEDNARODNA PODIPLOMSKA ŠOLA JOŽEFA STEFANA

JOŽEF STEFAN INTERNATIONAL POSTGRADUATE SCHOOL

SYNTHESIS OF LaF_3 NANOPARTICLES

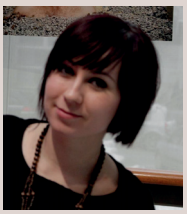

Olivija Plohl, univ.dipl.inž.kem.tehn.[a,b,*], Darja Lisjak[a,b,§], Darko Makovec[a,b,d], Miha Drofenik[a,c]

[a] „Jožef Stefan“ Institute, Department for materials synthesis, K8, Jamova cesta 39, 1000 Ljubljana

[b] „Jožef Stefan“ International postgraduate school, Jamova cesta 39, 1000 Ljubljana

*Programe: Nanosciences and nanotechnologies

§Supervisor: doc.dr. Darja Lisjak

[c] Faculty of chemistry and chemical engineering, Smetanova ulica 17, 2000 Maribor

[d] CENN Nanocenter, Jamova ulica 39, 1000 Ljubljana

INTRODUCTION

- Lanthanide-doped nanoparticles, which show upconversion, were proposed as alternative biomarkers for fluorescence imaging.
- Upconversion is a process, where sensitizer ion (i.e, Yb^{3+}) absorbs the excitation radiation with specific wavelenght and transfer it as a non-radiative energy to activator ion (i.e., Er^{3+}, Tm^{3+}, Ho^{3+}), which emits at shorter wavelenght.
- Most extensively studied host matrices are fluorides due to their ability to incorporate lanthanide ions, have low phonon energies and high chemical stability.
- One of suitable upconversion fluorescent host matrix is lanthanum fluoride (LaF_3).

APPLICATIONS

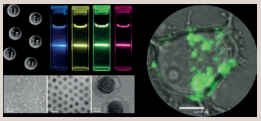

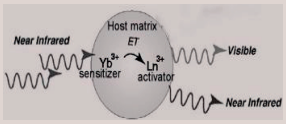

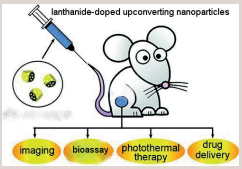

EXPERIMENTAL

LaF_3 nanoparticles were prepared with solvothermal synthesis at 160 °C or 180 °C for 6 h - 24 h using water or ethylene glycol (EG) as a solvent.

water

$La(NO_3)_3x6H_2O$ was used as La^{3+} source and $NaBF_4$ as F^- source. Citrate ion (Cit^{3-}) was used to form La-Cit complex.

EG

$NaBF_4$ was dissolved in 20 mL EG. Afterward, solution of $La(NO_3)_3x6H_2O$ in 20 mL EG was added into the above solution.

RESULTS

XRD ANALYSIS

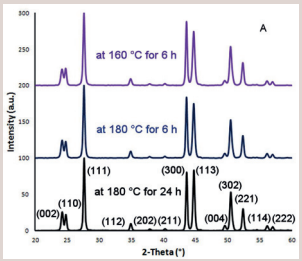

XRD patterns of as-prepared LaF_3 nanoparticles with hexagonal crystal structure (JCPDS 32-0483, A in water, B in EG).

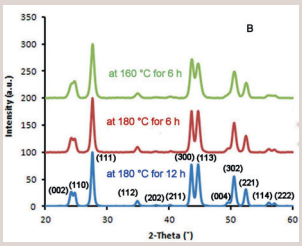

Crystalline size of as-prepared LaF_3.

water		EG	
Temperature and reaction time	Crystal size (nm)	Temperature and reaction time	Crystal size (nm)
180 °C for 24 h	80 ± 1	180 °C for 12 h	30 ± 1
180 °C for 6 h	60 ± 2	180 °C for 6 h	25 ± 2
160 °C for 6 h	60 ± 3	160 °C for 6 h	20 ± 1

Size of nanoparticles increases with increasing temperature and time of solvothermal reaction for both solvents.

ENERGY DISPERSIVE SPECTROSCOPY (EDXS)

EDXS analysis confirmed that the atomic ratio of the LaF_3 nanoparticles synthesized in water was La:F ≈ 1:3, although a minor fraction of oxygen was also detected. EDXS analysis of LaF_3 nanoparticles, synthesized in EG revealed, that the atomic ratio of the La:F was not stoichiometric as in LaF_3 and oxygen was also detected.

TEM ANALYSIS

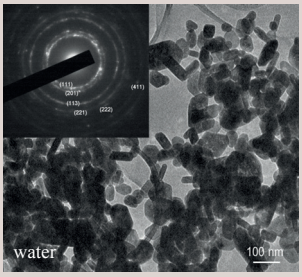

TEM images of LaF_3 nanoparticles, prepared under hydrothermal conditons at 180 °C for 24 h in water and at 180 °C for 6 h in EG.

SEM ANALYSIS

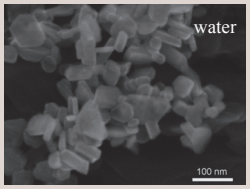

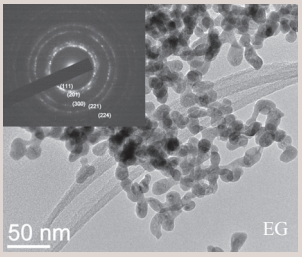

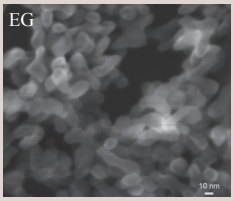

SEM images of LaF_3 nanoparticles prepared at 160 °C for 6 h in water and at 160 °C for 6 h in EG.

CONCLUSION

- We synthesized LaF_3 nanoparticles with enviromentally more friendly solvothermal synthesis using different solvents (i.e., water, EG).
- When water was used as a solvent, synthesized nanoparticles were composed of aggregated hexagonal nanoplates. Morphology of nanoparticles, synthesized in EG differs from those synthesized in water. Those nanoparticles were of irregular shape and were connected between each other.
- In both cases XRD results confirmed hexagonal LaF_3 crystal structure meanwhile EDXS and SAED analyses on some particles revealed the presence of oxygen, which can be incorporated into fluoride crystal lattice forming LaOF.
- One of possible solution to synthesize oxygen-free LaF_3 is to replace reagent $La(NO_3)_3$ with $LaCl_3$ and will be tested in future.

ACKNOWLEDGEMENT: This work was financially supported by ARRS. The autors acknowledge for the use of equipment in the CENN Nanocenter.

Magnetooptical time-resolved study of Eu^{2+} spin dynamics in $EuFe_2(As_{1-x}P_x)_2$ pnictide superconductor

Anna Pogrebna[1,2], Zuan Xu[4], Tomaž Mertelj[2], Dragan Mihailović[2,3]

[1] International postgraduate school Jozef Stefan, Ljubljana, Slovenia

[2] Complex Matter Department, Jozef Stefan Institute, Jamova 39, SI-1000 Ljubljana, Slovenia

[3] Center of Excellence on Nanoscience and Nanotechnology – Nanocenter (CENN Nanocenter),
Jamova 39, SI-1000 Ljubljana, Slovenia

[4] Department of Physics, Zhejiang University, Hangzhou 310027, People's Republic of China

anna.pogrebna@ijs.si

We investigate the Eu^{2+} dynamics in $EuFe_2(As_{0.7}P_{0.3})_2$ (EFAP) pnictide superconductor and parent nonsuperconducting $EuFe_2As_2$ (EFA) using optical pump-probe femtosecond spectroscopy in magnetic field. In both cases we observe an emergence of a slow anisotropic photoinduced relaxation component concurrent with Eu spin ordering. A remarkable change of the quasiparticle relaxation dynamics at the antiferromagnetic (AFM) spin density wave (SDW) transition temperature 200 K is observed.

The magnetic field dependence of the relaxation in the superconducting EFAP is different than in the nonsuperconducting EFA. In EFA we observe switching of the optical-transients anisotropy with increasing magnetic field attributed to a field-induced antiferromagnetic (AFM) to ferromagnetic (FM) phase transition. In the superconducting EFAP a large coherent magnon oscillation is observed at a similar metamagnetic transition. The oscillation is absent in the transient magneto-optical Kerr effect suggesting an interplay between the Eu^{2+} spin and charge degrees of freedom.

MEDNARODNA PODIPLOMSKA ŠOLA JOŽEFA STEFANA

JOŽEF STEFAN INTERNATIONAL POSTGRADUATE SCHOOL

Magnetooptical time-resolved study of Eu^{2+} spin dynamics in $EuFe_2(As_{1-x}P_x)_2$ pnictide superconductor

A.Pogrebna,[1,*] Z. A. Xu,*** T.Mertelj,* D.Mihailovic*,**

[1] International postgraduate school. Nanoscience and nanotechnologies

* Complex Matter Department, Jozef Stefan Institute, Jamova 39, SI-1000 Ljubljana, Slovenia

** Center of Excellence on Nanoscience and Nanotechnology – Nanocenter (CENN Nanocenter), Jamova 39, SI-1000 Ljubljana, Slovenia

*** Department of Physics, Zhejiang University, Hangzhou 310027, People's Republic of China

Abstract

We investigate the quasiparticle relaxation and Eu^{2+} spin dynamics in $EuFe_2(As_{0.7}P_{0.3})_2$ (EFAP) pnictide superconductor and parent nonsuperconducting $EuFe_2As_2$ (EFA) using optical pump-probe femtosecond spectroscopy in magnetic field. In both cases we observe an emergence of a slow anisotropic photoinduced relaxation component concurrent with Eu spin ordering. A remarkable change of the quasiparticle relaxation dynamics at the antiferromagnetic (AFM) spin density wave (SDW) transition temperature 200 K is observed.

The magnetic field dependence of the relaxation in the superconducting EFAP is different than in the nonsuperconducting EFA. In EFA we observe switching of the optical-transients anisotropy with increasing magnetic field attributed to a field-induced antiferromagnetic (AFM) to ferromagnetic (FM) phase transition. In the superconducting EFAP a large coherent magnon oscillation is observed at a similar metamagnetic transition. The oscillation is absent in the transient magneto-optical Kerr effect suggesting an interplay between the Eu^{2+} spin and charge degrees of freedom.

Introduction

$EuFe_2As_2$ is a peculiar member of iron arsenide AFeAs family. It exhibits a SDW transition around T_0 = 190 K related to the Fe_2As_2 layers. At T_N = 18K the magnetic moments of localized Eu^{2+} moments order antiferromagnetically [1]. The parent system $EuFe_2(As_{1-x}P_x)_2$ with the partial substitution of As with P was reported as the first ferromagnetic superconductor [2]. The phosphorus doping leads to a coexistence of superconductivity and ferromagnetism.

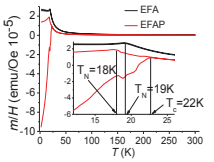

FIG. 1. The magnetic susceptibility measurement in H = 5 Oe

Magneto-optical experiment was performed using the standard pump-probe technique, with 50 fs optical pulses from a 250 kHz Ti:Al_2O_3 regenerative amplifier seeded with an Ti:Al_2O_3 oscillator with 1.55 eV photon energy. Samples were mounted in a 7-T optical magnet.

Phase transitions in pump-probe response

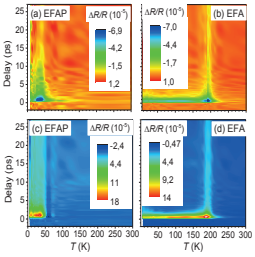

FIG. 2. The photoinduced reflectivity ($\Delta R/R$) transients at 4 μJ/cm² pump fluence as a function of temperature at different dopings and probe polarizations (a)-(b), (c)-(d). The top row (a)-(c) corresponds to the $\mathcal{P}^-$ and the bottom row (b)-(d) to the $\mathcal{P}^+$ polarization.

Variance of the anisotropy across the surface of the samples suggest a orthorhombic domain structure on the lengthscale of the probe beam diameter (~100 μm).

The undoped sample showed the SDW transition at the temperature T_{SDW} = 188 K, which is in consistent with previous results [3]. The SDW transition is also observed in doped EFAP at T_{SDW} = 35 K.

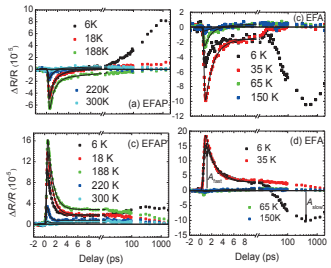

FIG. 3. $\Delta R/R$ transients from Fig. 2. at representative temperatures at different dopings for different polarizations. (a)-(c) corresponds to the $\mathcal{P}^-$ and the bottom row (b)-(d) to the $\mathcal{P}^+$ polarization.

The analysis shows at least two components in the signal with different dynamics. One decays on a sub picosecond timescale and disappears at 190 K and 35 K in the pure and doped sample, respectively. It corresponds to the SDW ordering of FeAs layers. Another one has a very slow risetime and long decay-time and disappears at 18 K. It corresponds to antiferromagnetic Eu^{2+} spin ordering. The superconducting transition in EFAP was not observed by optics.

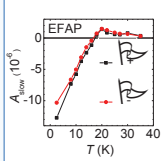

FIG. 5. Amplitudes of the raw reflectivity transients at the long delay as a function of temperature of EFAP at 4 μJ/cm².

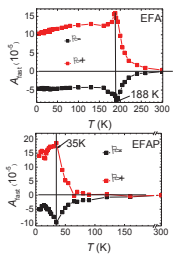

FIG. 4. Amplitudes of the raw reflectivity transients at the short delay as a function of temperature at different P dopings at 4 μJ/cm².

Metamagnetic transition in EFAP

A metamagnetic transition was observed in the doped sample (EFAP) at B = 0.5 T, where the amplitude of the slow part of the signal abruptly changes sign with increasing magnetic field.

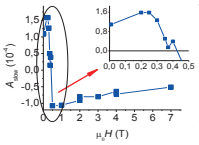

This transition is associated with a ferromagnetic ordering of Eu^{2+} spins induced by applied magnetic field [4].

In the doped EFAP unexpected magnon oscillations appear at the metamagnetic transition.

The frequency of oscillations only weakly depends on the magnetic field and the fluence of the exciting laser pulses. On the other hand, the oscillation amplitude saturates with increasing pump fluence and strongly depends on the magnetic field.

Simultaneously, the sample shows very weak magneto-optical Kerr effect signal suggesting an interplay between the Eu^{2+} spin and charge degrees of freedom.

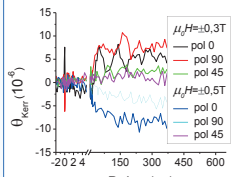

FIG. 7. The Kerr angle measurement in EFAP at applied magnetic fields B = 0,3 T and B = 0,5 T for different probe polarizations

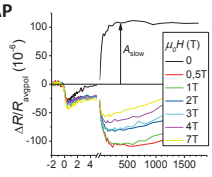

FIG. 5. $\Delta R/R$ transients as a function of magnetic field in EFAP

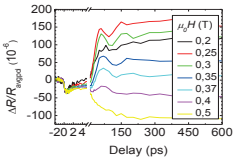

FIG. 6. $\Delta R/R$ transients as a function of magnetic field in EFAP

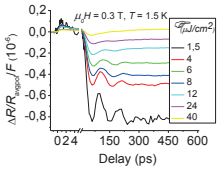

FIG. 8. $\Delta R/R$ transients as a function of laser pump fluence in EFAP

Anisotropy switching by magnetic field in undoped EFA

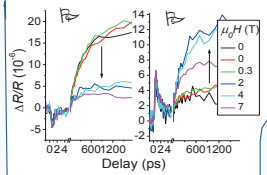

FIG. 9. $\Delta R/R$ transients for EFA as a function of magnetic field

In the undoped sample (EFA) no magnon oscillations were observed at the field induced AFM to FM transition. There is however a clear switching of the optical transient anisotropy concurrent with the transition.

References

[1] Zhi Ren et al. Phys. Rev. B 78. 052501 (2008).

[2] Zhi Ren et al., Phys. Rev. Lett. 102, 137002 (2009).

[3] S.Zapf et al. Phys.Rev. B 84, 140503(R) (2011).

[4] Z. Guguchia et al. Phys. Rev. B 84, 144506 (2011).

Conclusions

1. Both samples have a domain structure on ~100 μm lengthscale.

2. The slow part of the transient reflectivity, appearing below 18 K, corresponds to the dynamics of Eu^{2+} spins.

3. In both samples we observed a metamagnetic transition around 0,5 T corresponding to the FM ordering of the Eu^{2+} spins.

4. Strong magnon oscillations are observed in the transient reflectivity in the doped sample near the metamagnetic transition indicating a coupling between Eu^{2+} spins and charge degrees of freedom.

complexmatter Jožef Stefan Institute

Jožef Stefan Institute

Analysis of the background under the e-beam and x-ray induced Auger peaks

Besnik Poniku[1,2], **Igor Belič**[1], **Monika Jenko**[1]

[1] Institute of Metals and Technology, Ljubljana, Slovenia

[2] Jožef Stefan International Postgraduate School, Ljubljana, Slovenia

besnik.poniku@imt.si

Our research work aims to find suitable ways to achieve full automation of the Auger spectra processing. Apart from simplifying greatly the manipulation of data after the measurement, we believe this will also improve greatly the reliability of the results obtained.

In order to make this automation possible, a precondition is the removal of background and noise from the Auger spectra, in order to "feed" the program with the data which represent only the characteristic peaks of elements. For a successful removal, a better understanding of the background and noise, and the factors that contribute to them is needed. This work was done in order to understand better the contribution of the backscattered electrons to the background.

To complete this work the spectra of 11 samples in total were measured using Auger Electron Spectroscopy (AES) and X-ray Photoelectron Spectroscopy (XPS). Samples such as Al(100), Al(110), Al(111), Cu, Fe(100), Fe(110), Fe(111), Fe2%Si (100), Ni, Ti, and W(110) were used. The idea here was to use two different modes of excitation and observe the intensity under the Auger peaks of the same element. Since in AES an electron beam is involved and as a result backscattered electrons which constitute the background are also part of the signal measured, and on the other hand in XPS an X-ray beam is involved and therefore no backscattered electrons are involved, this made it possible to investigate the contribution of backscattered electrons to the background by taking the difference between the spectra measured in AES and those measured in XPS.

Since in the literature a power law is given to describe the contribution of backscattered electrons to the spectrum, having used a 10 keV beam the difference between the two spectra was expected to yield a smooth, steadily increasing line with increasing energy. But instead as a result was obtained something that resembled the peaks. This could be explained only by taking into consideration that the contribution of the backscattered electrons is not only a simple, smooth power law as it would be if they entered the sample and got back elastically, but due to inelastic collisions some of them which have enough energy excite additional Auger electrons on their way back as well.

MEDNARODNA PODIPLOMSKA ŠOLA JOŽEFA STEFANA

JOŽEF STEFAN INTERNATIONAL POSTGRADUATE SCHOOL

ANALYSIS OF THE BACKGROUND UNDER THE E-BEAM AND X-RAY INDUCED AUGER PEAKS

BESNIK PONIKU, mag. NiN
Study programme: Nanosciences and nanotechnologies,
Jozef Stefan International Postgraduate School
MENTOR: prof. dr. Monika Jenko
CO-MENTOR: doc. dr. Igor Belič
Institute of Metals and Technology, Lepi pot 11, 1000 Ljubljana

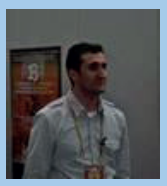

Auger transitions may be induced by using an electron beam, as well as by other modes of excitation, such as an X-ray beam.

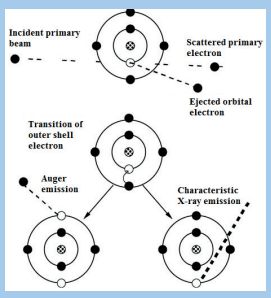

Here the LMM Auger transition for copper in an Auger spectrum (left) and an XPS spectrum (right) can be seen.

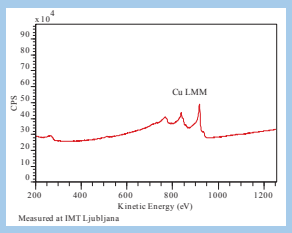

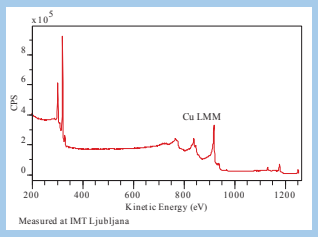

In this work we wanted to investigate the differences in intensity (measured in Counts Per Second - CPS) under the Auger peaks of the same element as they appear in the Auger electron spectrum and the XPS spectrum.

$$B_{e^-} = CPS_{AES} - CPS_{XPS} \qquad (1)$$

This was done by inspecting spectra measured using Microlab 310 - F at the IMT laboratory for Surface Analysis .

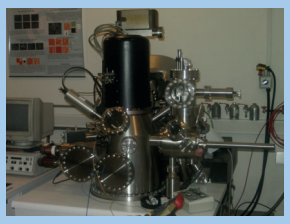

11 samples were used in total for the experimental work: Al(100), Al(110), Al(111), Cu, Fe(100), Fe(110), Fe(111), Fe2%Si (100), Ni, Ti, and W(110).

In general in the literature, the background is reported to consist of the backscattered electrons (left) and the secondary electrons (right).

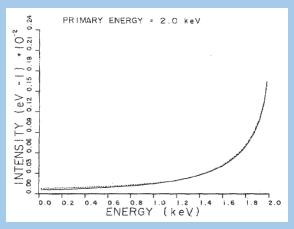

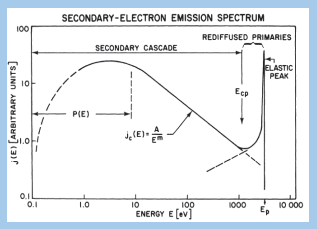

The contribution of the backscattered electrons to the spectrum is described by Eq.2:

$$n_B(E) \sim \exp(E/E1) \qquad (2)$$

And that of the secondary electrons by Eq. 3:

$$B(E) = AE^{-m} \qquad (3)$$

When using Eq. 1 to reveal the contribution of the backscattered electrons under the Auger peaks for the 11 samples that we measured, we obtained shapes which were not smooth, but which partially resembled the peaks.

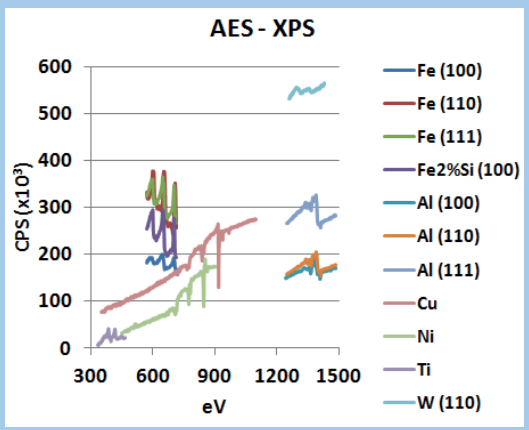

This is something totally unexpected if we take into consideration equations 2 and 3.

This observed difference from what was expected cannot be attributed to backscattered electrons per se, but they still are the cause of these observed “hills” in the difference spectrum which resembles the peaks. This can be explained as the extra Auger electrons that are being excited due to the traveling of the backscattered electrons on their way out of the sample. It seems that this fact is not taken into account in the models described above which are found in the literature.

Preparation of stable colloidal aqueous suspensions of magnetic iron-oxide nanoparticles using aspartic acid as surfactant

Klementina Pušnik[1,2], **Mihael Drofenik**[1,3], **Darko Makovec**[1,2,4]

[1] Department for Materials Synthesis, Jožef Stefan Institute, Ljubljana, Slovenia

[2] Jožef Stefan International Postgraduate School, Ljubljana, Slovenia

[3] Faculty of Chemistry and Chemical Engineering, Maribor, Slovenia

[4] CENN Nanocenter, Slovenia

klementina.pusnik@ijs.si

Nano-sized materials such as magnetic nanoparticles, which are a major class of nanoscale materials (ferro/ferrimagnetic materials, such as iron, nickel, cobalt, and magnetic oxides like iron oxides, including magnetite and maghemite), have fascinating physical-chemical properties that if tuned properly, can design new bio-diagnostics and therapeutic strategies, as well as, innovative biotechnology methodologies. The most common synthesis methods of iron-oxides nanoparticles are: co-precipitation, thermal decomposition, hydrothermal synthesis, microemulsion, sonochemical synthesis.

For biological applications, the magnetic nanoparticles are coated with biocompatible coating of organic molecules. Thus, the magnetic nanoparticles have usually core-shell structure. The organic shell prevents agglomeration of the iron-oxide nanoparticles in the aqueous suspensions and enables bonding of different molecules needed in application to their surfaces.

For in vivo applications, the organic shell of the surfactants should be nontoxic and biocompatible. One possible type of surfactant used in the stabilization of aqueous nanoparticles suspensions is amino acids. The amino acids also play an important role in the body. In our study, aspartic acids were successfully used as surfactant for preparation of stable aqueous suspensions of magnetic iron-oxide nanoparticles.

MEDNARODNA PODIPLOMSKA ŠOLA JOŽEFA STEFANA

JOŽEF STEFAN INTERNATIONAL POSTGRADUATE SCHOOL

Preparation of stable colloidal aqueous suspensions of magnetic iron-oxide nanoparticles using aspartic acid as surfactant

Klementina Pušnik [1,2], Mihael Drofenik [1,3], Darko Makovec [1,2,4]

[1]Department for Materials Synthesis, Jožef Stefan Institute, Ljubljana, Slovenia

[2]Jožef Stefan International Postgraduate School, Ljubljana, Slovenia

[3] Faculty for Chemistry and Chemical Engineering, Maribor, Slovenia

[4] Center of Excellence on Nanoscience and Nanotechnology – Nanocenter, Ljubljana, Slovenia

INTRODUCTION

STABLE AQUEOUS SUSPENSIONS OF MAGHEMITE NANOPARTICLES

are used for biomedical applications as:

- Drug-delivery systems for cell separation,
- As mediators in magnetic hyperthermia,
- As MRI contrast agents.

SURFACTANTS

- The organic shell of the surfactants for in-vivo applications should be biocompatible and should provide long blood-circulation times,
- The adsorption of the amino acids onto the magnetic nanoparticles is important for their targeting to a specific tissue in the human body using an external magnetic field.

AMINO ACIDS

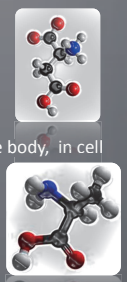

- Are biocompatible,
- Play an important role in the body, in cell growth or in tissue repair,.

EXPERIMENTAL SECTION AND RESULTS

ONE-STEP METHOD

- Amino acid was added to the solution before the precipitation of Fe^{3+} and Fe^{2+} ions (the molar ratio 2Fe(III):1Fe(II):3 aspartic acid (AA)),
- Solution of ammonium hydroxide was added under vigorous stirring till pH=11 ,
- Amino-acid-coated maghemite nanoparticles were dispersed in water at pH=11.

TWO-STEP METHOD

- Precipitation of Fe^{3+} and Fe^{2+} ions from their aqueous solutions with aqueous ammonia to synthesize maghemite nanoparticles,
- Amino acid was adsorbed onto the synthesized nanoparticles at pH=4.0,
- Amino-acid-coated maghemite nanoparticles were dispersed in water at pH=11.

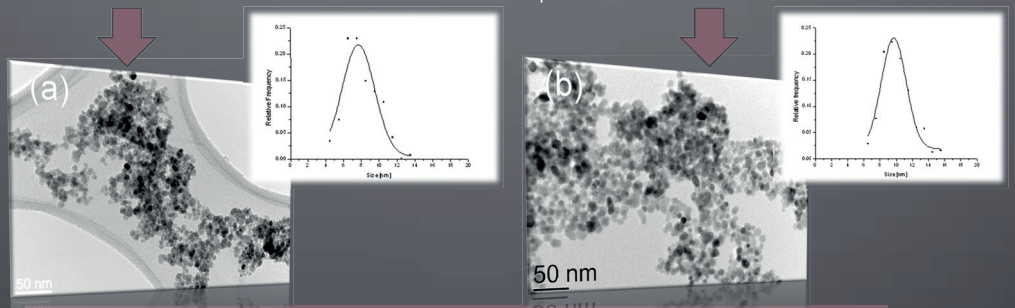

TEM image of aspartic-acid-adsorbed maghemite nanoparticles, prepared by one-step approach (a), two-step approach (b) with their correspond size distributions: a) 8± nm, b)10± nm.

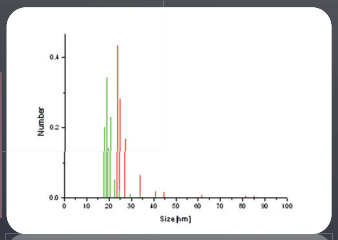

Particles size distributions of aspartic-acid-adsorbed maghemite nanoparticles in aqueous suspension: red-prepared by one-step approach (1mg/mL) and green- prepared by two-step (5mg/mL) approach.

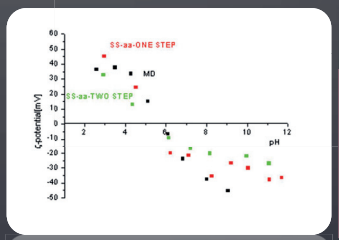

ζ-potential of: untreated maghemite nanoparticles (MD), aspartic-acid adsorbed nanoparticles prepared by one-step approach (SS-aa-ONE STEP), and AA-coated nanoparticles prepared by two-step approach (SS-aa-TWO STEP).

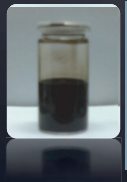

Aspartic-acid adsorbed maghemite nanoparticles suspensions (5 mg/mL).

Precipitation of Fe^{2+}/Fe^{3+} resulted in superparamagnetic maghemite nanoparticles of uniform size of 10 nm. The particles size of aspartic-acid-adsorbed maghemite nanoparticles decreases with adding a surfactant in one-step approach. So, we suggested that aspartic acid in one-step approach limits the particles growth. Zeta potential measurements showed no significant differences between untreated and AA-adsorbed nanoparticles. We proposed that the adsorption mechanism is due to the electrostatic repulsion between the ionized groups of aspartic acid. Therefore, by dispersing of the nanoparticles in water a stable suspension (ferrofluid) is obtained .

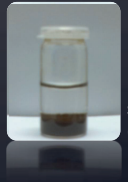

Maghemite nanoparticles suspensions (20 mg/mL).

CONCLUSIONS

We successfully synthesized stable aqueous suspensions of aspartic-acid-adsorbed maghemite nanoparticles using two different approaches, one-step approach of Fe^{2+}/Fe^{3+} precipitation in the presence of amino acid and two-step approach including separate synthesis of the nanoparticles and their subsequent coating with amino acid. Colloidal stability was achieved in using one-step and two-step approach. Hydrodynamic size of the aspartic-acid-adsorbed maghemite nanoparticles corresponded well with the size measured from TEM images.

ACKNOWLEDGEMENT

This work was financially supported by ARRS. The authors acknowledge the use of equipment in the Center of Excellence on Nanoscience and Nanotechnology–Nanocenter.

Obdelava polimernih podlag z nizkotlačno kisikovo plazmo za boljšo vezavo malignih človeških kostnih celic

Nina Recek[1,2], **Alenka Vesel**[1], **Miran Mozetič**[1]

[1] Odsek F4, Inštitut Jožef Stefan, Ljubljana, Slovenia

[2] Mednarodna podiplomska šola Jožefa Stefana, Ljubljana, Slovenia

nina.recek@ijs.si

Vakuumske tehnologije si postopoma utirajo pot v biologiji in medicini. Sodobni tehnološki postopek za obdelavo podlag, na katerih se razraščajo biološke celice, je obdelava z nizkotlačno plinsko plazmo. Polimeri imajo nizko površinsko energijo in zato tudi slabe adhezijske lastnosti in biokompatibilnost. Plazemske tehnologije so obetavna tehnika za spremembo površinskih lastnosti polimerov. Z plazemsko obdelavo polimerov ustvarimo na površini polimera nove funkcionalne skupine in s tem spremenimo kemijsko sestavo površine. Že kratkotrajna obdelava povzroči spremembo morfoloških lastnosti površine polimera, spremembo hrapavosti in omočljivosti površine, kar vodi k bistvenemu izboljšanju adhezije in proliferacije celic na plazemsko obdelanih podlagah. V prispevku opisujemo vpliv plazemske obdelave na morfološke in kemijske lastnosti polimera PS (Polistiren), ki ga uporabljamo kot podlago za razraščanje malignih človeških kostnih celic. Polimer PS je bil obdelan s kisikovo plazmo v ustreznem plazemskem reaktorju. Spremembo morfologije površine polimera smo spremljali s pomočjo mikroskopa na atomsko silo (AFM), spremembo kemijske sestave z rentgenskim fotoelektronskim spektrometrom (XPS), omočljivost polimerne površine pa smo določili z merjenjem kontaktnega kota vodne kapljice. Začetno fazo razraščanja celic smo opazovali z elektronsko mikroskopijo. Ugotovili smo, da maligne kostne celice že v kratkem času tvorijo nitaste (fibrilarne) strukture na podlagah, obdelanih z kisikovo plazmo, medtem, ko tega pojava nismo opazili na neobdelanih podlagah. Tovrstni eksperimenti predstavljajo prvi korak k selektivni vezavi rakastih celic na plazemsko obdelanih materialih.

MEDNARODNA PODIPLOMSKA ŠOLA JOŽEFA STEFANA

JOŽEF STEFAN INTERNATIONAL POSTGRADUATE SCHOOL

OBDELAVA POLIMERNIH PODLAG Z NIZKOTLAČNO KISIKOVO PLAZMO ZA BOLJŠO VEZAVO CELIC

Nina Recek, univ. dipl. inž. kem. tehn.
Študijski program: Nanoznanosti in nanotehnologije,
Mednarodna podiplomska šola Jožefa Stefana
MENTOR: doc. dr. ALENKA VESEL
SOMENTOR: prof. dr. MIRAN MOZETIČ
Inštitut Jožef Stefan, Jamova cesta 39, 1000 Ljubljana

RF (radio-frekvenčna) kisikova plazma

ZNANSTVENI TEMELJI

Sodobni tehnološki postopek za obdelavo podlag, na katerih se razraščajo biološke celice, je obdelava z nizkotlačno plinsko plazmo. PLAZMA je ioniziran plin (četrto agregatno stanje snovi) in predstavlja vir kemijsko aktivnih skupin (ionov, elektronov, atomov, radikalov in fotonov). Že kratkotrajna obdelava povzroči spremembo površinskih lastnosti polimera, kar vodi k bistvenemu izboljšanju adhezije in proliferacije celic, na plazemsko obdelanih polimerih. Tovrstni eksperimenti predstavljajo prvi korak k selektivni vezavi rakastih celic na plazemsko obdelanih materialih.

► želimo spremeniti zgolj površino polimera (modifikacija sega do nekaj nm v globino) ne da bi spremenili lastnosti celotnega materiala

► želimo tvoriti nove kemijske vezi na površini - z okolju prijazno tehnologijo (izognemo se uporabi mokrih kemijskih postopkov, ki so okolju škodljivi)

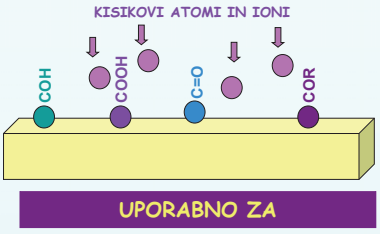

UPORABNO ZA

► spremembo morfoloških lastnosti površine

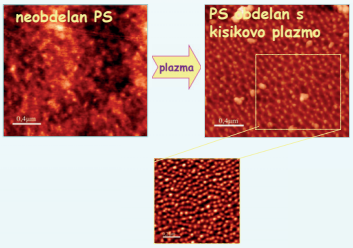

► Medicinske aplikacije (medicinski implantanti)

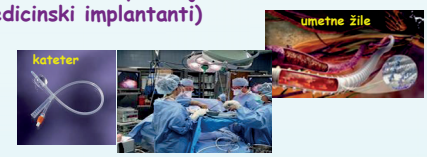

► spremembo hrapavosti površine

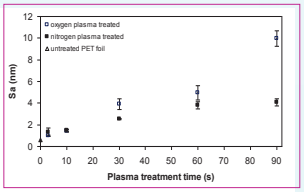

Izboljšanje adhezije celic

Neobdelani vzorci

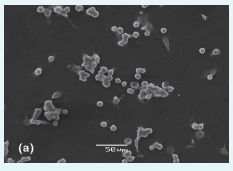

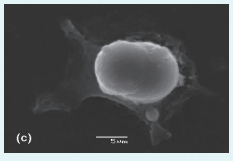

Plazemsko obdelani vzorci

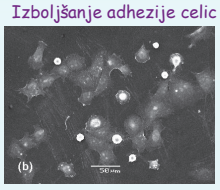

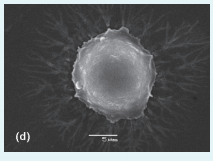

►spremembo omočljivosti površine

hidrofobna površina — hidrofilna površina

►spremembo kemijske sestave površine

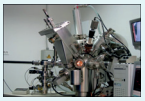

- 1.vrh: C-C in C-H vezi
- 2.vrh: C-O vezi
- 3.vrh: O=C-O vezi

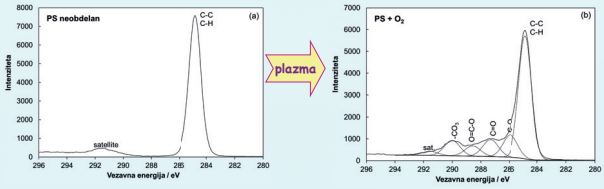

►Rezultati MTT testa, neobdelan PS in plazesmko obdelani PS po 2 in 6 dneh inkubacije celic.

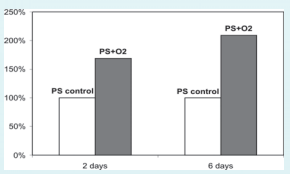

The effect of silica sol infiltration on the properties of dental 3Y-TZP ceramics

Anastasia Samodurova[1,2], **Andraž Kocjan, Irena Pribošič, Tomaž Kosmač**

[1] Department of Engineering Ceramics, Jožef Stefan Institute, Ljubljana, Slovenia

[2] Jožef Stefan International Postgraduate School, Ljubljana, Slovenia

anastasia.samodurova@ijs.si

Yttria partially stabilized tetragonal zirconia (Y-TZP) is becoming increasingly popular as an alternative material in restorative dentistry. One of the issues concerning tetragonal Y-TZP ceramics is their sensitivity to low temperature degradation (LTD), i.e. ageing. LTD appears from spontaneous transformation of metastable tetragonal grains to a more stable monoclinic phase in the presence of water or water vapour.

LTD resistance of dental zirconia can be improved by decreasing grain size or increasing the yttria content in the starting powder. Unfortunately, both of these approaches lead to the reduction of the mechanical properties of zirconia, thus making it unattractive for dental applications. Other way to tackle the problem is by adding of dopants.

Our research is focused on the study of the effects of silica on the phase composition, microstructure, mechanical properties and LTD of the Y-TZP ceramics in order to understand, whether ageing resistance can be increased without decreasing mechanical properties. The other goul of work is to understand the mechanism, by which silica gives rise to increasing ageing resistance of Y-TZP. The understanding of this can helps to explain the mechanism of LTD. In order to reach the desired final properties of tetragonal zirconia ceramics, the mechanism of LTD must be known.

MEDNARODNA PODIPLOMSKA ŠOLA JOŽEFA STEFANA

JOŽEF STEFAN INTERNATIONAL POSTGRADUATE SCHOOL

The effect of silica sol infiltration on the properties of dental 3Y-TZP ceramics

Anastasia Samodurova
Study programme: Nanosciences and Nanotechnologies,
Jožef Stefan International Postgraduate School
Supervisor: prof. dr. Tomaž Kosmač
Jožef Stefan Institute, Jamova 39, 1000 Ljubljana

Dental zirconia

Early 1990s

- Orthodontic brackets
- Root posts for anterior teeth

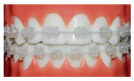

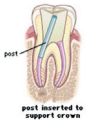

Nowadays

- Fixed partial dentures
- Implants

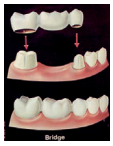

Why zirconia?

- High strength and fracture toughness
- Aesthetics
- Biocompatibility

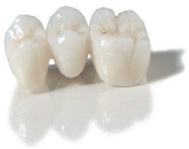

Problems:

- Porcelain chipping
- Low temperature degradation (LTD), i.e. ageing

Aim

To enhance the ageing resistance of Y-TZP by infiltration with silica sol without decreasing mechanical properties

Materials and methods

TZ-3YB
TZ-PX-242A
(Tosoh, Japan)
→ Uni-axial dry pressing, 150 kN, Ø 20mm
→ Pre-sintering, 900°C

Infiltration with silica sol

Infiltration with silica sol, synthesized *in situ* by the sol–gel method through hydrolysis of dynasylan. Specimens were immersed into a mixture of absolute ethanol and dynasylan. The hydrolysis was carried out by dropwise adding of an aqueous ammonia (%) at room temperature.

Final sintering, 1450°C, 4h
→ Autoclaving in water: 134°C, up to 48h
→ Characterization XRD, TEM, SEM

Results

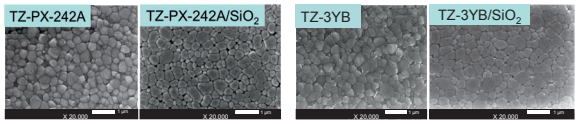

Fig. 1. SEM micrographs of polished and thermally etched specimens sintered at 1450 °C for 4 h.

Relative densities, %

	TZ-PX-242A	TZ-3YB
As sintered	98.6 ± 0.3	96.0 ± 0.7
SiO_2-doped	99.2 ± 0.5	96.5 ± 0.4

Average grain sizes, μm

	TZ-PX-242A	TZ-3YB
As sintered	0.29 ± 0.03	0.31 ± 0.04
SiO_2-doped	0.28 ± 0.02	0.32 ± 0.04

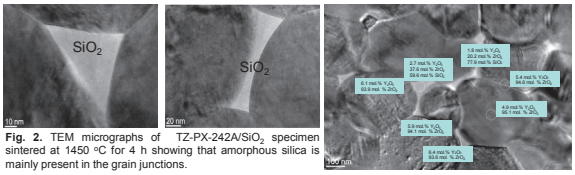

Fig. 2. TEM micrographs of TZ-PX-242A/SiO_2 specimen sintered at 1450 °C for 4 h showing that amorphous silica is mainly present in the grain junctions.

Mechanical properties

Sample	Flexural strength, MPa	Hardness, H_v (GPa)	Fracture toughness, K_{IC} (MPa·m$^{1/2}$)
TZ-PX-242A	1072 ± 48	15.2 ± 0.5	4.5 ± 0.7
TZ-PX-242A/SiO_2	1150 ± 150	14.1 ± 0.4	4.2 ± 0.3
TZ-3YB	1051 ± 136	14.5 ± 0.5	4.4 ± 0.3
TZ-3YB/SiO_2	1076 ± 114	13.9 ± 0.3	4.3 ± 0.1

In-vitro ageing behavior

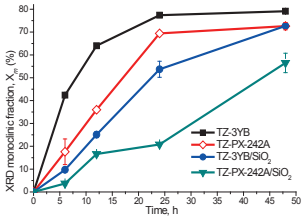

Fig. 3. Calculated monoclinic fraction versus in-vitro ageing time for monolithic and silica doped TZ-PX-242A and TZ-3YB materials.

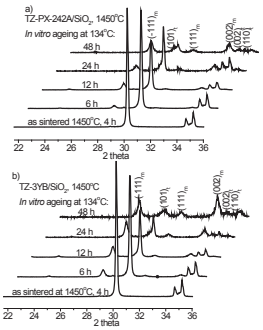

Fig. 4. XRD patterns obtained from a) SiO_2-TZ-PX-242A and b) SiO_2-TZ-3YB ceramic surfaces, sintered for 4 h at 1450 °C and aged in water at 134 °C for 6, 12, 24 and 48 h.

Conclusions

- Silica doped 3Y-TZP ceramics with the same grain size were prepeared by the pressureless infiltration of pre-sintered specimens with silica sol synthesized *in situ* by the sol-gel method
- The results of TEM analysis revealed that silica was mainly present as an amorphous phase concentrated at grain junctions
- The presence of silica substantially improves the LTD resistance without decreasing mechanical properties.

Bioactive Calcium Phosphate Coatings on Ceramic Bone Implants

Martin Štefanič[1], Tomaž Kosmač[1], Kristoffer Krnel

[1]Jožef Stefan International Postgraduate School, Ljubljana Slovenia
martin.stefanic@ijs.si

Calcium phosphate (Ca-P) coatings on zirconia bone implants have a great potential to improve the osseointegration of already-existing ceramic implants, owing to their bioactive and osteoconductive characteristics. A very promising approach for the preparation of Ca-P coatings is the so-called biomimetic method, which includes the immersion of the implant into a supersaturated Ca-P solution under physiological conditions. This method allows the synthesis of coatings with a good surface coverage on materials with complex shapes and good control over the coating composition. However, the drawbacks of the method are the relatively long time of the synthesis and, in particular, the poor adhesion of the coating to the substrate.

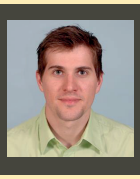

Bioactive Calcium Phosphate Coatings on Ceramic Bone Implants

MARTIN ŠTEFANIČ, univ. dipl. biokem.
Študijski program: Nanoznanosti in nanotehnologije,
Mednarodna podiplomska šola Jožefa Stefana
MENTOR: Prof. Dr. Tomaž Kosmač
SOMENTOR: doc. dr. Kristoffer Krnel

MEDNARODNA PODIPLOMSKA ŠOLA JOŽEFA STEFANA
JOŽEF STEFAN INTERNATIONAL POSTGRADUATE SCHOOL

Introduction

Calcium phosphate (Ca-P) coatings on zirconia bone implants have a great potential to improve the osseointegration of already-existing ceramic implants, owing to their bioactive and osteoconductive characteristics. A very promising approach for the preparation of Ca-P coatings is the so-called biomimetic method, which includes the immersion of the implant into a supersaturated Ca-P solution under physiological conditions. This method allows the synthesis of coatings with a good surface coverage on materials with complex shapes and good control over the coating composition. However, the drawbacks of the method are the relatively long time of the synthesis and, in particular, the poor adhesion of the coating to the substrate [1].

Objective

➢To synthesize Ca-P coatings on zirconia ceramics by applying a simple biomimetic method that would allow a high deposition rate.
➢To improve the attachement of the coating to the substrate by thermal and mechanical processing.

Experimental design

Materials

Polished Y-TZP discs

1. Deposition of coatings on ZrO_2 discs

2. Thermal processing of coatings
A) 600 °C, 1hour
B) 800 °C, 1 hour
*CIP - cold isostatic pressing

3. Bond strength evaluation
➢ISO 4624
➢Adhesive: HTK ULTRA BOND®

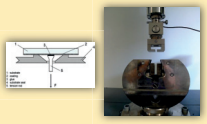

Results

1.) Deposition of coatings

➢Two-step synthesis:

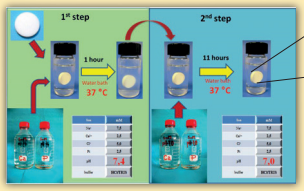

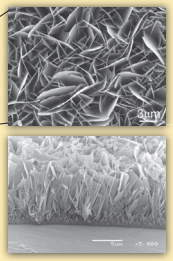

➢XRD

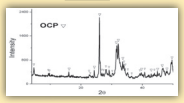

➢the coaitng is composed of octacalcium phosphate (OCP)

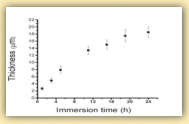

Coating thickness vs soaking time
➢Coating thickness was increasing with the time of immersion in the second solution (pH=7.0).

➢ Simple procedure
➢mild synthesis conditions
➢Rapid deposition

2.) Thermal processing of coatings

➢600 °C, 1h

➢Formation of hydroxyapatite (HAp).

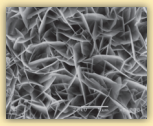

➢Preserved lamelar morphology.

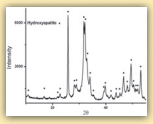

➢ OCP crstals transformed to hydroxyapatite (HAp) after firing at 600 ° C.

➢ 800 °C, 1h

➢Formation of β-tricalcium phosphate (β-TCP)

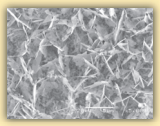

➢the coating became porous

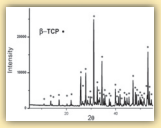

➢The coating lost its integrity, such that by applying a small force, (e. g. sonification in a water bath) a majority of the coating could be easily removed, except for the thin β-TCP layer remaining on the zirconia surface.

Ultra-sound bath

t ≈ 5 min

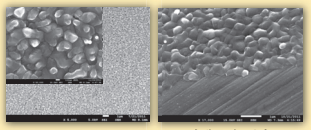

➢tilt angle = 35°

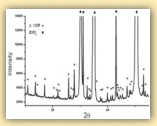

➢Thin β-TCP coating remained on the ceramic surface after short ultrasonic treatment

➢Coating thickness ≈ 500 nm

3.) Bond strength evaluation

Table: measured values of coatings bond strength

Sample	Bond strength (MPa)
As-deposited coating **(OCP)**	**1.8 ± 0.3**
600 °C, 1hour **(HAp)**	**3.2 ± 0.6**
800 °C, 1hour & sonification **(β-TCP)**	**29.3 ± 6.4**

➢6 samples for each experimental group

A) As-deposited coating (OCP)

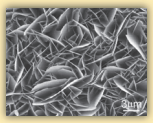

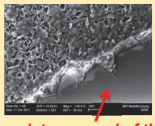

B) 600 °C, 1h (HAp)

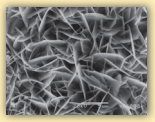

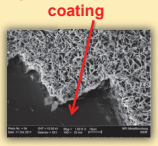

Complete removal of the coating

C) 800 °C, 1h & sonification (β-TCP)

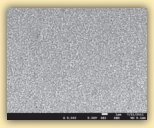

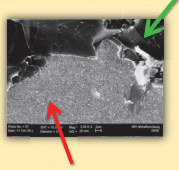

Adhesive

No detachement of the coating

Conclusions

➢A two-step wet-chemical biomimetic method was employed for the rapid deposition of Ca-P coatings on ZrO_2 ceramics.

➢The bond strength of the deposited coating is low (1.8 MPa), but can be significantly improved by thermal treatments.

➢Thermal treatments at 600 °C and 800 °C caused conversion in the composition of the coating from the initial OCP to the Hap (600 °C) and β-TCP (800 °C) phase, respectively.

➢Thin β-TCP coatings that were produced by firing the coated zirconia discs at 800 °C and subsequent short sonification, reached high value of bond strength (29.3 MPa). The coatings could not be detached from the substrate with our tensile test.

References

[1] León B, Jansen J. Thin Calcium Phosphate Coatings for Medical Implants, ISBN: 978-0-387-77718-4; Springer, 2009.

[2] Bigi A, Boanini E, Bracci B, Facchini A, Panzavolta S, Segatti F, Sturba L. Nanocrystalline hydroxyapatite coatings on titanium: a new fast biomimetic method. Biomaterials 2005;26:4085-9.

MoS2/P3HT composites for photovoltaic applications: Optical absorption and morphological properties

Peter Topolovšek[1], **Christoph Gadermaier**[1]

[1]Jožef stefan International Postgraduate School, Ljubljana, Slovenia
peter.topolovsek@ijs.si

This poster presents recent morphology analysis and optical absorption spectra of MoS_2/P3HT composites which have a potential to be used as an active layer in organic solar cells. Up to this date the most studied composite used in organic solar cells is a mixture of conjugated polymer P3HT [Poly(3-hexylthiophene-2,5-diyl)] used as an electron donor and PCBM [[6,6]-Phenyl C61 butyric acid methyl ester] as an electron acceptor. MoS_2, a member of layered transition metal dichalcogenides, might be a suitable substitute for PCBM due to its 2D structure, higher electron mobility (200 $cm^2V^{-1}s^{-1}$)[1] than that of a PCBM (10^{-3} $cm^2V^{-1}s^{-1}$)[2] and higher absorption in the visible light spectral region. Here we compare AFM images and optical absorption spectra of MoS_2/P3HT composite films deposited with three different techniques, two-component spray deposition, and drop casting and spin coating of MoS_2/P3HT mixture. Additionaly we performed thermal annealing in an inert atmosphere to observe changes in the morphology of the deposited film. We observed no clear phase separation of MoS_2 and P3HT on all differently deposited thin films, even with additional thermal annealing. This could be attributed to the relatively low wt % of MoS_2 in mixtures (up to 5 wt %) at which no significant aggregation can occur.

MEDNARODNA PODIPLOMSKA ŠOLA JOŽEFA STEFANA

JOŽEF STEFAN INTERNATIONAL POSTGRADUATE SCHOOL

MoS_2/P3HT composites for photovoltaic applications:

Optical absorption and morphological properties

Author: Peter Topolovšek; Jožef Stefan International Postgradual School
Program: Nanosciences and Nanotechnologies; Supervisor: Asst. Prof. Christoph Gadermaier.

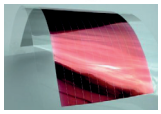

→ Optical absorption and morphological properties of spray and spin coated and drop casted MoS_2/P3HT composites for the use as active layer in plastic solar cells

→ Spray coating is the recommended method for large area covering, realizing large surface solar cells

MoS_2

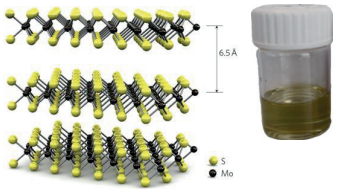

Deposition techniques:

Spray coating (2 component)

Spin coating (mixture)

Drop casting (mixture)

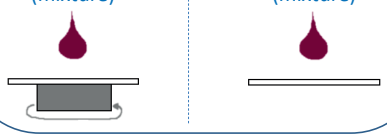

P3HT – Poly(3-hexylthiophene-2,5-diyl)

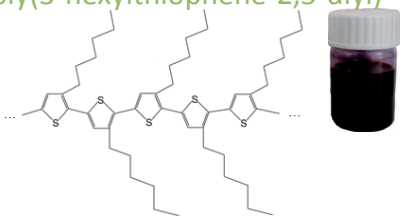

Two component spray deposition

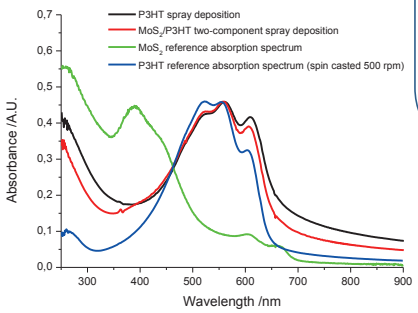

Annealing of spin coated 1 wt % MoS_2 samples

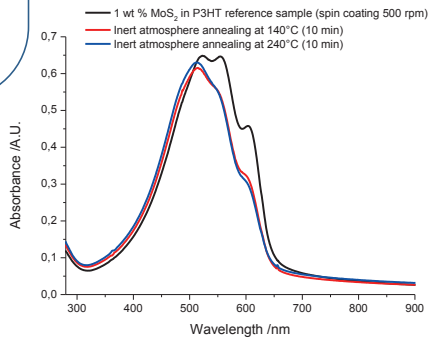

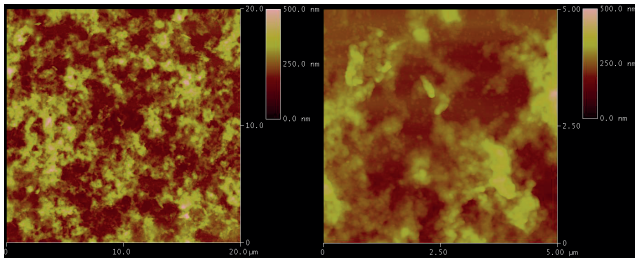

Drop casting deposition, 50 wt % MoS_2

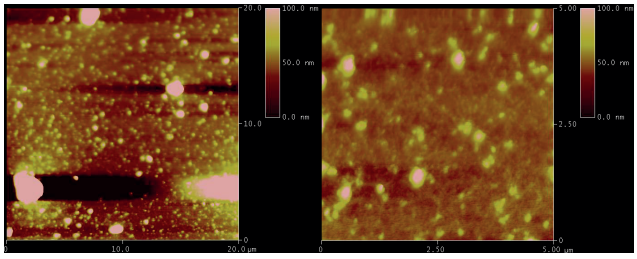

Reference sample, 1 wt % MoS_2 spin coated

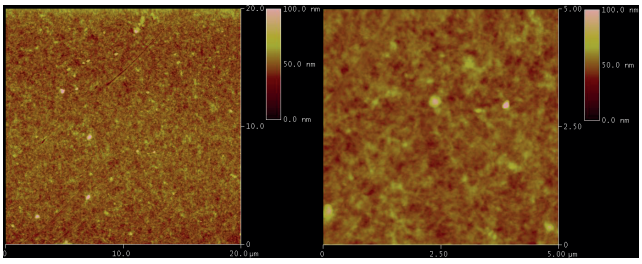

Annealed at 240°C in inert atmosphere

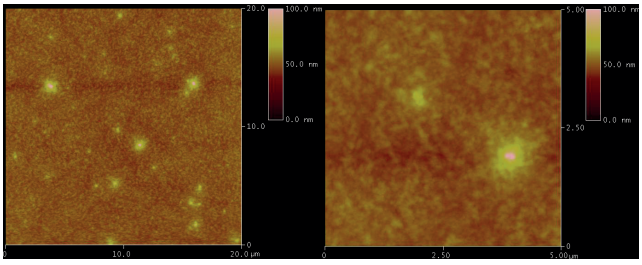

Conclusions

→ Spray coating produces rougher surface with slight phase separation

→ Drop casting method produces agreggates with various sizes, but enables deposition of high MoS_2 wt % samples

→ Annealing does not have an effect on aggregation (phase separation)

complexmatter

Prispevki iz industrije (Contributions from Industry)

Analyze topographical properties of robot laser hardened specimens with topological properties of visibility graphs

Matej Babič[1], Peter Kokol[2], Milan Zorman[2], Marko Marhl[3], Peter Panjan[4], Igor Belič[5], Matija Lokar[6], Andrej Mrvar[7], Milfelner Matjaž[8]

[1] Emo-Orodjarna d.o.o.,
[2]University of Maribor, Faculty of Electrical Engineering and Computer Science,
[3]University of Maribor, *Faculty of Education*
[4]Institute Jozef Stefan,
[5]Institute of metals and technology,
[6]University of Ljubljana, Faculty of Mathematics and Physics,
[7]University of Ljubljana, Faculty of Social Science,
[8]Tic-Lens d.o.o.

babicster@gmail.com

Visibility graphs have many applications, one of which is the analysis of trend lines of market graphs. It is possible to use *2D* visibility graphs for such analysis and the construction for *2D* visibility graphs is well known; however, in this paper, we will present analyze topographical properties of robot laser hardened specimens with topological properties of visibility graphs. The visibility graph is a fundamental geometric structure that is useful in many applications, including illumination and rendering, motion planning, pattern recognition and sensor networks. A graph *G* is called a visibility graph if there is a polygon *P*, such that the vertices of *P* are the vertices of *G* and two vertices are adjacent in *G* if they are visible in *P*. Robot laser surface hardening heat treatment is complementary to conventional flame or inductive hardening. The energy source for laser hardening is the laser beam, which heats up very quickly and the metal surface area of ponds up to *1.5* mm and a hardness of *65 HRC*. Laser hardening is a process of controlling projecting features, such as non-controlled energy intake, high performance constancy and accurate positioning. Hard martensitic microstructure provides improved surface properties, such as wear resistance and high strength. An algorithm for the construction of visibility graphs is very useful in many cases, including: illumination and rendering, motion planning, pattern recognition, computer graphics, computational geometry and sensor networks and the military and automotive industries. We use this new algorithm for pattern recognition.

Investing in your future
OPERATION PART FINANCED BY THE EUROPEAN UNION
European Social Fund

EMO ORODJARNA d.o.o.

Analyze topographical properties of robot laser hardened specimens with topological properties of visibility graphs

Matej Babič[1], Peter Kokol[2], Milan Zorman[2], Marko Marhl[3], Peter Panjan[4], Igor Belič[5], Matija Lokar[6], Andrej Mrvar[7], Milfelner Matjaž[8]

[1] Emo-Orodjarna d.o.o., [2]University of Maribor, Faculty of Electrical Engineering and Computer Science, [3]University of Maribor, Faculty of Education, [4]Institute Jozef Stefan, [5]Institute of metals and technology, [6]University of Ljubljana, Faculty of Mathematics and Physics, [7]University of Ljubljana, Faculty of Social Science, [8]Tic-Lens d.o.o.

ABSTRACT

Visibility graphs have many applications, one of which is the analysis of trend lines of market graphs. It is possible to use *2D* visibility graphs for such analysis and the construction for *2D* visibility graphs is well known; however, in this paper, we will present analyze topographical properties of robot laser hardened specimens with topological properties of visibility graphs. The visibility graph is a fundamental geometric structure that is useful in many applications, including illumination and rendering, motion planning, pattern recognition and sensor networks. A graph *G* is called a visibility graph if there is a polygon *P*, such that the vertices of *P* are the vertices of *G* and two vertices are adjacent in *G* if they are visible in *P*. Robot laser surface hardening heat treatment is complementary to conventional flame or inductive hardening. The energy source for laser hardening is the laser beam, which heats up very quickly and the metal surface area of ponds up to *1.5* mm and a hardness of *65 HRC*. Laser hardening is a process of controlling projecting features, such as non-controlled energy intake, high performance constancy and accurate positioning. Hard martensitic microstructure provides improved surface properties, such as wear resistance and high strength. An algorithm for the construction of visibility graphs is very useful in many cases, including: illumination and rendering, motion planning, pattern recognition, computer graphics, computational geometry and sensor networks and the military and automotive industries. We use this new algorithm for pattern recognition.

iNTRODUCTION

The visibility graph [1-2] is a fundamental geometric structure which is useful in many applications, including illumination and rendering, motion planning, pattern recognition, and sensor networks. A graph *G* is called a visibility graph if there is a polygon *P* such that the vertices of *P* are the vertices of *G*, and two vertices are adjacent in *G* if they are visible in *P*. Visibility graph analysis is a spatial analysis technique for urban and building spaces pioneered at the *VR* Centre, which may also be applied to landscapes. The method involves taking a selection of points across a space, and forming graph edges between those points if they are mutually visible, to form a visibility graph. Visibility graph is widely studied for *2D* scenes, but we inerestinfg for study *3D* visibility complex. Visibility calculations are central to any computer graphics application. We stady how complex are microstructure of robot laser hardenend specimen. We can present a microstructure in *3D* space. Thus we use *3D* visibility graph for desribe this microstructure.

Robot laser surface hardening heat treatment is complementary to the conventional flame or inductive hardening. The energy source for laser hardening, the laser beam which heats up very quickly and the metal surface area of ponds up to *1.5* mm and a hardness of *65 HRC*. Laser hardening is a process of projecting features such as non controlled energy intake, high performance constancy and accurate positioning process. Hard martensitic microstructure provides improved surface properties such as wear resistance and high strength.

Robot laser hardening is have many application on fast development military, avtomoto and aerospece industry. But, here have we many open problems. We will knoe how parameters of robot laser cell impact on microstructure. In this paper, we present a new method, algorithem for describe 3D visibility graph, for analize microstructure of robot laser hardening specimens. We know many process of hardening: Inductive, flame, hardening in hardening furnace and most important robot laser hardening.

In this work we have used scanning electronic microscope (*SEM*) [6], analyze the picture of microstructure of the robot laser hardened specimen. The aim of the study is to develop the algorithm for *3D* classifikation microstructure of robot laser hardenend specimen. An application of the algorithm for construction *3D* visibility graph is in analize microstructure of laser technic in hardening specimen

MATERIAL PREPARATION AND METHOD

The study was undertaken using tool steel standard label DIN standard 1.7225. The chemical composition of the material contained 0.38 to 0.45% C, 0.4% maximum Si, 0.6–0.9% Mn, 0.025% maximum P, 0.035% maximum S and 0.15–0.3% Mo [7]. The specimen test section was in a cylindrical form with dimensions of 25×10mm. Specimens were prepared by laser technique, followed by hardening at $T \in [1000, 1400]$ °C and $v \in [2, 5]$ mm/s. First, we changed two parameters of the robot laser cell: speed $v \in [2, 5]$ mm/s with steps of 1 mm/s and temperature $T \in [1000, 1400]$ °C in steps of 100 °C.
After hardening we polish [8] all specimens. After hardening the test specimen was cut into smaller parts. We use a field emission scanning electron microscope, JEOL JSM-7600F to made pictures (Fig. 2) on surface and on depth of robot laser hardenend specimens. We made pictures on different magnification (5000×, 10000×, 20000×, 30000× and 50000×). To analize a picture we used software program ImageJ.

We develop new algorithm for for construction visibility graph in 3D space. This algorithm we use to analyze mechanical properties of robot laser hardenend specimens. Firstly, we analize profile graph of microstructure picture with visibility graph. Algorithm for 2D visibility graph already exist [9]. On Graph 1 and Graph 2 is presented profile graph of Fig. 1.

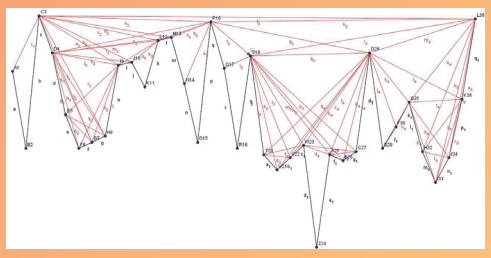

Graph 1: Profile graph of surface hardened specimen

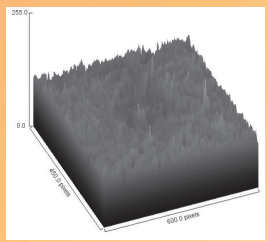

Graph 2: Three dimensional graph

RESULTS

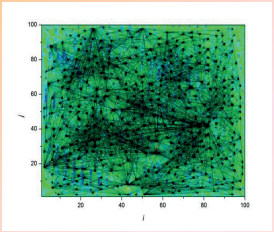

Graph 3: Connection in 3D visibility graph

CONCLUSION

The visibility graph problem itself has long been studied in computational geometry and has been applied to a variety of areas. *3D* visibility graph can be used in many *3D* geometric problems. Finally, in this work the visibility network in *3D* space, which contains more information than the visibility graph, has been used to analize microstructure of robot laser hardened specimens. This algoritm is also usefull in many cases, including illumination and rendering, motion planning, pattern recognition, computer graphics, computational geometry and sensor networks.

REFERENCES

[1] B. Ben-Moshe, O. Hall-Holt, M. J. Katz, J. S. B. Mitchell. Computing the visibility graph of points within a polygon.
[2] Overmars, M. H., and E. Welzl, New methods for constructing visibility graphs. *In Proceedings of the 4th Annual ACM Symposium on Computational Geometry, Urbana, IL* (1988), pp. 164-171.
[3] Grumm J., Žerovnik, P., Šturm, R. 1996, Measurement and analysis of residual stresses after laser hardening and laser surface melt hardening on flat specimens; Proceedings of the Conference "Quenching '96", Ohio, Cleveland.
[4] Babič, M., Milfelner, M., Stepišnik, S. 2010, Laser hardening metals. Y: PERME, Tomaž(ur.), ŠVETAK, Darko (ur.), BALIČ, Jože (ur.). IRT Industrial Forum, Portoroz, 7–8 June 2010. Source of knowledge and experience for the profession: Proceedings of the Forum. Skofljica: Profidtp.

Numerical model of the continuous casting of steel in Štore Steel company

Robert Vertnik[1,2]**, Bojan Senčič**[1,4]**, Agnieszka Guštin**[3]**, Božidar Šarler**[2,3]

[1]Štore Steel d.o.o., Research, Železarska c. 3, 3220, Štore

[2]University of Nova Gorica, Laboratory for Multiphase Processes, Vipavska 13, 5000 Nova Gorica

[3]Institute of Metals and Technology, Laboratory for Simulation of Materials and Processes, Lepi pot 11, 1000 Ljubljana

[4]Jožef Stefan International Postgraduate School, Jamova 39, 1000 Ljubljana

robert.vertnik@store-steel.si

The Štore Steel company is producing rounds and flats of a huge spectrum of different steel quality and has a long tradition in delivering top quality steels to the major European spring and automotive producers. One of the research strategies to improve the quality of the product is optimization of the process parameters by the numerical modeling of the processes in the production chain. This work represents the developed numerical models for the continuous casting process of steel.

NUMERICAL MODEL OF THE CONTINUOUS CASTING OF STEEL IN ŠTORE STEEL COMPANY

Robert Vertnik[1,2], Bojan Senčič[1,4], Agnieszka Guštin[3], Božidar Šarler[2,3]
1-Štore Steel d.o.o., Research, Železarska c. 3, 3220 Štore
2-University of Nova Gorica, Laboratory for Multiphase Processes, Vipavska 13, 5000 Nova Gorica
3-Institute of Metals and Technology, Laboratory for Simulation of Materials and Processes, Lepi pot 11, 1000 Ljubljana
4-Jožef Stefan International Postgraduate School, Jamova 39, 1000 Ljubljana

The Štore Steel company is producing rounds and flats of a huge spectrum of different steel quality and has a long tradition in delivering top quality steels to the major European spring and automotive producers. One of the research strategies to improve the quality of the product is optimization of the process parameters by the numerical modeling of the processes in the production chain. This work represents the developed numerical models for the continuous casting process of steel.

1. Continuous casting of steel

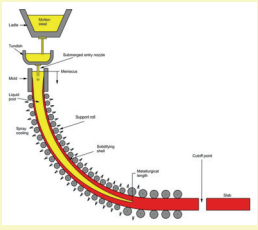

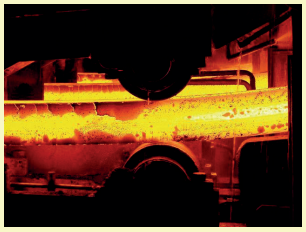

Scheme of the casting process

2. Two-dimensional heat flow model

-simulation of a temperature field with grain structure
-heat flow in longitudinal direction of the billet is neglected
-much faster calculation time in comparison to full 3D model
-can be used in on-line monitoring of the strand and in qualitative sensitivity studies

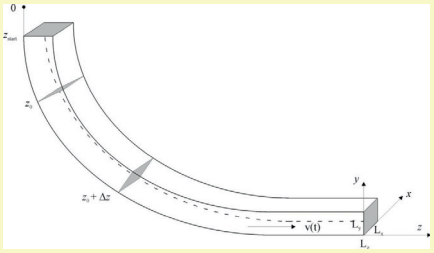

Scheme of the 2D slice model

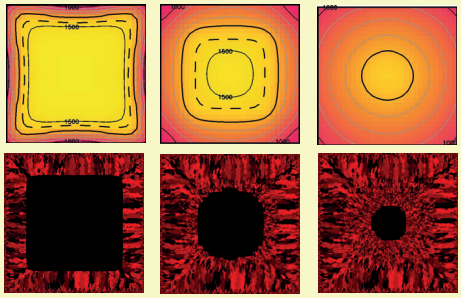

Top: temperature field, Bottom: grain structure at different slice positions

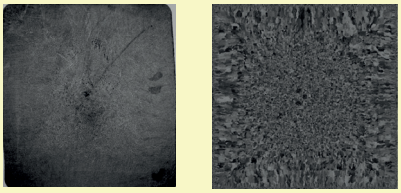

Left: Baumann print of the 51CrV4 steel billet
Right: simulated grain structure

3. Three-dimensional heat and fluid flow model with turbulence

-complex physical model
-much slower then 2D slice model
-~600.000 calculation points – parallelization is needed
-used for optimization of the SEN geometry, particle tracking and macrosegregation in the mould

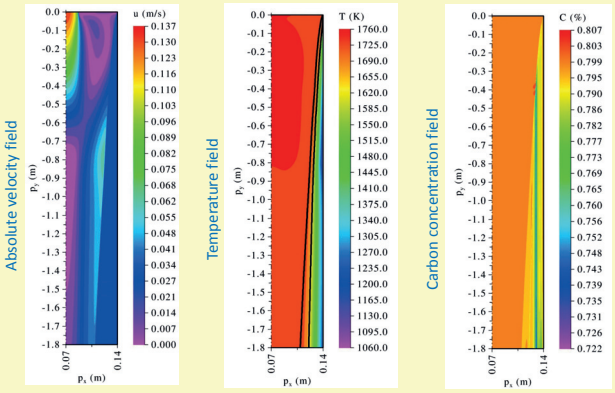

Calculated fields of the longitudinal cross section

4. Validation of the numerical models

-validation is performed based on the temperature measurements of the billet surface with a two-color pyrometer

-schell thickness measured with hammering the nails into the billet

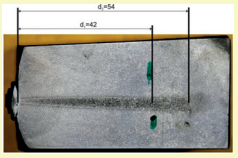

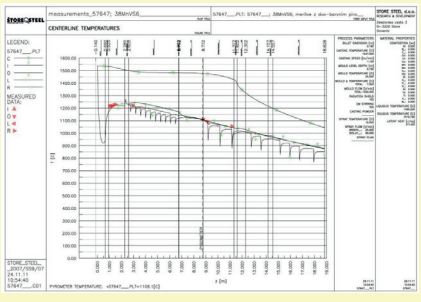

Solid black line – simulation, red symbols - measurements

MEDNARODNA PODIPLOMSKA ŠOLA JOŽEFA STEFANA
Jamova 39, 1000 Ljubljana

Tel: (01) 477 31 00
Faks: (01) 477 31 10
E-pošta: info@mps.si
http://www.mps.si/